UNIVERSIDADE FEDERAL DO RIO GRANDE DO SUL
ESCOLA DE ENGENHARIA
PROGRAMA DE PÓS-GRADUAÇÃO EM ENGENHARIA ELÉTRICA

MATHIAS GIORDANI TITTON

STABILITY AND STABILIZATION OF SAMPLED-DATA CONTROL FOR LURE SYSTEMS

Porto Alegre
2021

MATHIAS GIORDANI TITTON

STABILITY AND STABILIZATION OF SAMPLED-DATA CONTROL FOR LURE SYSTEMS

Thesis presented to Programa de Pós-Graduação em Engenharia Elétrica of Universidade Federal do Rio Grande do Sul in partial fulfillment of the requirements for the degree of Master in Electrical Engineering.
Area: Control and Automation

ADVISOR: Prof. Dr. João Manoel Gomes da Silva Jr.

Porto Alegre
2021

MATHIAS GIORDANI TITTON

STABILITY AND STABILIZATION OF SAMPLED-DATA CONTROL FOR LURE SYSTEMS

This thesis was considered adequate for obtaining the degree of Master in Electrical Engineering and approved in its final form by the Advisor and the Examination Committee.

Advisor: _____
Prof. Dr. João Manoel Gomes da Silva Jr., UFRGS
Doutor pela Université Paul Sabatier – Toulouse, França

Examination Committee:

Prof. Dr. Eugenio de Bona Castelan Neto, UFSC
Doutor pela Université Paul Sabatier – Toulouse, França

Prof. Dr. Jeferson Vieira Flores, UFRGS
Doutor pela Universidade Federal do Rio Grande do Sul – Porto Alegre, Brasil

Prof. Dr. Sérgio Luís Haffner, UFRGS
Doutor pela Universidade Estadual de Campinas – São Paulo, Brasil

Coordinator of PPGEE: _____
Prof. Dr. Sérgio Luís Haffner.

Porto Alegre, June 2021.

DEDICATÓRIA

Dedico este trabalho aos meus pais, avós e à minha namorada.

AGRADECIMENTOS

À minha família, em especial aos meus pais Ari e Maritana e à minha namorada Paula pelo apoio incondicional, pela compreensão e por auxiliarem continuamente no meu desenvolvimento pessoal e profissional.

Aos meus avós Dornélio, Ana e Zelaide e aos meus tios Altair e Etacir pelo apoio. À minha prima Bruna e aos meus sogros Marinês e Paulo pela companhia e momentos de lazer.

Ao meu orientador, Dr. João Manoel, por proporcionar um tema de pesquisa relevante na área, pelas trocas de ideias nas reuniões e por transmitir conhecimentos e segurança ao longo da pesquisa. Posso afirmar que a orientação foi da melhor qualidade possível. Agradeço também ao Dr. Giórgio Valmórbida e ao Dr. Marc Jungers pela contribuição na pesquisa e por participarem do processo de elaboração dos artigos.

Aos meus amigos que estão próximos e também aqueles que estão distantes, aos novos e aos antigos pelos quais tenho muito apreço, em especial ao Rodrigo, Osvaldo, Éverton e ao meu primo Maurício, que proporcionaram momentos de descontração e de troca de ideias.

À Dra. Alessandra, por ter sido uma segunda orientadora que auxiliou na resolução de diversas questões. Agradeço pela disponibilidade do seu tempo e por ter transmitido um pouco do seu conhecimento.

Aos colegas, pela companhia e auxílio nas tarefas desenvolvidas.

Aos professores, pelos conhecimentos transmitidos.

Ao Programa de Pós-Graduação em Engenharia Elétrica, PPGEE, e seus servidores pela oportunidade de realizar meu mestrado.

À CAPES pela provisão da bolsa de mestrado.

À banca pelas contribuições.

ABSTRACT

This work presents a new method for stability analysis and stabilization of sampled-data controlled Lure systems, subject to aperiodic sampling and nonlinearities that are sector bounded and slope restricted, in both global and regional contexts. We assume that the states of the plant are available for measurement and that the nonlinearities are known, which leads to a more general formulation of the problem. The states are acquired by a digital controller which updates the control input at aperiodic discrete-time instants, keeping it constant between successive sampling instants. The approach here presented is based on the use of a new class of looped-functionals and a generalized Lure-type function, which leads to stability and stabilization conditions that are written in the form of Linear Matrix Inequalities (LMIs) and quasi-LMIs, respectively. On this basis, optimization problems are formulated aiming to compute the maximal intersampling interval or the maximal sector bounds for which the asymptotic stability of the origin of the sampled-data closed-loop system is guaranteed. In the case where the sector conditions hold only locally, the solution of these problems also provide an estimate of the region of attraction for the continuous-time trajectories of the closed-loop system. As the synthesis conditions are quasi-LMIs, a Particle Swarm Optimization (PSO) algorithm is proposed to deal with the involved nonlinearities in the optimization problems, which arise from the product of some decision variables. Numerical examples are presented throughout the work to highlight the potentialities of the method.

Keywords: Sampled-data Control, Lure Systems, Stability and Stabilization, Looped-Functional Approach, Particle Swarm Optimization Algorithm.

RESUMO

Este trabalho apresenta um novo método para a análise de estabilidade e estabilização de sistemas do tipo Lure com controle amostrado, sujeitos a amostragem aperiódica e não linearidades que são limitadas em setor e restritas em derivada, em ambos contextos global e regional. Assume-se que os estados da planta estão disponíveis para medição e que as não linearidades são conhecidas, o que leva a uma formulação mais geral do problema. Os estados são adquiridos por um controlador digital que atualiza a entrada de controle em instantes de tempo discretos e aperiódicos, mantendo-a constante entre dois instantes sucessivos de amostragem. A abordagem apresentada neste trabalho é baseada no uso de uma nova classe de *looped-functionals* e em uma função do tipo Lure generalizada, que leva a condições de estabilidade e estabilização que são escritas na forma de desigualdades matriciais lineares (LMIs) e quasi-LMIs, respectivamente. Com base nestas condições, problemas de otimização são formulados com o objetivo de computar o intervalo máximo entre amostragens ou os limites máximos do setor para os quais a estabilidade assintótica da origem do sistema de dados amostrados em malha fechada é garantida. No caso em que as condições de setor são válidas apenas localmente, a solução desses problemas também fornece uma estimativa da região de atração para as trajetórias em tempo contínuo do sistema em malha fechada. Como as condições de síntese são quasi-LMIs, um algoritmo de otimização por enxame de partículas é proposto para lidar com as não linearidades envolvidas nos problemas de otimização, que surgem do produto de algumas variáveis de decisão. Exemplos numéricos são apresentados ao longo do trabalho para destacar as potencialidades do método.

Palavras-chave: Controle Amostrado, Sistemas Lure, Estabilidade e Estabilização, Abordagem *Looped-Functional*, Algoritmo de Otimização por Enxame de Partículas.

LIST OF FIGURES

LIST OF TABLES

LIST OF ABBREVIATIONS

BMI	Bilinear Matrix Inequality
LF	Lyapunov Function
LKF	Lyapunov Krasovskii Functional
LMI	Linear Matrix Inequality
LTI	Linear Time Invariant
MIMO	Multiple Input Multiple Output
NCS	Networked Controlled Systems
PSO	Particle Swarm Optimization
SDC	Sampled Data Control
SDP	Semi Definite Programming
SISO	Single Input Single Output
ZOH	Zero Order Hold

LIST OF SYMBOLS

$c \in \mathcal{C}$	c is an element of the set $\mathcal{C}$;
$c \notin \mathcal{C}$	c is not an element of the set $\mathcal{C}$;
$\mathcal{C} \subset \mathcal{D}$	$\mathcal{C}$ is a subset of $\mathcal{D}$;
$\mathcal{C} \subseteq \mathcal{D}$	$\mathcal{C}$ is a subset of $\mathcal{D}$ and it is allowed that $\mathcal{C} = \mathcal{D}$;
Re[z]	Real part of a complex number $z = a + bj$;
Im[z]	Imaginary part of a complex number $z = a + bj$;
$\forall$	For all;
$\exists$	There exists;
$\triangleq$	Equal by definition;
$\sum_{i=a}^{b}$	Sum of $x_a, x_{a+1}, \ldots, x_b$;
$\bigcup_{k \in \mathbb{N}} s_k$	Union of $s_0, s_1, \ldots, s_k$, $\forall k \in \mathbb{N}$;
$\mathbb{N}$	The set of the natural numbers;
$\mathbb{R}$	The set of the real numbers;
$\mathbb{R}^+$	The set of positive real numbers;
$\mathbb{R}^{n \times n}$	$n \times n$-dimensional real space;
$v \in \mathbb{R}^n$	v is a vector of dimension n;
v_i	The ith element of the vector v;
$M \in \mathbb{R}^{n \times n}$	M is a matrix of dimension $n \times n$;
M_i	The ith row of the matriz M;
M^T	The transpose of M;
$\mathbb{S}^n$	The space of all symmetric matrices of dimension $n \times n$;
$S \in \mathbb{S}^n$	S is a symmetric matrix of dimension $n \times n$;
$S \succ 0$	S is positive definite;
$S \succeq 0$	S is positive semidefinite;
$S \prec 0$	S is negative definite;

$S \preceq 0$	S is negative semidefinite;
$\star$	Symmetric terms in a symmetric matrix;
$\mathbb{D}^n$	The space of all diagonal matrices of dimension $n \times n$;
$S \in \mathbb{D}^n$	S is a diagonal matrix of dimension $n \times n$;
$S \in \mathbb{D}^n_{\succeq 0}$	S is a positive semi-definite diagonal matrix of dimension $n \times n$;
diag$(e_1, \ldots, e_n)$	The diagonal matrix of blocks $e_1, \ldots, e_n$;
I	A identity matrix of appropriate dimensions;
0	A zero matrix of appropriate dimensions;
∂	Sub-differential operator;
$\partial\mathcal{S}$	Defines the boundary of a set $\mathcal{S}$;
$\dot{x}$	Time-derivative of a time function x;
$f(\cdot)$	A function f with the argument suppressed;
$\mathbb{K}_{\mathcal{T}}$	The set of continuous functions from an interval $[0, \mathcal{T}]$ to $\mathbb{R}^n$, where $\mathcal{T}$ is a positive scalar;
He$\{A\}$	He$\{A\} \triangleq A + A^T$, where $A \in \mathbb{S}^n$;
$JF(y)$	The jacobian of a function $F(y)$;
$\lvert \cdot \rvert$	The absolute value of a scalar;
$\lVert \cdot \rVert$	The Euclidean norm;
$\lim_{x \to c} f(x) = K$	The limit of $f(x)$ as x approaches c equals K;
rank(A)	The number of linearly independent rows or columns of the matrix A;
det(A)	Determinant of a matrix A;
$\overline{\text{co}}(\mathcal{A})$	The closed convex hull of the set $\mathcal{A}$;

CONTENTS

1 INTRODUCTION

Sampled-Data Control (SDC) has attracted a lot of researchers' attention in the last decades (HESPANHA; NAGHSHTABRIZI; XU, 2007), (ZHANG *et al.*, 2019). This field of study comprehends the analysis of stability and stabilization of systems evolving in continuous-time, whereas a digital controller delivers inputs at discrete-time instants. More precisely, the signals of the plant are sampled and then transmitted to the controller, which updates the plant control input according to a pre-defined law, keeping it constant between successive sampling instants. This effect may induce complex behaviors, like oscillations and instability for the closed-loop system. In some situations, for instance, a large sampling period may be sufficient enough to destabilize a system. On the other hand, small sampling times may stabilize a system naturally unstable.

In the classical problem of linear SDC systems considering periodic sampling, the stability can be evaluated indirectly by obtaining a discrete model through exact discretization of the continuous-time plant, *i.e.*, assessed from a discrete model whose state values coincides to the ones of the continuous-time plant at the periodic sampling instants. Difficulties arises when dealing with uncertain systems, as the uncertainties appears at the exponent of the transition matrix. On the other hand, for nonlinear systems, approximate discretization techniques such as Euler and Bilinear ones are commonly used to assess the system stability. However, these techniques may fail for longer sampling periods, leading to system instability.

Although there exist a well-established theory for periodic SDC for linear systems, as for example in (CHEN; FRANCIS, 2012), (ÅSTRÖM; WITTENMARK, 2013) and the references therein, in the last years authors have shown concern over the issue of stability and stabilization of aperiodic SDC (FRIDMAN, 2010), (SEURET; GOMES DA SILVA JR., 2012), (HETEL *et al.*, 2017), (ZENG *et al.*, 2020). This is motivated by the increasing demand in the industry for embedded systems (microprocessed systems dedicated exclusively to predefined tasks) and Networked Control Systems (NCS), which are spatially distributed systems where the communication between sensors, actuators, controllers and devices occurs through a shared and band-limited digital communication network (HESPANHA; NAGHSHTABRIZI; XU, 2007), (ZAMPIERI, 2008). In this

context, the study of aperiodic SDC emerged as a modelling abstraction which allows to understand the behavior of systems with sampling jitters, packet drop-outs or fluctuations (HETEL *et al.*, 2017), caused generally by computer architecture, operating system, protocols with no guarantee of an uniform sampling rate (ANTSAKLIS; BAILLIEUL, 2007) or by a heavy temporary load of computation in a processor, which can corrupt the sampling period of a given controller (SEURET, 2012). Hence, these variations on the sampling period can dramatically affect the stability properties of the controlled system. Furthermore, when a SDC is updated aperiodically, then the exact discretization is no longer valid even for the linear case. Thus, the hybrid behavior resulting from the discrete- and continuous-time dynamics should be taken explicitly into account.

A more challenging task is to obtain conditions that guarantee stability for nonlinear SDC systems. Nonlinearities also degrades the performance of a control loop and may lead to instability of the controlled system. In this context, several nonlinear systems can be represented through a generic class denominated Lure systems, which is composed of a linear, time-invariant system fed back by a (vector-valued) nonlinearity that is supposed to belong to a cone-bunded sector, *e.g.* in (SUYKENS; VANDEWALLE; DE MOOR, 1998), (ZENG *et al.*, 2011), (VALMORBIDA; DRUMMOND; DUNCAN, 2016). Concerning the stability issue of Lure systems, graphical criteria such as the Circle and Popov ones or Lyapunov-based approaches are generally used to assess the stability of continuous-time systems (KHALIL, 2002). However, as will be discussed in the next chapters, there are lack of works concerning stability and stabilization of sampled-data controlled Lure systems, which motivates researches in this area.

In this study, sufficient conditions for the stability analysis and stabilization of a sampled-data controlled Lure system subject to aperiodic sampling and nonlinearities that are sector and slope restricted are proposed. The method is based on a looped-functional approach that focus on the behavior in the intersampling interval, ensuring that a positive definite function is strictly decreasing at the sampling instants, which implies the asymptotic convergence of the continuous-time trajectories of the system to the origin (SEURET, 2012), (SEURET; GOMES DA SILVA JR., 2012). In this context, from a new class of looped-functionals and Lure-type functions, we derive stability and stabilization conditions for the sampled-data closed-loop system in the form of Linear Matrix Inequalities (LMIs) or quasi-LMIs (that is, LMIs by fixing some parameters). On this basis, several optimization problems are stated, while ensuring global or regional asymptotic stability for the trajectories of the closed-loop system, aiming for instance, to maximize the intersampling intervals, the admissible sector bounds or to maximize the estimate of the region of attraction.

The outline of this dissertation is as follows. In Chapter 2, a bibliographic review about modelling techniques and approaches for stability analysis of sampled-data systems is presented. A review of Lure systems is also presented, with the intent of a characteri-

zation of the study inside this field of research.

In Chapter 3, a representation of the Lure system with a generic aperiodic sampled-data control law is formalized. Regarding the looped-functional approach, preliminary theorems for assessing the stability of the closed-loop system with SDC in both global and regional contexts are presented.

In Chapter 4, from the given control law, LMI conditions for analysing global and regional asymptotic stability are derived, using the preliminary results from Chapter 3 as basis. Numerical examples and a comparative result with a work in the literature is provided.

In Chapter 5, conditions of Chapter 4 are modified to compute feedback gains and synthesize global or regional stabilizing controllers. A criterion to improve the time response of the trajectories of the controlled system is also presented. As the obtained stabilization conditions are in the form of quasi-LMIs, it is proposed an evolutionary algorithm to test the feasibility of the inequalities while searching for the best combination of parameters that optimize the results according to each stated problem. As examples, some numerical simulations are executed by an appropriate algorithm to illustrate the methodology.

Finally, in Chapter 6, conclusions and some discussions on the prospects for future work are presented. Additionally, the Appendix provides some basic theoretical tools. Along the reading, it will be referenced when its content might be helpful.

2 LITERATURE REVIEW: STABILITY OF SAMPLED-DATA CONTROL SYSTEMS

In this chapter, a literature review on topics related to the scope of this dissertation is presented. In Section 2.1, modelling techniques, representations and approaches for sampled-data systems are discussed. Next, Section 2.2 introduces the Lure systems and presents a summary of works regarding SDC Lure systems, with the main ideas of their approaches.

2.1 Sampled-Data Control Systems

Dynamical systems are often classified as either continuous-time or discrete-time systems. For instance, one can easily recognize that classical mechanical systems and analog electronic circuits evolving in time according to physical laws such as Newton's and Kirchhoff's have continuous dynamics. On the other hand, financial and stock markets, where asset prices rise or fall, optimization algorithms and digital systems of all kinds that use binary logic can naturally be classified as discrete-time dynamical systems.

However, there exist many systems which combines qualitatively the behavior of discrete and continuous-time systems, making it difficult to classify them in a definite way (GOEBEL; SANFELICE; TEEL, 2012). In a switched electrical circuit, for example, voltages and currents that change continuously according to classical electrical network laws also change discontinuously due to the switching of the transistors (GOEBEL; SANFELICE; TEEL, 2009). Biological reactions, mechanisms subject to impact and any system involving both digital and analog components also have discontinuous dynamics when receiving an impulse stimulus.

Sampled-data systems are inserted in this context, as they also exhibits both discrete and continuous-time behavior, since the control updates occur at discrete-time instants, while the overall system naturally has continuous dynamics. As we are interested in the stability of this kind of systems, along this chapter we will discourse about the two main approaches existing in the literature to model and to deal with them. The first one is the hybrid approach, which models the SDC system through difference and differential

equations and maps the update in the control signal at the sampling instants. A direct implication is that the obtained model is finite-dimensional. The second approach is the time-delay approach, where the sampling is translated into a time-varying input delay that keeps the control signal constant between two successive sampling instants, thus resulting in an infinite-dimensional model. In the sequence, we detail each one of these approaches, starting with the hybrid.

2.1.1 Hybrid Approach

According to GOEBEL; SANFELICE; TEEL (2012), a hybrid dynamical system, or just a hybrid system, is a dynamical system that exhibits characteristics of both continuous and discrete-time dynamical systems or a dynamical system that is modelled with a combination of common modelling tools for continuous and discrete-time dynamical systems. Essentially, a closed-loop system may be modelled through a merge of differential equations and difference equations, since the former cannot describe changes on logical variables and the latter is not capable to completely characterize the system dynamics. A hybrid system can be formally represented, for instance, by the following model (GOEBEL; SANFELICE; TEEL, 2009):

$$\begin{cases} \dot{x}(t) = f(x(t)), & \forall x(t) \in \mathcal{C} \\ x^{+}(t) = g(x(t)), & \forall x(t) \in \mathcal{D} \end{cases}, \tag{1}$$

where $x \in \mathbb{R}^n$ is the vector of states of the system, $\dot{x}$ is the vector of its derivatives with respect to time, x^+ is the vector of the values of the states after an instantaneous change, f and g are, respectively, the flow map and the jump map, with $\mathcal{C}$ and $\mathcal{D}$ being, respectively, the flow and jump sets. In this representation, the states of the hybrid system changes according to a differential equation $\dot{x}(t) = f(x(t))$ while in the set $\mathcal{C}$, and to a difference equation $x^+(t) = g(x(t))$ while in the set $\mathcal{D}$, whose solution is a discontinuous function of time. This allows to capture the dynamics of purely continuous-time or discrete-time systems. Note that f and g must be completely defined on the flow and jump sets.

According to HETEL *et al.* (2017), the first mentions to SDC systems as hybrid dynamical systems came from the work of MOUSA; MILLER; MICHEL (1986), where it was performed a stability analysis given some input-output properties of the continuous-time plant. Later, hybrid systems were applied, for example, to linear SDC systems with uniform and multi-rate sampling aiming to solve $\mathcal{H}_2$ and $\mathcal{H}_\infty$ problems (TOIVONEN, 1992), (KABAMBA; HARA, 1993), (SUN; NAGPAL; KHARGONEKAR, 1993). An extension to nonlinear SDC systems was addressed in (HOU; MICHEL; YE, 1997), (YE; MICHEL; HOU, 1998). For a solid theoretical foundation of hybrid systems, the reader is encouraged to see (GOEBEL; SANFELICE; TEEL, 2009), (GOEBEL; SANFELICE; TEEL, 2012) and the references therein.

One of the most important classes of hybrid systems used to deal with sample-and-

hold circuits is the class of impulsive ones, described by Ordinary Differential Equations (ODEs) and instantaneous state jumps or impulses (HESPANHA; LIBERZON; TEEL, 2008), (GOEBEL; SANFELICE; TEEL, 2009), (BRIAT; SEURET, 2012a). In this case, the difference equation activates the discrete-time dynamics at the impulse instants, which introduces discontinuities in the trajectories of the system. A finite-dimensional, SDC system in the impulsive framework may be expressed, for instance, by the following equations:

$$\begin{cases} \dot{x}(t) = f(x(t), u(t)), & \forall t \notin \Theta; \\ x(t) = x(t^-), & \forall t \in \Theta, \quad t \neq 0; \\ u(t) = g(x(t^-)), & \forall t \in \Theta, \quad t \neq 0; \\ \dot{u}(t) = 0, & \forall t \notin \Theta; \\ x(0) = x_0, \quad u(0) = K_x x_0, & t = 0, \end{cases} \tag{2}$$

where $\Theta = \{t \in \mathbb{R}^+ : t = t_k, t_{k+1} > t_k, k \in \mathbb{N}\}$ is the set containing the time sequence of impulsive updates t_k, $x \in \mathbb{R}^n$ is the plant state variable, x_0 is the vector of initial conditions of the states of the system, $u \in \mathbb{R}^q$ is the control signal, $K_x \in \mathbb{R}^{q \times n}$ is the states gains matrix, f and g are the flow and jump maps. The limit from below of the signal $x(t)$ is defined as $x(t^-) = \lim_{\tilde{t} \to t,\ \tilde{t} < t} x(\tilde{t})$ and the left-hand side derivative of x with respect to t, as $\dot{x}(t) = \lim_{\tilde{t} \to t,\ \tilde{t} < t} \frac{x(\tilde{t}) - x(t)}{\tilde{t} - t}$. Observe in representation (2) that if the difference between two successive sampling times (also called dwell-time) is constant, we have a periodic SDC. Otherwise, we have an aperiodic SDC.

In this context, the modelling as impulsive systems had been used in the literature in the last decades to assess the stability of SDC systems. For instance, impulsive systems with aperiodic sampling had been developed in (TOIVONEN, 1992), (DULLERUD; LALL, 1999), (MICHEL; HU, 1999). In (SIVASHANKAR; KHARGONEKAR, 1994), necessary and sufficient conditions were provided regarding the stability of linear systems and $\mathcal{L}_2$-gain analysis in the form of differential equation with jumps. The impulsive model was also applied to sampled-data stabilization of linear uncertain systems subject to periodic sampling (HU *et al.*, 2003) by using a piecewise linear in time quadratic Lyapunov Function (LF) and further extended to aperiodic sampling with a known upper bound in (NAGHSHTABRIZI; HESPANHA; TEEL, 2008), which introduced a method based on a discontinuous LF.

More recently, the analysis of stability of linear impulsive systems was done through the use of looped-functionals as in (BRIAT; SEURET, 2012a), (BRIAT; SEURET, 2012b), providing reduction on the conservatism in comparison to the existing results. In (BRIAT, 2013), conditions for robust stability analysis and stabilization of periodic and aperiodic uncertain SDC systems are derived considering a quadratic clock-dependent LF and a link of this approach and the looped-functional one is discussed in (BRIAT, 2016). Regarding yet the impulsive system framework, results of linear systems subject to input

saturation and aperiodic sampling are given in (FIACCHINI; GOMES DA SILVA JR., 2018), (FAGUNDES; GOMES DA SILVA JR.; JUNGERS, 2019).

2.1.2 Time-Delay Approach

The time-delay approach, or also known as input-delay approach, was introduced by (MIHEEV; SOBOLEV; FRIDMAN, 1988) and further developed by (FRIDMAN, 1992). It consists in modelling the aperiodic sample-and-hold operations by a delayed control input, whereas the system evolves in continuous-time. An LTI system with a sampled-data control law may be expressed, for instance, by the following time-delay system:

$$\begin{cases} \dot{x}(t) = Ax(t) + B_u u(t - \tau(t)); \\ \tau(t) = t - t_k, \qquad\qquad \forall t \in [t_k, t_{k+1}), \quad k \in \mathbb{N}; \end{cases} \tag{3}$$

where $x \in \mathbb{R}^n$ is the plant state variable, $u \in \mathbb{R}^q$ is the control signal, which is a function that depends on the plant and the controller states delayed in time, $A \in \mathbb{R}^{n\times n}$ is the dynamical matrix and $B_u \in \mathbb{R}^{n\times q}$ is the input matrix. Representation (3) corresponds to the case where the time-varying delay $\tau(t)$ is piecewise-linear with derivative $\dot{\tau}(t) = 1$ for $t \neq t_k$. Note that when a sampling occurs, the delay is reset to zero, *i.e.*, $\tau(t_k) = 0$.

In the case where the derivative of the delay is less than or equal to one, robust stability conditions for linear systems with time-varying delays were derived via Lyapunov-Krasovskii Functionals (LKF), as for example in (FRIDMAN, 2014) and the references therein. On the other hand, for time-varying delays without any restrictions on its derivative (also known as fast-varying delays), the stability issue has initially been treated through the use of Lyapunov-Razumikhin functions (see CAO; SUN; CHENG (1998) and some references in (HALE; LUNEL, 2013) and (KOLMANOVSKII; MYSHKIS, 2012)), leading to results that are possibly conservative. These methods became very popular in the NCS literature to analyse and design linear uncertain systems under aperiodic samplings with the known upper bound on the sampling intervals (FRIDMAN; SEURET; RICHARD, 2004), (YU *et al.*, 2005), (GAO; CHEN, 2008), (JIANG *et al.*, 2008).

In (FRIDMAN; SEURET; RICHARD, 2004) robust stability conditions for sampled-data control were developed for linear systems by using a LKF and assuming that the delay is restricted to evolve at the same rate of time $\dot{\tau} = 1$ as in (3), reducing the conservatism in comparison to the Lyapunov-Razumikhin approach without loss of generality, since the restriction of $\dot{\tau}$ is intrinsic to the SDC system. Improvements to the existing results were provided in (MIRKIN, 2007) and (FUJIOKA, 2009) by using the small gain theorem. These methods were very relevant at the time, because differently from the discrete-time approaches, they were able to deal with uncertain systems or systems with time-varying parameters. In the works of (SEURET, 2009), (LIU; SUPLIN; FRIDMAN, 2010) and (FRIDMAN, 2010), conditions were refined to provide less restrictive results, with the latter introducing a novel time-dependent Lyapunov functional-based technique

for aperiodic sampled-data control which does not grow after the sampling times. This LKF used in (FRIDMAN, 2010) is given as follows:

$$V_{LK}(t,x(t),\dot{x}(t)) = \overline{V}_{LK}(t) = x^T(t)Px(t) + (t_{k+1}-t)\int_{t_k}^{t}\dot{x}^T(s)U\dot{x}(s)\mathrm{d}s$$
$$+(t_{k+1}-t)\xi^T(t)\begin{bmatrix}\frac{X+X^T}{2} & -X+X_1\\ \star & -X_1-X_1^T+\frac{X+X^T}{2}\end{bmatrix}\xi(t), \quad t\in[t_k,t_{k+1}), \qquad (4)$$

where $P\in\mathbb{S}^n_{\succ 0}$, $U\in\mathbb{S}^n_{\succ 0}$, $X\in\mathbb{R}^{n\times n}$, $X_1\in\mathbb{R}^{n\times n}$, $\xi(t)=[x^T(t)\ x^T(t_k)]^T$. Note that the terms dependent on U and X, X_1 vanishes at the sampling instants. Thus, this functional is continuous, since $\lim_{t\to t_k}\overline{V}_{LK}(t)=\overline{V}_{LK}(t_k)$. The main idea of this method is to prove that a positive definite LKF as in (4) is upper and lower bounded by two positive scalars and that $\dot{\overline{V}}_{LK}(t)<0$, $t\in[t_k,t_{k+1})$.

However, according to SEURET (2012), this approach was still conservative, since it requires the positivity-definiteness of the functional. To overcome this, the author introduced the looped-functional approach, in which the functional does not require to be positive definite. This method was firstly applied to obtain sufficient conditions for asymptotic and exponential stability by considering a linear system with a sampled-data control, subject to periodic and aperiodic sampling and uncertain systems.

Recently, a new two-sided looped-functional was introduced in (ZENG; TEO; HE, 2017) in the context of sampled-data linear systems, which takes into account the information on both intervals $x(t)$ to $x(t_k)$ and $x(t)$ to $x(t_{k+1})$. The obtained conditions substantially improved those ones in the literature, as the results were nearly approximated to those obtained from the theoretical bound (*i.e.*, by eigenvalue analysis). In (ZENG *et al.*, 2020), conditions were improved to take into account the presence of time-delays in the network by using a two-sided looped-functional which depends on the information on the intervals $x(t_k)$ to $x(t)$, $x(t)$ to $x(t_{k+1})$, $x(t_k-\tau)$ to $x(t-\tau)$ and $x(t-\tau)$ to $x(t_{k+1}-\tau)$. Less restrictive results were obtained, and connections between the impact of communication delay and sampling action are investigated, where it has been noticed that time-delays may improve rather than deteriorate the system performance in some cases.

2.2 Lure Systems

According to (KHALIL, 2002), many nonlinear physical systems can be represented as a feedback connection of an LTI dynamical system $G(s)$ with a nonlinear element ϕ, which satisfies the so-called sector conditions. Such class of systems is known as Lure systems. The structure of a Lure system is illustrated in Fig. 1.

Figure 1: Basic structure of a Lure system.

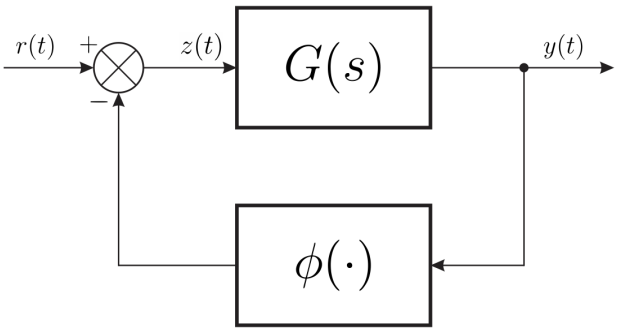

Font: Adapted from (KHALIL, 2002).

The state space mathematical description of an unforced $(r(t) = 0)$ Lure system corresponding to Fig. 1 is given by:

$$\begin{cases} \dot{x} &= Ax + Bz \\ y &= Cx + Dz \\ z &= -\phi(t, y), \end{cases} \tag{5}$$

where $x \in \mathbb{R}^n$, $z \in \mathbb{R}^m$, $y \in \mathbb{R}^m$, (A, B) is controllable, (A, C) is observable, and $\phi : [0, \infty) \times \mathbb{R}^m \to \mathbb{R}^m$, $\phi(t, 0) = 0$. We assume that the algebraic loop is well-posed, *i.e.*, has as unique solution z for every (t, x) in the domain of interest. This is always the case when $D = 0$. The transfer function matrix of the linear system is given by $G(s) = C(sI - A)^{-1}B + D$, and it is square and proper. The nonlinearity ϕ is a memoryless function, possibly time-varying, which is piecewise continuous in t and locally Lipschitz in y, and satisfies a sector condition according to *Definition 1*.

Definition 1. *Let $\underline{\Delta} = diag(\underline{\delta}_1, \underline{\delta}_2, \ldots, \underline{\delta}_m)$, $\overline{\Delta} = diag(\overline{\delta}_1, \overline{\delta}_2, \ldots, \overline{\delta}_m)$, with real constants $\underline{\delta}_i$ and $\overline{\delta}_i > \underline{\delta}_i, \forall i$. A memoryless nonlinearity $\phi : [0, \infty) \times \mathbb{R}^m \to \mathbb{R}^m$ is said to belong to the sector $[\underline{\Delta}, \overline{\Delta}]$, where $\tilde{\Delta} = \overline{\Delta} - \underline{\Delta}$ is a positive definite symmetric matrix, if*

$$[\phi(t, y) - \underline{\Delta} y]^T [\phi(t, y) - \overline{\Delta} y] \leq 0, \quad \forall t \geq 0, \quad \forall y \in \mathcal{Y}_0 \subset \mathbb{R}^m, \tag{6}$$

where the interior of $\mathcal{Y}_0$ is connected and contains the origin.

The sector condition (6) can be verified globally, that is the case when $\mathcal{Y}_0 = \mathbb{R}^m$, or locally, *i.e.*, for a finite domain $\mathcal{Y}_0$ defined as follows:

$$\mathcal{Y}_0 \triangleq \{y(t) \in \mathbb{R}^m; y_i(t) \in [\underline{y}_i, \overline{y}_i], \forall i = 1, \ldots, m\}, \tag{7}$$

where $\underline{y}_i \in \mathbb{R}$, $\overline{y}_i \in \mathbb{R}$, $\underline{y}_i < 0 < \overline{y}_i$. Then, $\mathcal{Y}_0$ is a convex region that contains the origin and if the sector condition holds in $\mathcal{Y}_0$, then this region is defined as a region of validity of the sector condition. Thus, given nonlinearities ϕ, we conclude that:

- If $\mathcal{Y}_0$ is strictly contained in $\mathbb{R}^m$, then the sector conditions are satisfied locally;
- If $\mathcal{Y}_0$ match the whole space in $\mathbb{R}^m$, then the sector conditions are satisfied globally.

Figure 2 illustrates scalar functions verifying the sector conditions locally or globally. The nonlinearity ϕ_i in Fig. 2(a) belongs to a sector $[\underline{\delta}_i, \overline{\delta}_i]$ locally, with validity region given by (7). On the other hand, Fig. 2(b) represents a nonlinearity that globally belongs to a sector $[\underline{\delta}_i, \overline{\delta}_i]$.

Figure 2: Sector condition - (a) Local case and (b) Global case.

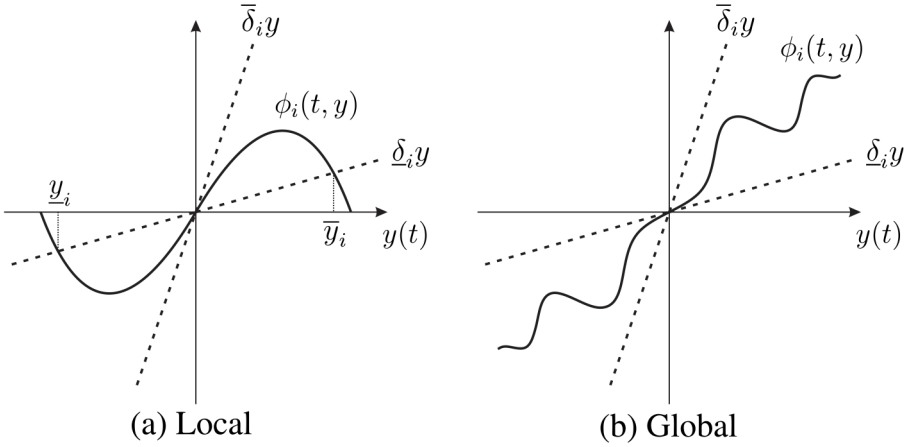

Font: Author.

Remark 1. *It is well-known that a function $\phi_i(\cdot)$ contained in the sector $[\underline{\delta}_i, \overline{\delta}_i]$ can be transformed through a loop transformation into a function $\tilde{\phi}_i(\cdot)$ in the sector $[0, \tilde{\delta}_i]$, with $\tilde{\delta}_i = \overline{\delta}_i - \underline{\delta}_i \succ 0$, without loss of generality. Thus, the system presented in Fig. 1 can be equivalently represented by the system given in Fig. 3.*

Figure 3: Loop transformation.

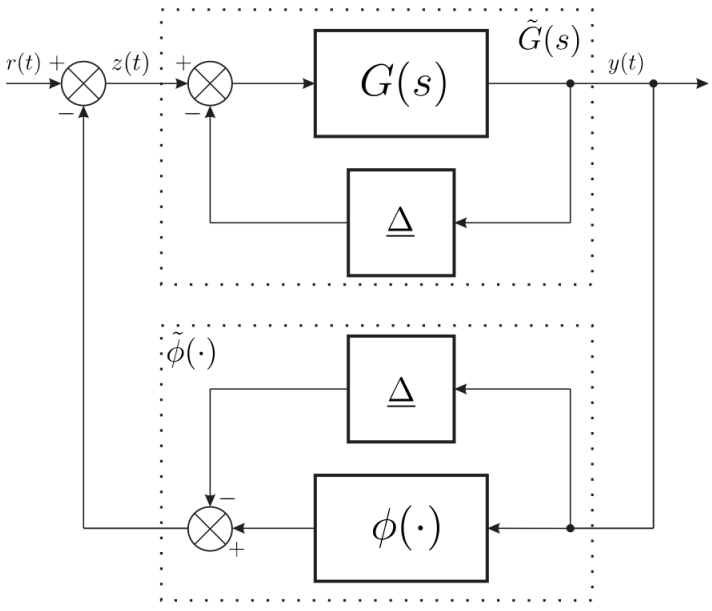

Font: Author.

This process defines a new linear system $\tilde{G}(s) = G(s)[I + \underline{\Delta}G(s)]^{-1}$ *and a new nonlinearity* $\tilde{\phi}(t, y) = \phi(t, y) - \underline{\Delta}y$*. Note that a constant negative feedback gain* $\underline{\Delta}y$ *is applied around the linear component of the system which effect is offset by subtracting* $\underline{\Delta}y$ *from the output of the nonlinearity.*

We should point out that other restrictions for the nonlinearities can be taken into account, *e.g.* slope bounds (TURNER; KERR, 2014), (VALMORBIDA; DRUMMOND; DUNCAN, 2016), (VALMORBIDA; DRUMMOND; DUNCAN, 2018).

2.2.1 Absolute Stability

Regarding Lure systems, the main problem of interest is to study the stability of the origin $x = 0$ (which is an equilibrium point of the system), not for a given nonlinearity, but for a class of nonlinearities that satisfy a given sector condition. If we succeed in certifying the stability of the origin for all nonlinearities in the sector, then the system is said to be absolutely stable, according to the following definition:

Definition 2 (KHALIL (2002))**.** *Consider system (5), where* ϕ *satisfies a sector condition per Definition 1. The system is absolutely stable if the origin is globally uniformly asymptotically stable for any nonlinearity in the given sector. It is absolutely stable with a finite domain if the origin is uniformly asymptotically stable.*

To determine if a Lure system is absolutely stable for all nonlinearities satisfying a given sector, we must analyse the asymptotic stability of its origin. To handle with this problem, two classes of methods are used. The first one uses graphical tools which are based on the frequency response of the linear system, leading to well-known frequency-based techniques, such as the Circle and Popov criteria. On the other hand, the second class is based on the Lyapunov's direct method, where the main idea is to obtain sufficient conditions that guarantees the stability of the origin by using a given Lyapunov function candidate. In the sequence, we recall the Circle and Popov criteria.

2.2.1.1 Circle Criterion

The Circle Criterion provides graphical conditions based on the Nyquist diagram to verify if a continuous-time Lure system in the form (5) is absolutely stable. Using the concepts from strictly positive real (SPR) functions stated in *Lemma 14* (see the Appendix), we present the following theorem regarding the multivariable Circle Criterion.

Theorem 1 (Multivariable Circle Criterion (KHALIL, 2002))**.** *The system (5) is absolutely stable if*

- $\phi \in [\underline{\Delta}, \infty]$ *and* $G(s)[I + \underline{\Delta}G(s)]^{-1}$ *is strictly positive real, or*
- $\phi \in [\underline{\Delta}, \overline{\Delta}]$*, with* $\tilde{\Delta} = \overline{\Delta} - \underline{\Delta} = \tilde{\Delta}^T \succ 0$*, and* $Z(s) = [I + \overline{\Delta}G(s)][I + \underline{\Delta}G(s)]^{-1}$ *is strictly positive real.*

If the sector condition is satisfied only on a set $\mathcal{Y}_0 \subset \mathbb{R}^m$, then the foregoing conditions ensure that the system is absolutely stable with a finite domain.

Conditions from *Theorem 1* can be verified graphically for the scalar case $m = 1$, by examining the Nyquist plot of $G(j\omega)$ (KHALIL, 2002). For $\phi \in [\underline{\delta}, \overline{\delta}]$, with $\overline{\delta} > \underline{\delta}$, we have that the system is absolutely stable if the scalar transfer function $Z(s) = \frac{1+\overline{\delta}G(s)}{1+\underline{\delta}G(s)}$ is SPR. From *Lemma 14*, this condition can be easily checked if $Z(s)$ is Hurwitz, that is, the poles of all elements of $Z(s)$ have negative real parts, and if the following inequality is satisfied:

$$\mathrm{Re}\left[\frac{\frac{1}{\overline{\delta}} + G(j\omega)}{\frac{1}{\underline{\delta}} + G(j\omega)}\right] > 0, \quad \forall\omega \in (-\infty, \infty). \tag{8}$$

To establish the connections between the Nyquist plot of $G(j\omega)$ and (8), one needs to distinguish three different cases that arises from possible changes on the sign of $\underline{\delta}$. Figure 4 illustrates a particular case for $0 < \underline{\delta} < \overline{\delta}$, which is explained below.

Figure 4: Representation of the Circle Criterion.

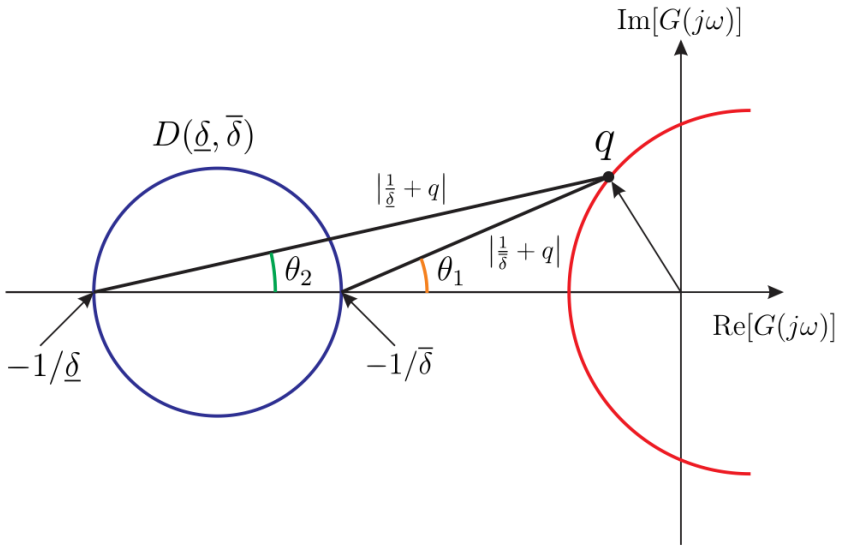

Font: Adapted from (KHALIL, 2002).

From Fig. 4, observe that from a point q of the Nyquist plot of $G(j\omega)$ (depicted in red), two lines can be drawn to connect q to the limits of the closed disk $D(\underline{\delta}, \overline{\delta})$ over the real axis, given by the points $-(1/\overline{\delta}) + j0$ and $-(1/\underline{\delta}) + j0$. We have that the ratio of $(q - (-1/\underline{\delta}))$ with $(q - (-1/\overline{\delta}))$ presents positive real part when the angle difference between them $(\theta_1 - \theta_2)$ is less than $\pi/2$, fact that occurs when q is outside the disk $D(\underline{\delta}, \overline{\delta})$. As $0 < \underline{\delta} < \overline{\delta}$ and since (8) is required to hold for all ω, we conclude that the Nyquist plot must be strictly outside the disk $D(\underline{\delta}, \overline{\delta})$. From the Nyquist criterion, we have that $Z(s)$ is Hurwitz if $G(s)[1 + \underline{\delta}G(s)]^{-1}$ is Hurwitz. This property holds, if and only if the Nyquist plot of $G(j\omega)$ does not intersect the point $-(1/\underline{\delta}) + j0$ (that is the case where the

Nyquist plot of $G(j\omega)$ does not enter the disk $D(\underline{\delta}, \overline{\delta})$) and encircles it exactly k times in the counterclockwise direction, where k is the number of poles of $G(s)$ in the open right-half complex plane. Hence, conditions of *Theorem 1* are satisfied, and absolute stability is assessed.

The following theorem summarizes the graphical stability conditions for these three mentioned cases, yielding to the Circle Criterion, stated as follows.

Theorem 2 (Circle Criterion (KHALIL, 2002))**.** *Consider a scalar system in the form (5), where $\{A, B, C, D\}$ is a minimal realization of $G(s)$ and $\phi \in [\underline{\delta}, \overline{\delta}]$. Then, the system is absolutely stable if one of the following conditions is satisfied, as appropriate:*

(i) If $0 < \underline{\delta} < \overline{\delta}$, the Nyquist plot of $G(j\omega)$ does not enter the disk $D(\underline{\delta}, \overline{\delta})$ and encircles it k times in the counterclockwise direction, where k is the number of poles of $G(s)$ with positive real parts.

(ii) If $0 = \underline{\delta} < \overline{\delta}$, $G(s)$ is Hurwitz and the Nyquist plot of $G(j\omega)$ lies to the right of the vertical line defined by $\mathrm{Re}[s] = -1/\overline{\delta}$.

(iii) If $\underline{\delta} < 0 < \overline{\delta}$, $G(s)$ is Hurwitz and the Nyquist plot of $G(j\omega)$ lies in the interior of the disk $D(\underline{\delta}, \overline{\delta})$.

If the sector condition is satisfied only on an interval $[\underline{y}, \overline{y}]$, then the foregoing conditions ensure that the system is absolutely stable with a finite domain.

An important feature of the Nyquist plot is that by raising the frequency response curve of the system from experimental data, one can investigate the absolute stability of the system. On the other hand, for the multivariable case, the stability can be verified by analytical means through the conditions stated in the following lemma.

Lemma 1 (Kalman-Yakubovich-Popov Lemma. (KHALIL, 2002))**.** *Let $Z(s) = \overline{C}(sI - \overline{A})^{-1}\overline{B} + \overline{D}$ be a $m \times m$ transfer function matrix, where $\overline{A}$ is Hurwitz, $(\overline{A}, \overline{B})$ is controllable, and $(\overline{A}, \overline{C})$ is observable. Then $Z(s)$ is strictly positive real if and only if there exist a positive symmetric matrix P, matrices W and L and a positive constant ε such that*

$$P\overline{A} + \overline{A}^T P = -L^T L - \varepsilon P \tag{9}$$

$$P\overline{B} = \overline{C}^T - L^T W \tag{10}$$

$$W^T W = \overline{D} + \overline{D}^T. \tag{11}$$

If these conditions hold for $Z(s) = [I + \overline{\Delta}G(s)]$, then it can be shown that a quadratic Lyapunov function $V(x) = x^T P x$ certifies the asymptotic stability of the origin of the system (5), with $D = 0$, for nonlinearity ϕ that belongs to a sector $[0, \overline{\Delta}]$ as given in (6). In the case that ϕ satisfies the sector condition only for $y \in \mathcal{Y}_0 \subset \mathbb{R}^m$, then the previous analysis is valid only in a neighbourhood of the origin. In what follows, we present the second frequency-based approach denominated Popov Criterion.

2.2.1.2 *Popov Criterion*

Consider a particular case of system (5), given by

$$\begin{cases} \dot{x} &= Ax + Bz \\ y &= Cx \\ z_i &= -\phi_i(y_i), \end{cases} \tag{12}$$

$i = 1, \ldots, m$, where $x \in \mathbb{R}^n$, $z \in \mathbb{R}^m$, $y \in \mathbb{R}^m$, (A, B) is controllable, (A, C) is observable, $\phi_i : \mathbb{R} \to \mathbb{R}$ is a locally Lipschitz memoryless nonlinearity that belongs to the sector $[0, \overline{\delta}_i]$. The transfer function $G(s) = C(sI - A)^{-1}B$ is strictly proper and ϕ is time invariant and decoupled, that is, $\phi_i(y) = \phi_i(y_i)$. Then, we present the Popov Criterion, given by *Theorem 3*.

Theorem 3 (Popov Criterion (KHALIL, 2002))**.** *The system (12) is absolutely stable if, for* $1 \leq i \leq m$, $\phi_i \in [0, \overline{\delta}_i]$, $0 < \overline{\delta}_i \leq \infty$, *there exists a constant* $\lambda_i \geq 0$, *with* $(1 + \sigma_k \lambda_i) \neq 0$ *for every eigenvalue* σ_k *of* A, *such that* $M + (I + s\Lambda)G(s)$ *is strictly positive real, where* $\Lambda = diag(\lambda_1, \ldots, \lambda_m)$ *and* $M = diag(1/\overline{\delta}_1, \ldots, 1/\overline{\delta}_m)$. *If the sector condition* $\phi_i \in [0, \overline{\delta}_i]$ *is satisfied only on a set* $\mathcal{Y}_0 \subset \mathbb{R}^m$, *then the foregoing conditions ensure that the system is absolutely stable with a finite domain.*

Considering the scalar case $m = 1$, the SPR of $Z(s) = (1/\overline{\delta}) + (1 + s\lambda)G(s)$ can be verified graphically. From *Lemma 14* (see the Appendix), $Z(s)$ is SPR if

$$\frac{1}{\overline{\delta}} + \mathrm{Re}[G(j\omega)] - \lambda\omega \mathrm{Im}[G(j\omega)] > 0, \quad \forall \omega \in [-\infty, \infty], \tag{13}$$

where $G(j\omega) = \mathrm{Re}[G(j\omega)] + j\mathrm{Im}[G(j\omega)]$. If the plot of $\mathrm{Re}[G(j\omega)]$ versus $\omega\mathrm{Im}[G(j\omega)]$, with ω as a parameter, lies to the right of the the line intercepting the point $(-1/\overline{\delta})$ with a slope $1/\lambda$, then condition (13) is satisfied. The graphical representation of the Popov Criterion is illustrated in Fig. 5.

Figure 5: Representation of the Popov Criterion.

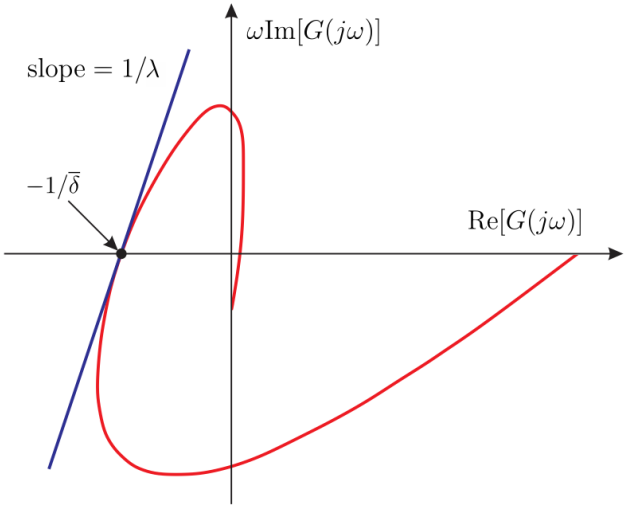

Font: Adapted from (KHALIL, 2002).

Note that the axis of the Popov plot are different from those of the Nyquist plot. If condition (13) is satisfied only for the open interval $\omega \in (-\infty, \infty)$, while the left-hand side approaches zero as $\omega \to \infty$, *e.g.* in the case when $\overline{\delta} = \infty$ and $G(s)$ has relative degree two, then one needs also to verify that

$$\lim_{\omega \to \infty} \omega^2 \left\{ \frac{1}{\overline{\delta}} + \mathrm{Re}[G(j\omega)] - \lambda \omega \mathrm{Im}[G(j\omega)] \right\} > 0. \tag{14}$$

Note also that if $\lambda_i = 0$, the conditions of Circle criterion are recovered for the case $\phi \in [0, \overline{\delta}]$. From the KYP Lemma, $M + (I + s\Lambda)G(s)$ is SPR if and only if there exists a positive definite symmetric matrix P, matrices W and L and a positive constant ε, such that

$$PA + A^T P = -L^T L - \varepsilon P \tag{15}$$

$$PB = (C + \Lambda CA)^T - L^T W \tag{16}$$

$$W^T W = 2M + \Lambda CB + B^T C^T \Lambda. \tag{17}$$

In particular, if (15)-(17) holds, the asymptotic stability of the system (12) is certified by the Lyapunov function $V = (1/2)x^T Px + \sum_{i=1}^{m} \lambda_i \int_0^{y_i} \phi_i(s)\mathrm{d}s$, which is known as a Lure-Postnikov function. In the case that ϕ satisfies the sector condition only for $y \in \mathcal{Y}_0 \subset \mathbb{R}^m$, then the previous analysis is valid only in a neighbourhood of the origin.

However, despite the importance of both Circle and Popov approaches, they are not suitable to deal with more complex formulations, such as, for example, the introduction of the sampling effect or uncertainties on Lure systems. In the sequence, we present a brief discussion of the Lyapunov-based approaches, which are more flexible in this sense.

2.2.1.3 Lyapunov-Based Approaches

Alternatively to the frequency-based approaches provided for instance by the Circle and Popov criteria, one can use the Lyapunov's theory to determine if the origin of the Lure system is absolutely stable. Here, we refer to the Lyapunov's direct method, which consists in searching for a Lyapunov function such that the stability of the nonlinear system can be assessed (for more details, see the appendix).

For this, consider a continuous-time system given, for example, by (5) and let $V : \mathcal{D}_x \to \mathbb{R}^+$ be a continuously differentiable function defined in a domain $\mathcal{D}_x \subset \mathbb{R}^n$ that contains the origin, with $V(0) = 0$ and $V(x) > 0$ in $\mathcal{D}_x - \{0\}$. If the time derivative of V in respect to time denoted by $\dot{V}(x)$ is negative, then V will decrease along the solutions of the system. From this, we conclude that if $\dot{V} \leq 0$ in $\mathcal{D}_x$, then $x = 0$ is stable. Moreover, if $\dot{V} < 0$, then $x = 0$ is asymptotically stable. If these conditions are satisfied, then this function is a Lyapunov function. Note, however, that the existence of a LF provides only sufficient, not necessary conditions for stability. For the case when $\mathcal{D}_x = \mathbb{R}^n$, then there is an interest in study global stability properties of the system. Otherwise, when

global stability can not be assessed, then the analysis of stability is focused only for a region in the neighbourhood of the origin. Moreover, the sector conditions are frequently incorporated in the inequalities $V(x) > 0$ and $\dot{V}(x) < 0$ through S-Procedure (see the Appendix) as done in (CASTELAN; TARBOURIECH; QUEINNEC, 2008), aiming to satisfy them only for nonlinearities ϕ that belongs to the sector, allowing to obtain less conservative and numerically tractable conditions.

In this context, different classes of LFs have been considered to study Lure systems, like quadratic ones (KHALIL, 2002), (CASTELAN; TARBOURIECH; QUEINNEC, 2008), (GOMES DA SILVA JR *et al.*, 2013), quadratic functions with respect to the state, with crossed terms between the state and the nonlinearity (GONZAGA; JUNGERS; DAAFOUZ, 2012), Lure-Postnikov LFs (HADDAD; KAPILA, 1995), (PARK; BANJERDPONGCHAI; KAILATH, 1998), (PARK, 2002), Lure-Postnikov LFs with components on both the states and nonlinearities (SUYKENS; VANDEWALLE; DE MOOR, 1998), (TURNER; KERR, 2014), composite LFs (HU; HUANG; LIN, 2004) and generalized Lure function (VALMORBIDA; DRUMMOND; DUNCAN, 2018).

It is desirable that for a given function, stability and stabilization conditions can be formulated as convex optimization problems. As observed in most of the works mentioned above, the stability constraints are generally written as linear matrix inequalities, which are convex on the decision variables, and therefore can be easily solved numerically through Semi-Definite Programming (SDP) tools. It should, however, be highlighted that the derived conditions are applied to continuous-time systems or discrete-time ones. For systems with sampled-data control, new approaches are required for a formal stability assessment.

In what follows, we give a brief review on the works concerning sampled-data Lure systems, which are the focus of this dissertation, highlighting the main points of each approach. In (HAO; ZHAO, 2010) and (ZENG *et al.*, 2011), the stability of a Lure system with time-varying network-induced delays is assessed through a Lyapunov-Krasovskii functional-based method, which requires the positivity of the quadratic part and does not take into account informations about the nonlinearity as well its possible slope restrictions. These works employs a state-feedback law delayed in time. In (LOUIS; JUNGERS; DAAFOUZ, 2015), the stability issue of Lure systems governed by a control law stabilising their forward Euler approximate model is investigated. Although the obtained conditions are LMIs, this approach is limited to periodic control updates. In (SEIFULLAEV; FRADKOV, 2013), the authors derive stability conditions by using a Lyapunov-Krasovskii functional and a state feedback sampled-data control law in the framework of the input-delay approach. The cases of both periodic and aperiodic sampling are covered, and conditions for exponential stability are provided. An extension of the results regarding uncertain systems is given in (SEIFULLAEV; FRADKOV, 2016) and in (SEIFULLAEV; FRADKOV, 2015), the authors use an approach from the standpoint of systems

passification, with control by static output feedback.

Finally, in (ZANI; FLORES; GOMES DA SILVA JR., 2018) the authors conducted a study on the master-slave synchronization problem of chaotic Lure systems subject to aperiodic sampled-data control with nonlinearities described by a piecewise-linear function. Stability conditions are derived by using similar theoretical tools to those will be employed in this work, such as a Lure-type functions and looped-functionals. However, we emphasize that this work cover a wider class of nonlinearities, also differing in the consideration of the slope restrictions, which allow us to incorporate new terms on the functional. Combining this with the use of a generalized Lure-type function (which will be applied for the first time for stability analysis of sampled-data controlled Lure systems), less restrictive conditions can be obtained, thus potentially reducing the conservatism of the approach.

2.3 Final Comments

The literature review presented in this chapter assists to understand how stability analysis is generally assessed by considering a particular class of nonlinear systems denominated Lure systems. Modelling techniques and approaches are presented and discussed.

However, as exposed in the previous sections, few studies regarding the stability and stabilization of sampled-data controlled Lure systems with aperiodic control updates have been conducted. Motivated by the above facts, our contributions will stand on the development of new stability conditions in the looped-functional framework.

The contents of the next chapters are composed of these contributions, starting from the representation of the Lure system in the sampled-data context. Based on a generalized Lure function, a particular looped-functional and a generic control law that consider the feedback of both the states and the nonlinearities, preliminary results are presented in Chapter 3, which leads to stability and stabilization conditions in both global and regional contexts in the further chapters.

3 PROBLEM FORMULATION AND PRELIMINARIES

3.1 Introduction

This chapter will present the mathematical formulation of a sampled-data controlled Lure system composed of an LTI plant evolving in continuous-time, with nonlinearities assumed to be both sector and slope restricted. In the sampled-data context, the signals of the plant are acquired at periodic or aperiodic time intervals and then sent to a digital controller, which delivers inputs that are held constant between two successive sampling instants to the Lure system aiming its stabilization. More specifically, we are interested in the case where the admissible variation of the sampling instants are delimited by a lower and an upper bound.

Regarding the studied Lure system, we present conditions to guarantee the existence and uniqueness of a solution for the algebraic loop contained in the argument of the nonlinearity and we recall the classical sector conditions, which are useful for incorporating the sector and slope restrictions into the analysis. These are fundamental elements to introduce the looped-functional approach that will allow us to assess the stability of the sampled-data Lure system. From the above mentioned, we provide base theorems for assessing the stability of the sampled-data closed-loop system in both global and regional contexts. Finally, in order to derive testable conditions in the next chapters, we introduce a new class of looped-functionals that takes into account the Lure nonlinearity and recall the generalized Lure function proposed in (VALMORBIDA; DRUMMOND; DUNCAN, 2018).

3.2 Problem Formulation

Consider the continuous-time plant described by the following Lure system:

$$\begin{cases} \dot{x}(t) = Ax(t) + B_u u(t) + B_\phi \phi(y(t)) \\ y(t) = Cx(t) + D_\phi \phi(y(t)) \end{cases}, \tag{18}$$

where $x \in \mathbb{R}^n$ represents the states of the plant, $u \in \mathbb{R}^q$ represents the control input and $y \in \mathbb{R}^m$ is the argument of the nonlinearity ϕ. Matrices $A \in \mathbb{R}^{n\times n}$, $B_u \in \mathbb{R}^{n\times q}$,

$B_\phi \in \mathbb{R}^{n\times m}$, $C \in \mathbb{R}^{m\times n}$, $D_\phi \in \mathbb{R}^{m\times m}$ are known and constant.

The nonlinearity $\phi : \mathcal{Y} \to \mathbb{R}^m$, $\mathcal{Y} \subseteq \mathbb{R}^m$ is assumed to be time-invariant, memoryless, Lipschitz on $\mathcal{Y}$, decentralized, sector bounded and slope restricted, *i.e.*, $\phi(y) = [\phi_1(y_1), \ldots, \phi_m(y_m)]^T$, with $\phi_i(y_i)$ satisfying, $\forall i = 1, \ldots, m$:

$$\phi_i(0) = 0 \tag{19a}$$

$$\frac{\phi_i(y_i)}{y_i} \in [\underline{\delta}_i, \overline{\delta}_i], \ \ \forall y \in \mathcal{Y}_0 \subseteq \mathcal{Y} \tag{19b}$$

$$\partial\phi_i(y_i) \in [\underline{\gamma}_i, \overline{\gamma}_i], \ \ \forall y \in \mathcal{Y}_0 \subseteq \mathcal{Y}, \tag{19c}$$

where $\underline{\delta}_i \in \mathbb{R}$, $\overline{\delta}_i \in \mathbb{R}$, $\underline{\delta}_i \leq \overline{\delta}_i$ are, respectively, the lower and upper sector bounds for the ith nonlinearity and $\underline{\gamma}_i \in \mathbb{R}$, $\overline{\gamma}_i \in \mathbb{R}$, $\underline{\gamma}_i < \overline{\gamma}_i$ are, respectively, the lower and upper slope bounds for the ith nonlinearity. From these bounds, denote $\underline{\Delta} \triangleq \text{diag}(\underline{\delta}_1, \ldots, \underline{\delta}_m)$, $\overline{\Delta} \triangleq \text{diag}(\overline{\delta}_1, \ldots, \overline{\delta}_m)$, $\underline{\Gamma} \triangleq \text{diag}(\underline{\gamma}_1, \ldots, \underline{\gamma}_m)$ and $\overline{\Gamma} \triangleq \text{diag}(\overline{\gamma}_1, \ldots, \overline{\gamma}_m)$ to express the sector and slope conditions in matrix format. The Lipschitz assumption on ϕ implies that $\partial\phi_i(y_i) = \frac{\mathrm{d}\phi_i}{\mathrm{d}y_i}$ almost everywhere, relaxing the requirement for the nonlinearity to be continuously differentiable.

We suppose that the control signal u is computed by a digital controller and is updated at sampling instants denoted by t_k, remaining constant between two successive sampling instants through a zero-order holder (ZOH). In particular, we consider the following sampled-data control law:

$$u(t) = K_x x(t_k) + K_\phi \phi(y(t_k)), \ \ \forall t \in [t_k, t_{k+1}), \tag{20}$$

where $K_x \in \mathbb{R}^{q\times n}$, $K_\phi \in \mathbb{R}^{q\times m}$. At the sampling time t_k, $k \in \mathbb{N}$, the plant state $x(t_k)$ is sent to the controller and the control law is computed. Then, the control signal is sent back to the plant to be used as soon as it arrives. Note that $\phi(y(t_k))$ can be obtained by solving the implicit equation $y(t_k) - D_\phi\phi(y(t_k)) = Cx(t_k)$, which will be detailed in the sequence.

We consider the generic case of aperiodic sampling, and we assume that there exist two positive scalars $\mathcal{T}_1 \leq \mathcal{T}_2$, such that the difference between two successive sampling instants $T_k = t_{k+1} - t_k$ satisfies

$$0 < \mathcal{T}_1 \leq T_k \leq \mathcal{T}_2, \ \ \forall k \in \mathbb{N}. \tag{21}$$

Thus, $\{t_k\}_{k\in\mathbb{N}}$ is an increasing sequence of positive scalars such that $\bigcup_{k\in\mathbb{N}}[t_k, t_{k+1}) = [0, +\infty)$. Note that the periodic sampling appears as a particular case, in which T_k must have the same value $\forall k \in \mathbb{N}$, *i.e.*, $T_k = \mathcal{T}_1 = \mathcal{T}_2$, $\forall k$. In a networked control context, the bounds $\mathcal{T}_1$ and $\mathcal{T}_2$ can represent, for instance, network conditions that can affect sampling rate, *e.g.* lag induced by computer operating system or communication protocol.

Figure 6 shows a block diagram of the controlled system.

Figure 6: Structure of the closed-loop system, $\forall t \in [t_k, t_{k+1})$.

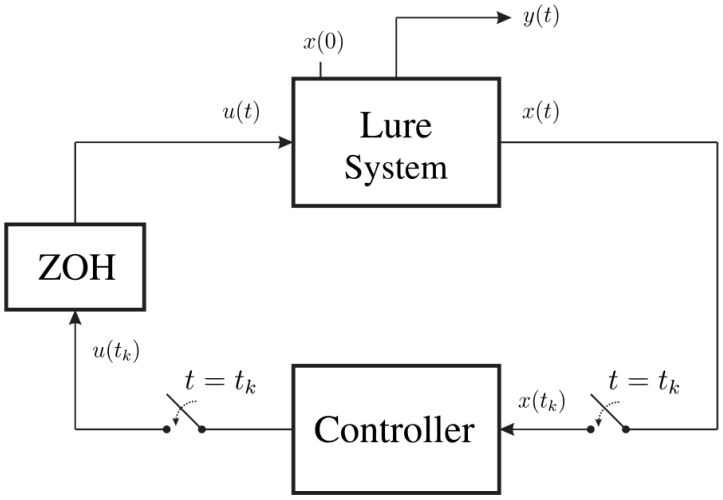

Font: Author.

Remark 2. *Note that the generic control law (20) allows to use information about the nonlinearities (CASTELAN; TARBOURIECH; QUEINNEC, 2008) through the term $K_\phi\phi$. As we assume that the states can be measured and ϕ is a function of x, if the nonlinearities are known they can be directly evaluated by the controller by solving the implicit equation in (18), thus obtaining $\phi(y(t_k))$. However, if the nonlinearities are unknown or cannot be measured, the control law becomes simply a linear state-feedback, i.e., $K_\phi = 0$.*

3.2.1 Algebraic Loop

From system (18), note that the second equation is an implicit one, as we consider that y depends also on $\phi(y)$ if $D_\phi \neq 0$, which characterizes an algebraic loop. The well-posedness of this algebraic loop is guaranteed if there exists a unique solution to the implicit equation $F(y) \triangleq y - D_\phi\phi(y) = Cx$, that is, a mapping $y(Cx)$ satisfying $F(y(Cx)) = Cx$. In (VALMORBIDA; DRUMMOND; DUNCAN, 2018) it is shown that for functions ϕ that are differentiable almost everywhere, a condition for the algebraic loop to be well-posed is that the Jacobian of $F(y)$, $JF(y) = I - D_\phi\partial\phi(y)$, belongs to a compact and convex set of invertible (nonsingular) matrices for almost all values of y.

Given the slope restriction of ϕ in (19c) for almost all y, we have that $JF(y) \in \mathcal{M} \triangleq \overline{\text{co}}(\{I - D_\phi\Gamma, \Gamma \in \mathcal{G}\})$, where

$$\mathcal{G} \triangleq \{\Gamma \in \mathbb{D}^m : \Gamma = \text{diag}(\gamma_1,\gamma_2,\ldots,\gamma_m),\gamma_i \in [\underline{\gamma}_i, \overline{\gamma}_i], \forall i\}.$$

From the above, we have that the set $\mathcal{M}$ is convex and compact. The following proposition provides conditions for the matrices in the set $\mathcal{M}$ to be nonsingular, thus guaranteeing that the solution to the algebraic loop exists and is unique.

Proposition 1. *(VALMORBIDA; DRUMMOND; DUNCAN, 2018). Assume that* $(I - D_\phi \underline{\Gamma})$ *is nonsingular. If there exists a matrix* $N \in \mathbb{D}^m_{\succeq 0}$*, such that*

$$2N - \mathrm{He}\{N(I - D_\phi \underline{\Gamma})^{-1} D_\phi(\overline{\Gamma} - \underline{\Gamma})\} \succ 0,$$

then the algebraic loop $F(y) = y - D_\phi \phi(y) = Cx$ *is well-posed for all matrices* Γ *belonging to the set* $\mathcal{G}$*.*

Proof. If $(I - D_\phi \Gamma)$ is singular, then there exists $z \in \mathbb{R}^m$, $z \neq 0$ such that

$$\begin{aligned} 0 = (I - D_\phi \Gamma)z &= ((I - D_\phi \underline{\Gamma}) - D_\phi(\Gamma - \underline{\Gamma}))z \\ &= (I - D_\phi \underline{\Gamma})z - (D_\phi(\overline{\Gamma} - \underline{\Gamma})(\overline{\Gamma} - \underline{\Gamma})^{-1}(\Gamma - \underline{\Gamma}))z. \end{aligned}$$

Define $\overline{z} \triangleq (\overline{\Gamma} - \underline{\Gamma})^{-1}(\Gamma - \underline{\Gamma})z$ to obtain

$$(I - D_\phi \underline{\Gamma})[z - (I - D_\phi \underline{\Gamma})^{-1} D_\phi(\overline{\Gamma} - \underline{\Gamma})\overline{z}] = 0.$$

Multiply the above expression on the left by $\overline{z}^T N(I - D_\phi \underline{\Gamma})^{-1}$ to obtain

$$\overline{z}^T N z - \overline{z}^T N(I - D_\phi \underline{\Gamma})^{-1} D_\phi(\overline{\Gamma} - \underline{\Gamma})\overline{z} = 0. \tag{22}$$

Since for $\underline{\gamma}_i \leq \gamma_i < \overline{\gamma}_i$, $0 \leq (\overline{\gamma}_i - \underline{\gamma}_i)^{-1}(\gamma_i - \underline{\gamma}_i) \leq 1$ and as $\overline{\Gamma}$, $\underline{\Gamma}$, Γ and N are diagonal matrices, we have

$$\overline{z}^T N z = z^T(\overline{\Gamma} - \underline{\Gamma})^{-1}(\Gamma - \underline{\Gamma}) N z \geq z^T(\overline{\Gamma} - \underline{\Gamma})^{-2}(\Gamma - \underline{\Gamma})^2 N z = \overline{z}^T N \overline{z}. \tag{23}$$

Thus, if $(I - D_\phi \Gamma)$ is singular, by combining (22) and (23) we must have

$$\overline{z}^T \left(N - \frac{1}{2}\mathrm{He}\left\{ N(I - D_\phi \underline{\Gamma})^{-1} D_\phi(\overline{\Gamma} - \underline{\Gamma}) \right\} \right) \overline{z} \leq 0,$$

which contradicts the inequality of the claim. Hence, if the inequality in the claim holds, the matrix $(I - D_\phi \Gamma)$ is nonsingular for any $\Gamma \in \mathcal{G}$. □

Provided *Proposition 1* holds, we can define the following set

$$\mathcal{X}_0 = \{x \in \mathbb{R}^n \mid y \in \mathcal{Y}_0, F(y) = Cx\}, \tag{24}$$

where $\mathcal{Y}_0 \subseteq \mathcal{Y} \subseteq \mathbb{R}^m$ corresponds to the set where the sector and slope restrictions defined in (19) holds. If the sector (19b) and slope bounds (19c) hold globally, *i.e.*, $\mathcal{Y}_0 = \mathbb{R}^m$, global properties are obtained by setting $\mathcal{X}_0 = \mathbb{R}^n$.

3.2.2 Sector Conditions

In this subsection, we present the inequalities verified by the sector and slope bounded nonlinearity. The classical sector condition presented in *Definition 1* is very convenient to use in the analysis of stability of nonlinear systems, due to the fact that it can be easily incorporated into LMIs restrictions, *e.g.* as demonstrated in (ARCAK; LARSEN; KOKOTOVIĆ, 2003), (CASTELAN; TARBOURIECH; QUEINNEC, 2008) and (VALMORBIDA; DRUMMOND; DUNCAN, 2018). From this, define $S_\Delta : \mathbb{R}^{m\times m}\times\mathbb{R}^m\times\mathbb{R}^m \to \mathbb{R}$, $S_\Gamma : \mathbb{R}^{m\times m} \times \mathbb{R}^m \times \mathbb{R}^m \to \mathbb{R}$ as

$$S_\Delta(U, \phi(\kappa), \kappa) \triangleq (\phi(\kappa) - \underline{\Delta}\kappa)^T U(\overline{\Delta}\kappa - \phi(\kappa))$$
$$S_\Gamma(U, \dot{\phi}(\kappa), \dot{\kappa}) \triangleq (\dot{\phi}(\kappa) - \underline{\Gamma}\dot{\kappa})^T U(\overline{\Gamma}\dot{\kappa} - \dot{\phi}(\kappa)).$$

Then, we state the following lemmas:

Lemma 2. *(KHALIL, 2002). If $U_1 \in \mathbb{D}^m_{\geq 0}$ and $\phi : \mathcal{Y} \to \mathbb{R}^m$, $\mathcal{Y} \subseteq \mathbb{R}^m$, satisfies (19), then*

$$S_\Delta(U_1, \phi(\kappa), \kappa) \geq 0, \tag{25}$$

for all $\kappa \in \mathcal{Y}_0 \subseteq \mathcal{Y}$.

Lemma 3. *(VALMORBIDA; DRUMMOND; DUNCAN, 2018). If $U_2 \in \mathbb{D}^m_{\geq 0}$ and $\phi : \mathcal{Y} \to \mathbb{R}^m$, $\mathcal{Y} \subseteq \mathbb{R}^m$, satisfies (19), then*

$$S_\Gamma(U_2, \dot{\phi}(\kappa), \dot{\kappa}) \geq 0, \tag{26}$$

almost everywhere for $\kappa \in \mathcal{Y}_0 \subseteq \mathcal{Y}$.

We emphasize that these inequalities will play a very important role to obtain conditions to assess the stability of the closed-loop system (18)-(20).

3.3 Preliminary Results

In this section, we address the Lure problem through a looped-functional approach for sampled-data systems, aiming to assess the stability of the origin of the system (18) with the sampled-data control law (20). For this, two main theorems are presented, which provide sufficient conditions to guarantee the asymptotic stability of the origin of the SDC system, in a global and regional context, respectively. These theorems are inspired in the works of (SEURET, 2012) and (SEURET; GOMES DA SILVA JR., 2012), and focuses on the interconnections between the discrete and continuous-time Lyapunov theorems, as sampled-data systems are naturally at the boundary of these two theories.

It is shown that if the time derivative of a positive function along the trajectories of the continuous-time model is strictly negative, then a function V is strictly decreasing for the

discrete-time asynchronous system. Differently from the Lyapunov-Krasovskii based approches, adopted for instance in (FRIDMAN; SEURET; RICHARD, 2004), (NAGHSHTABRIZI; HESPANHA; TEEL, 2008), (FRIDMAN, 2010), this approach does not require the positivity-definiteness of the functional for the global case.

3.3.1 Looped-Functional Approach

Define, as in (SEURET, 2012), $x_k(\tau) \triangleq x(t_k + \tau)$, $y_k(\tau) \triangleq y(t_k + \tau)$ and $\phi_k(\tau) \triangleq \phi(y_k(\tau))$. Hence, the closed-loop behavior in the interval $[t_k,\, t_{k+1})$ can be described by:

$$\begin{cases} \dot{x}_k(\tau) = Ax_k(\tau) + B_\phi\phi_k(\tau) + B_u(K_x x_k(0) + K_\phi\phi_k(0)) \\ y_k(\tau) = Cx_k(\tau) + D_\phi\phi_k(\tau), \qquad\qquad \forall\tau \in [0, T_k), \end{cases} \tag{27}$$

where $\dot{x}_k(\tau) = \frac{\mathrm{d}}{\mathrm{d}\tau}x_k(\tau)$. In this representation, we introduce the variable τ, which expresses the behavior of the closed-loop system between successive sampling instants. When a update of the control arises, then τ is set to zero and then evolves continuously in time until the next sampling t_{k+1}. Fig. 7 illustrates the evolution of τ for periodic sampling ($T_k \in [2.0, 2.0]$) and aperiodic sampling ($T_k \in [0.001, 2.0]$).

Figure 7 – Evolution of the variable τ: (a) periodic sampling case (b) aperiodic sampling case.

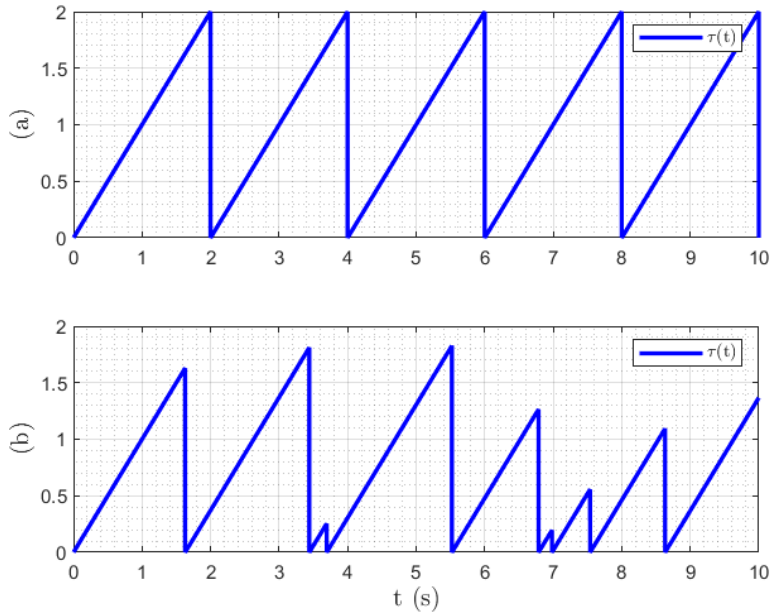

Font: Author.

Using representation (27), and inspired by the results in (SEURET; GOMES DA SILVA JR., 2012) for linear sampled-data control systems subject to actuator saturation, we state the following theorem regarding the looped-functional approach that allows to assess the closed-loop stability of a Lure-type system.

Theorem 4. *Consider system (18), with (19) being satisfied $\forall y \in \mathbb{R}^m$, and the control law (20), with T_k satisfying (21). Let $V : \mathbb{R}^n \to \mathbb{R}^+$ be a differentiable function for which there exist real numbers $\mu_1, \mu_2 > 0$ and $p > 1$ such that*

$$\mu_1 \|x\|^p \leq V(x) \leq \mu_2 \|x\|^p, \ \forall x \in \mathbb{R}^n, \tag{28}$$

and let $\mathcal{W}_0 : [0, \mathcal{T}_2] \times \mathbb{K}_{\mathcal{T}_2} \times [\mathcal{T}_1, \mathcal{T}_2] \to \mathbb{R}$ be a continuous and differentiable functional, which satisfies for all $z(\cdot) \in \mathbb{K}_{\mathcal{T}_2}$[1] and for all $T_k \in [\mathcal{T}_1, \mathcal{T}_2]$

$$\mathcal{W}_0(T_k, z(\cdot), T_k) = \mathcal{W}_0(0, z(\cdot), T_k). \tag{29}$$

Then, if

$$\dot{W}(\tau, x_k, T_k) = \frac{\mathrm{d}}{\mathrm{d}\tau}[V(x_k(\tau)) + \mathcal{W}_0(\tau, x_k, T_k)] < 0, \tag{30}$$

$\forall k \in \mathbb{N}$, $T_k \in [\mathcal{T}_1, \mathcal{T}_2]$ and $\tau \in [0, T_k)$ along the trajectories of (27), it follows that

- *(i) $\Delta V(k) = V(x_{k+1}(0)) - V(x_k(0)) = V(x(t_{k+1})) - V(x(t_k))) < 0$, $\forall k \in \mathbb{N}$, $T_k \in [\mathcal{T}_1, \mathcal{T}_2]$;*
- *(ii) The origin of the nonlinear closed-loop system composed by (18) and the sampled-data control law (20) is globally asymptotically stable (GAS), i.e., it follows that $x(t) \to 0$ as $t \to \infty$, $\forall x(0) \in \mathbb{R}^n$.*

Proof. First note that, by continuity of the system trajectories $x_k(T_k) = x_{k+1}(0)$. Integrating now (30) in the interval $[0,T_k]$ and using (29), we conclude that this inequality implies that $\Delta V(k) = V(x_{k+1}(0)) - V(x_k(0)) = V(x(t_{k+1})) - V(x(t_k)) < 0, \forall k \in \mathbb{N}$. Thus, we can conclude that $x_k(0) = x(t_k) \to 0$ as $k \to \infty$.

To conclude the proof, we need to show that $x(t)$ is uniformly bounded $\forall t \in [t_k, t_{k+1})$, $\forall k$, and that the continuous-time trajectories also converge to the origin, *i.e.*, $x(t) \to 0$ as $t \to \infty$. For this, note that as $\frac{\phi_i(y_i)}{y_i} \in [\underline{\delta}_i, \overline{\delta}_i]$, it follows that, $\forall t$, there exist scalars $\alpha_i(t)$, $0 \leq \alpha_i(t) \leq 1$ such that

$$\phi_i(y_i(t)) = [\alpha_i(t)\underline{\delta}_i + (1 - \alpha_i(t))\overline{\delta}_i]y_i(t) = \upsilon_i(t)y_i(t), \tag{31}$$

with $\upsilon_i(t) \in [\underline{\delta}_i, \overline{\delta}_i]$. Thus, we can write $\phi(y(t)) = \Upsilon(\upsilon(t))y(t)$, with $\Upsilon(\upsilon(t)) = \text{diag}(\upsilon_1(t), \upsilon_2(t), \ldots, \upsilon_m(t))$, $\upsilon(t) \in \mathcal{U}_\upsilon = \{\upsilon \in \mathbb{R}^m | \underline{\delta}_i \leq \upsilon_i \leq \overline{\delta}_i, \ i = 1, \ldots, m\}$. In this case, as the algebraic loop is supposed to be well-posed, we have $y(t) = Cx(t) + D_\phi \Upsilon(t)y(t)$, or equivalently

$$y(t) = (I - D_\phi \Upsilon(\upsilon(t)))^{-1} Cx(t). \tag{32}$$

[1] We recall from the notations, that $\mathbb{K}_{\mathcal{T}_2}$ is the set of continuous functions from an interval $[0, \mathcal{T}_2]$ to $\mathbb{R}^n$.

Hence, the closed-loop system can be represented by the following linear time-varying system, $\forall t \in [t_k,\ t_{k+1})$

$$\dot{x}(t) = Ax(t) + B_u(K_x x(t_k) + K_\phi \phi(y(t_k))) + B_\phi \Upsilon(\upsilon(t))(I - D_\phi \Upsilon(\upsilon(t)))^{-1} Cx(t). \tag{33}$$

Considering the lifted-variables, one has

$$\dot{x}_k(\tau) = (A + B_\phi \Upsilon(\upsilon_k(\tau))(I - D_\phi \Upsilon(\upsilon_k(\tau)))^{-1} C)x_k(\tau) + B_u(K_x x_k(0) + K_\phi \phi_k(0)). \tag{34}$$

Define $\upsilon_k(\tau) \triangleq \upsilon(t_k + \tau)$. For each admissible $\upsilon_k \in \mathbb{K}_{\mathcal{T}_2}$, such that $\upsilon_k(\tau) \in \mathcal{U}_\upsilon$, define the transition matrix for the system (33) as $\Psi_{\upsilon_k}(\tau, s) \triangleq \Psi_\upsilon(t_k + \tau, t_k + s)$. Thus, it follows that

$$x_k(\tau) = \Psi_{\upsilon_k}(\tau, 0)x_k(0) + \int_0^\tau \Psi_{\upsilon_k}(\tau, s) B_u \begin{bmatrix} K_x & K_\phi \end{bmatrix} \begin{bmatrix} x_k(0) \\ \phi_k(0) \end{bmatrix} \mathrm{d}s. \tag{35}$$

Thus, we have that

$$\begin{aligned}
\|x_k(\tau)\| &\leq \|\Psi_{\upsilon_k}(\tau, 0)\|\ \|x_k(0)\| + \left\| \int_0^\tau \Psi_{\upsilon_k}(\tau, s)\mathrm{d}s \right\| \left\| B_u \begin{bmatrix} K_x & K_\phi \end{bmatrix} \begin{bmatrix} x_k(0) \\ \phi_k(0) \end{bmatrix} \right\| \\
&\leq \Bigg(\|\Psi_{\upsilon_k}(\tau, 0)\| + \left\| \int_0^\tau \Psi_{\upsilon_k}(\tau, s)\mathrm{d}s \right\| \big(\|B_u K_x\| \\
&\qquad + \|B_u K_\phi\|\ \|\Upsilon(\upsilon_k(0))(I - D_\phi \Upsilon(\upsilon_k(0)))^{-1} C\| \big) \Bigg) \|x_k(0)\| \\
&\leq \Bigg(\|\Psi_{\upsilon_k}(\tau, 0)\| + \int_0^{\mathcal{T}_2} \|\Psi_{\upsilon_k}(\tau, s)\mathrm{d}s\| \big(\|B_u K_x\| \\
&\qquad + \|B_u K_\phi \Upsilon(\upsilon_k(0))(I - D_\phi \Upsilon(\upsilon_k(0)))^{-1} C\| \big) \Bigg) \|x_k(0)\|.
\end{aligned} \tag{36}$$

As $\upsilon_k(\tau) \in \mathcal{U}_\upsilon$, $\forall \tau \in [0, \mathcal{T}_2]$, there exist a scalar μ_Ψ,

$$\mu_\Psi = \sup_{\substack{\upsilon_k \in \mathbb{K}_{\mathcal{T}_2} \\ \text{s.t. } \upsilon_k(\tau) \in \mathcal{U}_\upsilon}} \left(\|\Psi_{\upsilon_k}(\tau, 0)\| + \int_0^{\mathcal{T}_2} \|\Psi_{\upsilon_k}(\tau, s)\mathrm{d}s\| (\|B_u K_x\| + \|B_u K_\phi \mu_\upsilon\|) \right), \tag{37}$$

with $\mu_\upsilon = \max_{\upsilon \in \mathcal{U}_\upsilon} \|\Upsilon(\upsilon)(I - D_\phi \Upsilon(\upsilon))^{-1} C\|$, such that $\|x_k(\tau)\| \leq \mu_\Psi \|x_k(0)\|$. Hence, if $x_k(0) \to 0$ as $k \to \infty$, *i.e.*, $x(t_k) \to 0$ as $k \to \infty$, then $x(t_k + \tau) = x_k(\tau) \to 0$ as $k \to \infty$, $\forall \tau \in [0, T_k)$, that is $x(t) = x(t_k + \tau) \to 0$ as $t \to \infty$. □

Basically, the idea of *Theorem 4* is to ensure that a function V is strictly decreasing at the sampling instants, *i.e.*, $\Delta V(k) < 0$, $\forall k$, and that between the sampling instants the trajectories are uniformly bounded, which ensures the convergence of the continuous-time trajectories to the origin. In this case, this is achieved by ensuring the positivity of V and $\dot{W} < 0$.

A graphical illustration of the proof of *Theorem 4* is shown in Fig. 8. Observe that $\mathcal{W}_0$ decreases continually with the sequence of samplings and coincides with the function V at the sampling instants. Furthermore, the introduction of the functional allows V to be locally increasing, as it need to be decreasing only at the sampling instants.

Figure 8: Illustration of the proof of *Theorem 4*.

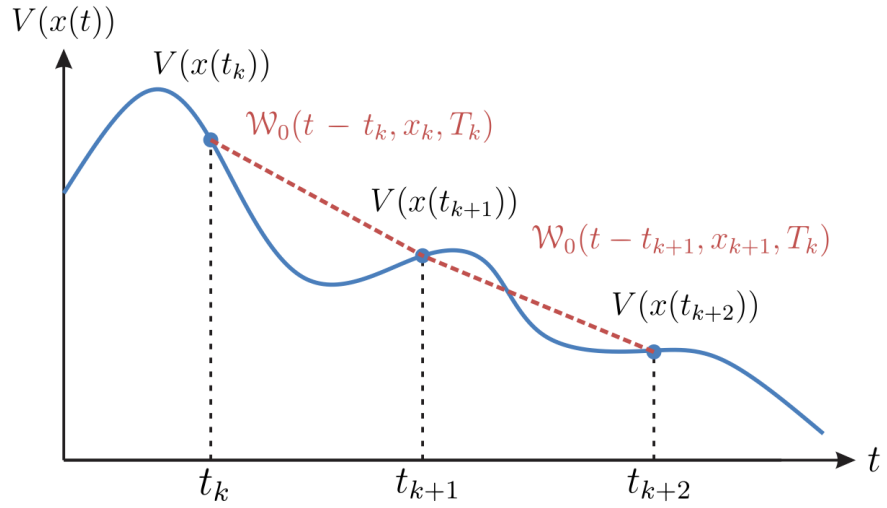

Font: Adapted from (SEURET, 2012) and (SEURET; GOMES DA SILVA JR., 2012).

When the nonlinearities does not hold the sector conditions globally, regional stability conditions are provided by the following theorem, which is similar to the ones presented in (MOREIRA *et al.*, 2019) and (PALMEIRA; GOMES DA SILVA JR; FLORES, 2020).

Theorem 5. *Consider system (18), with (19) being satisfied* $\forall y \in \mathcal{Y}_0 \subset \mathbb{R}^m$ *and* $\mathcal{Y}_0$ *as defined in (7), and the control law (20), with* T_k *satisfying (21). Consider a compact domain* $\mathcal{D}_x \subseteq \mathcal{X}_0 \subset \mathbb{R}^n$ *containing the origin and let* $V : \mathbb{R}^n \to \mathbb{R}^+$ *be a differentiable function for which there exist real numbers* $\mu_1, \mu_2 > 0$ *and* $p > 1$ *such that*

$$\mu_1 \|x\|^p \leq V(x) \leq \mu_2 \|x\|^p, \quad \forall x \in \mathcal{D}_x - \{0\}. \tag{38}$$

Let $\mathcal{L}(V, \rho) = \{x \in \mathbb{R}^n | V(x) \leq \rho\}$, *with* $\rho > 0$, *be the level sets of* V *and a continuous-time functional* $\mathcal{W}_0 : [0, \mathcal{T}_2] \times \mathbb{K}_{\mathcal{T}_2} \times [\mathcal{T}_1, \mathcal{T}_2] \to \mathbb{R}^+$, *such that*

$$\begin{aligned} &\mathcal{W}_0(0, x_k, T_k) = \mathcal{W}_0(T_k, x_k, T_k) = 0, \\ &\mathcal{W}_0(\tau, x_k, T_k) > 0, \forall \tau \in [0, T_k), \forall T_k \in [\mathcal{T}_1, \mathcal{T}_2], \forall x_k \text{ such that } x_k(\tau) \in \mathcal{D}_x - \{0\}. \end{aligned} \tag{39}$$

Define $W(\tau, x_k, T_k) = V(x_k(\tau)) + \mathcal{W}_0(\tau, x_k, T_k)$ *and let* $\dot{W}(\tau, x_k, T_k)$ *be the derivative of* $W(\tau, x_k, T_k)$ *with respect to* τ. *If the inequality*

$$\dot{W}(\tau, x_k, T_k) < 0 \tag{40}$$

is satisfied for $x_k(\tau) \in \mathcal{D}_x \subset \mathbb{R}^n$, $\forall \tau \in [0, T_k)$, $\forall T_k \in [\mathcal{T}_1, \mathcal{T}_2]$, $\forall k \in \mathbb{N}$, *then for any initial condition* $x(0) = x_0(0)$ *lying inside any level set* $\mathcal{L}(V, \rho) \subset \mathcal{D}_x$, *it follows that:*

(i) $\Delta V(k) = V(x_{k+1}(0)) - V(x_k(0)) < 0$, $\forall k \in \mathbb{N}$;

(ii) The corresponding trajectories of the closed-loop system, formed by (18) and (20) never leave $\mathcal{L}(V,\rho)$ *and converge asymptotically to the origin.*

Proof. Suppose that $x(0) = x_0(0) \in \partial\mathcal{L}(V,\rho) \subset \mathcal{D}_x$ and that (40) is satisfied. Then, it follows that

$$W(\tau, x_0, T_0) < W(0, x_0, T_0), \quad \forall \tau \in (0, T_0]. \tag{41}$$

Taking into consideration (41) and the properties of $\mathcal{W}_0$ stated in (39), it follows that $V(x_0(\tau)) < W(\tau, x_0, T_0) < W(0, x_0, T_0) = V(x_0(0))$, $\forall \tau \in (0, T_0]$, implying that $x_0(\tau) \in \mathcal{L}(V,\rho) \subset \mathcal{D}_x$, $\forall \tau \in (0, T_0]$. Now, integrating (40) over the interval $[0, T_0]$ and considering (39), one obtains that $V(x_0(T_0)) - V(x_0(0)) < 0$. Noting now by continuity of trajectories that $x_0(T_0) = x_1(0)$, we conclude that $\Delta V(0) < 0$ and thus $V(x_1(0)) < V(x_0(0))$, which implies that $V(x_1(0)) < \rho$, *i.e.*, $x_1(0) \in \partial\mathcal{L}(V,\rho_1) \subset \mathcal{L}(V,\rho)$ for some $\rho_1 < \rho$. Repeating this reasoning for $k = 1, 2, \ldots, \infty$, it follows that $\Delta V(k) < 0$, $\forall k \in \mathbb{N}$, which proves item (i). As a consequence, it follows that $\lim_{k\to\infty} x_k(0) = \lim_{k\to\infty} x(t_k) = 0$. Moreover, since $V(x_k(\tau)) < V(x_k(0))$, we conclude that $\mathcal{L}(V,\rho)$ is a positively invariant set and, as from (i) $\lim_{k\to\infty} V(x_k(0)) = 0$, we conclude that $\lim_{k\to\infty} V(x_k(\tau)) = 0$ and hence $x_k(\tau) \to 0$ for $k \to \infty$, which concludes the proof of item (ii). □

Remark 3. *Differently from Theorem 4, here we need a functional that is positive definite and satisfies* $\mathcal{W}_0(0, x_k, T_k) = \mathcal{W}_0(T_k, x_k, T_k) = 0$*, to ensure that the trajectories do not leave* $\mathcal{D}_x$ *between two sampling instants. Note however that function* V *is not required to be strictly decreasing with respect to the continuous-time trajectory, which implies that* $\mathcal{L}(V,\rho)$ *is positively invariant but not continuously contractive.*

In this work, we will use the following functional to derive the stability and stabilization conditions presented in the next chapters:

$$\begin{aligned}
\mathcal{W}_0(\tau, x_k, T_k) &= (T_k - \tau)\tau \begin{bmatrix} x_k(0) \\ \phi_k(0) \end{bmatrix}^T X \begin{bmatrix} x_k(0) \\ \phi_k(0) \end{bmatrix} \\
&+ (T_k - \tau)\left\{ \int_0^\tau \dot{x}_k^T(\theta) R_x \dot{x}_k(\theta) \mathrm{d}\theta + (x_k(\tau) - x_k(0))^T [F_x(x_k(\tau) - x_k(0)) + 2G_x x_k(0)] \right\} \\
&+ (T_k - \tau)\left\{ \int_0^\tau \dot{\phi}_k^T(\theta) R_\phi \dot{\phi}_k(\theta) \mathrm{d}\theta + (\phi_k(\tau) - \phi_k(0))^T [F_\phi(\phi_k(\tau) - \phi_k(0)) + 2G_\phi \phi_k(0)] \right\}
\end{aligned} \tag{42}$$

with $F_x \in \mathbb{S}^n$, $G_x \in \mathbb{R}^{n\times n}$, $X \in \mathbb{S}^{n+m}$, $F_\phi \in \mathbb{S}^m$, $G_\phi \in \mathbb{R}^{m\times m}$, $R_x \in \mathbb{S}^n_{\succ 0}$ and $R_\phi \in \mathbb{S}^m_{\succ 0}$. Its inspiration came from previous works in the literature. The terms F_x and G_x were

firstly introduced in the work of NAGHSHTABRIZI; HESPANHA; TEEL (2008). The integral term was considered in (FRIDMAN, 2010). The term $\tau(T_k - \tau)x_k(0)^T X x_k(0)$ was presented by (SEURET, 2012). Our contribution stands on the terms depending on the nonlinearity ϕ, which allows to take into account the slope bounds of the nonlinearities that may lead to less conservative results. Regarding the conditions for the functional stated in *Theorem 4*, since $(T_k - \tau) = 0$ when $\tau = T_k$ and $x_k(\tau) - x_k(0) = 0$ when $\tau = 0$, it follows that this functional satisfies (29). Moreover, it is continuous at all sampling instants and differentiable over $[0, T_k)$. Observe that the looped-functional approach focuses on the behavior of the intersampling intervals, *i.e.*, for $t \in [t_k, t_{k+1})$, $\forall k$, which the evolution of the closed-loop system in time is mapped to the lifted domain through the variable $\tau \in [0, T_k)$.

Finally, to evaluate the conditions stated in the previous theorems, one needs to choose a candidate function V. This subject will be discussed in the sequence.

3.3.2 Generalized Lure Lyapunov Function

Consider the generalized Lure function $V_{LG} : \mathbb{R}^n \to \mathbb{R}^+$, proposed in (VALMORBIDA; DRUMMOND; DUNCAN, 2018) and defined as follows:

$$V_{LG}(x) \triangleq V_{QG}(x) + \sum_{i=1}^{m} \lambda_i \int_0^{y_i} (\phi_i(s) - \underline{\delta}_i s)\mathrm{d}s, \tag{43}$$

where $y_i = C_i x + D_{\phi_i}\phi(y)$, $i = 1, \ldots, m$ and

$$V_{QG}(x) \triangleq \begin{bmatrix} x \\ \phi(y) \end{bmatrix}^T \begin{bmatrix} P_{11} & P_{12} \\ P_{12}^T & P_{22} \end{bmatrix} \begin{bmatrix} x \\ \phi(y) \end{bmatrix}. \tag{44}$$

This function is an extended version of the traditional Lure function, where the matrix P and the scalars λ_i (also known as Lure-Postnikov coefficients), $\Lambda \triangleq \mathrm{diag}(\lambda_1, \ldots, \lambda_i)$, $i = 1, \ldots, m$, are necessarily positive definite. Note that this form does not require the positive-definiteness of P, nor the non-negativity of the coefficients λ_i (VALMORBIDA; DRUMMOND; DUNCAN, 2018).

As discussed in (VALMORBIDA; DRUMMOND; DUNCAN, 2016) and (VALMORBIDA; DRUMMOND; DUNCAN, 2018), the function (43) is a generalization of the following LF considered in (TURNER; KERR, 2014):

$$\hat{V}(x) = \begin{bmatrix} x \\ \phi(y) \end{bmatrix}^T \hat{P} \begin{bmatrix} x \\ \phi(y) \end{bmatrix} + \sum_{j=1}^{4} \sum_{i=1}^{m} \mu_{j,i} \int_0^{y_i(x)} g_{j,i}(s)\mathrm{d}s, \tag{45}$$

where $g_{1,i}(s) \triangleq \phi_i(s)$, $g_{2,i}(s) \triangleq \overline{\delta}_i s - \phi_i(s)$, $g_{3,i}(s) \triangleq (\overline{\gamma}_i - \partial\phi_i(s))s$, $g_{4,i}(s) \triangleq \partial\phi_i(s)(\overline{\delta}_i s - \phi_i(s))$, with $\hat{P} \succ 0$ and $\mu_{j,i} \geq 0$, $i = 1, \ldots, m$, $j = 1, \ldots, 4$.

In this case, the positivity-definiteness of the function $V_{LG}(x)$ defined in (43) should be ensured by other means, as stated in the following lemma.

Lemma 4. *(VALMORBIDA; DRUMMOND; DUNCAN, 2018). Consider V_{LG} in (43) where ϕ satisfies (19a)-(19b) and Proposition 1 holds. If there exists a matrix $\tilde{\Lambda} \in \mathbb{D}^m_{\geq 0}$ such that*

$$\Lambda \succeq -\tilde{\Lambda}, \tag{46}$$

$$V_{QG}(x) - \frac{1}{2} y^T (\overline{\Delta} - \underline{\Delta}) \tilde{\Lambda} y > 0, \quad \forall x \in \mathcal{X}_0, \tag{47}$$

then $V_{LG}(x) > 0$, $\forall x \in \mathcal{X}_0 \subset \mathbb{R}^n$.

Proof. The idea is to use (46) to obtain a positive definite lower bound for (43) as follows. We assume the well-posedness of the algebraic loop for all $x \in \mathcal{X}_0$. First, note that the following relation holds:

$$\begin{aligned}
V_{LG}(x) &= V_{QG}(x) + \sum_{i=1}^{m} \lambda_i \int_0^{y_i} (\phi_i(s) - \underline{\delta}_i s) \mathrm{d}s \\
&\geq V_{QG}(x) - \sum_{i=1}^{m} \tilde{\lambda}_i \int_0^{y_i} (\phi_i(s) - \underline{\delta}_i s) \mathrm{d}s \\
&= V_{QG}(x) - \sum_{i=1}^{m} \tilde{\lambda}_i \int_0^{y_i} (\phi_i(s) - \underline{\delta}_i s) \mathrm{d}s - \frac{1}{2} y^T (\overline{\Delta} - \overline{\Delta}) \tilde{\Lambda} y \\
&= V_{QG}(x) - \sum_{i=1}^{m} \tilde{\lambda}_i \int_0^{y_i} \phi_i(s) \mathrm{d}s - \frac{1}{2} y^T (\overline{\Delta} - \overline{\Delta} - \underline{\Delta}) \tilde{\Lambda} y \\
&= V_{QG}(x) + \sum_{i=1}^{m} \tilde{\lambda}_i \int_0^{y_i} (\overline{\delta}_i s - \phi_i(s)) \mathrm{d}s - \frac{1}{2} y^T (\overline{\Delta} - \underline{\Delta}) \tilde{\Lambda} y.
\end{aligned} \tag{48}$$

Hence, from (47) and the fact that

$$\sum_{i=1}^{m} \tilde{\lambda}_i \int_0^{y_i} (\overline{\delta}_i s - \phi_i(s)) \mathrm{d}s \geq 0,$$

we can conclude that $V_{LG}(x) > 0$, provided (46) and (47) are satisfied. □

A relaxed version of *Lemma 4*, considering the coupling between x and ϕ (through y) can be stated as follows.

Lemma 5. *(VALMORBIDA; DRUMMOND; DUNCAN, 2018). Assume that (46) is satisfied. If there exist a matrix $U_0 \in \mathbb{D}^m_{\geq 0}$ such that*

$$V_{QG}(x) - \frac{1}{2} y^T (\overline{\Delta} - \underline{\Delta}) \tilde{\Lambda} y - S_\Delta(U_0, \phi, y) > 0, \tag{49}$$

then $V_{LG}(x) > 0$, $\forall x \in \mathcal{X}_0 \subset \mathbb{R}^n$.

Proof. Assume that (46) is satisfied. From *Lemma 2*, we have that if $x \in \mathcal{X}_0$, then $S_\Delta(U_0, \phi, y) \geq 0$ and thus $V_{QG}(x) - \frac{1}{2} y^T (\overline{\Delta} - \underline{\Delta}) \tilde{\Lambda} y > S_\Delta(U_0, \phi, y) \geq 0$. □

The generalized function $V_{LG}(x)$ will be used along the work to derive stability conditions. In order to show the potential advantage and the conservatism reduction induced by the generalized Lure function, we present along this work results considering particular structures of the function $V_{LG}(x)$ defined in (43) that have been used in the literature, as detailed in Table 1.

Table 1: Particular structures of the generalized Lure function.

Function	V_{LG} with
$V_Q = x^T P_{11} x$	$P_{12} = 0, P_{22} = 0, \lambda_i = 0, \forall i$
$V_{QG} = \begin{bmatrix} x \\ \phi(y) \end{bmatrix}^T \begin{bmatrix} P_{11} & P_{12} \\ P_{12}^T & P_{22} \end{bmatrix} \begin{bmatrix} x \\ \phi(y) \end{bmatrix}$	$\lambda_i = 0, \forall i$
$V_L = x^T P_{11} x + \sum_{i=1}^{m} \lambda_i \int_0^{y_i} (\phi_i(s) - \underline{\delta}_i s) \mathrm{d}s$	$P_{12} = 0, P_{22} = 0, \lambda_i > 0, \forall i$
$V_R = \begin{bmatrix} x \\ \phi(y) \end{bmatrix}^T \begin{bmatrix} P_{11} & P_{12} \\ P_{12}^T & P_{22} \end{bmatrix} \begin{bmatrix} x \\ \phi(y) \end{bmatrix} + \sum_{i=1}^{m} \lambda_i \int_0^{y_i} \phi_i(s)\, \mathrm{d}s$	$\lambda_i > 0, \underline{\delta}_i = 0, \forall i$

More specifically, we evaluate the feasibility of the inequalities such that them also hold, for instance, for a quadratic function $V_Q(x)$, for a generalized quadratic function $V_{QG}(x)$ and for a Lure-Postnikov function $V_L(x)$. Note that we also introduced the function $V_R(x)$, which will be used later to derive stabilization conditions.

3.4 Final Comments

In this chapter, it was presented a formal representation of a Lure system with sampled-data control, subject to aperiodic sampling and nonlinearities that are sector and slope restricted. We have introduced some aspects related to the sector inequalities and then we have stated the looped-functional approach, which provides sufficient conditions to assess the stability of the closed-loop system. This approach aims at linking the continuous and discrete-time Lyapunov theories, which main objective is to ensure that a positive function is strictly decreasing at the sampling instants, thus guaranteeing the convergence of the trajectories of the continuous-time system to the origin.

Based on this theoretical foundation, the main contribution from this chapter are the *Theorem 4* and the *Theorem 5*, concerning respectively to the global and local stability assessment of the closed-loop system composed by a Lure system and a sampled-data control law. Regarding these, we have introduced a novel class of functionals which main feature is on the terms that depend on the nonlinearities and their derivatives and we have presented a generalized Lure function that does not require the positivity of the quadratic part, nor of the Lure-Postnikov coefficients.

From these elements and the results of *Theorem 4* and *Theorem 5*, in the next chapters we will provide LMI conditions to analyse and synthesize sampled-data feedback laws in order to ensure the stability of the closed-loop system.

4 STABILITY ANALYSIS

4.1 Introduction

This chapter concerns the stability analysis of the sampled-data closed-loop control system presented in Fig. 6, formally expressed by

$$\begin{cases} \dot{x}(t) = Ax(t) + B_u(K_x x(t_k) + K_\phi \phi(y(t_k))) + B_\phi \phi(y(t)) \\ y(t) = Cx(t) + D_\phi \phi(y(t)) \end{cases}, \text{for } t \in [t_k, t_{k+1}). \quad (50)$$

In this case, we assume that K_x and K_ϕ are given *i.e.*, they were previously computed. Recapitulating the last chapter, *Theorem 4* and *Theorem 5* were presented to provide sufficient conditions to ensure the stability of the sampled-data controlled system, in both global and regional contexts, respectively, through a looped-functional approach. Based on these results, the idea here is to derive testable conditions in the form of linear matrix inequalities by considering a particular looped-functional defined in (42) and a generalized Lure function given in (43).

Section 4.2 addresses the stability problem through a global perspective, *i.e*, it deals with the case where the sector and slope restrictions hold globally. The obtained conditions allow to formulate optimization problems regarding the maximization of the upper intersampling bound, the maximal jitter over a nominal sampling time or the admissible sector bounds on the nonlinearities for which global stability is guaranteed.

Section 4.3 focuses on the regional stability analysis, which comprehends the case where the sector conditions hold only locally. From this, we present optimization problems in order to provide the highest estimates of the region of attraction while maximizing the upper intersampling bound, the jitter or the sector bounds.

Along this chapter, numerical examples are provided to highlight the potentialities of the method.

4.2 Global Results

In this section, we derive conditions in the form of linear matrix inequalities to assess the global asymptotic stability of the origin of the sampled-data closed-loop system (50),

under aperiodic sampling satisfying $T_k \in [\mathcal{T}_1, \mathcal{T}_2]$ and considering that the nonlinearities satisfy the sector and slope conditions given in (19) globally, *i.e.*, they hold $\forall y \in \mathbb{R}^m$. These are given by the following theorem.

Theorem 6. *For given* $0 < \mathcal{T}_1 \leq \mathcal{T}_2$*, assume that there exist matrices* $P \in \mathbb{S}^{n+m}$, $\Lambda \in \mathbb{D}^m$, $\tilde{\Lambda} \in \mathbb{D}^m_{\succeq 0}$, $U_h \in \mathbb{D}^m_{\succeq 0}$, $h = 0, \ldots, 3$, $F_x \in \mathbb{S}^n$, $G_x \in \mathbb{R}^{n\times n}$, $F_\phi \in \mathbb{S}^m$, $G_\phi \in \mathbb{R}^{m\times m}$, $R_x \in \mathbb{S}^n_{\succ 0}$, $R_\phi \in \mathbb{S}^m_{\succ 0}$, $Q_x \in \mathbb{R}^{(3n)\times n}$, $Q_\phi \in \mathbb{R}^{(3m)\times m}$, $X \in \mathbb{S}^{n+m}$, $L \in \mathbb{R}^{3(n+m)\times n}$ *that satisfy, for* $i = 1,2$*:*

$$\Psi_1(\mathcal{T}_i) = \Pi_1 + \mathcal{T}_i\Pi_2 + \mathcal{T}_i\Pi_3 \prec 0 \tag{51}$$

$$\Psi_2(\mathcal{T}_i) = \begin{bmatrix} \Pi_1 - \mathcal{T}_i\Pi_3 & \mathcal{T}_i M_{135}^T Q_x & \mathcal{T}_i M_{246}^T Q_\phi \\ \star & -\mathcal{T}_i R_x & 0 \\ \star & \star & -\mathcal{T}_i R_\phi \end{bmatrix} \prec 0 \tag{52}$$

$$\Lambda \succeq -\tilde{\Lambda} \tag{53}$$

$$P - \frac{1}{2}\begin{bmatrix} C^T \\ D_\phi^T \end{bmatrix}(\overline{\Delta} - \underline{\Delta})\tilde{\Lambda}\begin{bmatrix} C & D_\phi \end{bmatrix} + \mathrm{He}\left\{\frac{1}{2}\begin{bmatrix} (\underline{\Delta}C)^T \\ (\underline{\Delta}D_\phi - I)^T \end{bmatrix} U_0 \begin{bmatrix} \overline{\Delta}C & (\overline{\Delta}D_\phi - I) \end{bmatrix}\right\} \succ 0, \tag{54}$$

with

$$\begin{aligned}
\Pi_1 &= \mathrm{He}\{M_{12}^T P M_{34}\} - M_{15}^T F_x M_{15} - M_{26}^T F_\phi M_{26} - \mathrm{He}\{M_{26}^T G_\phi M_6\} - \mathrm{He}\{M_{15}^T G_x M_5\} \\
&\quad - \mathrm{He}\left\{\frac{1}{2}(M_1^T(\underline{\Delta}C)^T + M_2^T(\underline{\Delta}D_\phi - I)^T)\Lambda C M_3\right\} \\
&\quad - \mathrm{He}\left\{\frac{1}{2}(M_1^T(\underline{\Delta}C)^T + M_2^T(\underline{\Delta}D_\phi - I)^T)\Lambda D_\phi M_4\right\} \\
&\quad + \mathrm{He}\{M_2^T(I - (\underline{\Delta}D_\phi)^T) - M_1^T(\underline{\Delta}C)^T)U_1(\overline{\Delta}C M_1 + (\overline{\Delta}D_\phi - I)M_2)\} \\
&\quad + \mathrm{He}\{M_4^T(I - (\underline{\Gamma}D_\phi)^T) - M_3^T(\underline{\Gamma}C)^T)U_2(\overline{\Gamma}C M_3 + (\overline{\Gamma}D_\phi - I)M_4)\} \\
&\quad + \mathrm{He}\{M_6^T(I - (\underline{\Delta}D_\phi)^T) - M_5^T(\underline{\Delta}C)^T)U_3(\overline{\Delta}C M_5 + (\overline{\Delta}D_\phi - I)M_6)\} \\
&\quad - \mathrm{He}\{M_{135}^T Q_x M_{15}\} - \mathrm{He}\{M_{246}^T Q_\phi M_{26}\} + \mathrm{He}\{L M_0\} \\
\Pi_2 &= M_3^T R_x M_3 + \mathrm{He}\{M_3^T(F_x M_{15} + G_x M_5)\} + \mathrm{He}\{M_4^T(F_\phi M_{26} + G_\phi M_6)\} \\
&\quad + M_4^T R_\phi M_4 \\
\Pi_3 &= M_{56}^T X M_{56},
\end{aligned} \tag{55}$$

where[1]

$$
\begin{aligned}
M_0 &= [A \;\; B_\phi \;\; -I \;\; 0 \;\; B_u K_x \;\; B_u K_\phi] \\
M_1 &= [I \;\; 0 \;\; 0 \;\; 0 \;\; 0 \;\; 0] \qquad M_2 = [0 \;\; I \;\; 0 \;\; 0 \;\; 0 \;\; 0] \qquad M_3 = [0 \;\; 0 \;\; I \;\; 0 \;\; 0 \;\; 0] \\
M_4 &= [0 \;\; 0 \;\; 0 \;\; I \;\; 0 \;\; 0] \qquad M_5 = [0 \;\; 0 \;\; 0 \;\; 0 \;\; I \;\; 0] \qquad M_6 = [0 \;\; 0 \;\; 0 \;\; 0 \;\; 0 \;\; I] \\
M_{15} &= M_1 - M_5 \qquad M_{26} = M_2 - M_6 \\
M_{12} &= [M_1^T \;\; M_2^T]^T \qquad M_{34} = [M_3^T \;\; M_4^T]^T \qquad M_{56} = [M_5^T \;\; M_6^T]^T \\
M_{135} &= [M_1^T \;\; M_3^T \;\; M_5^T]^T \quad M_{246} = [M_2^T \;\; M_4^T \;\; M_6^T]^T.
\end{aligned}
$$

Then the origin of the sampled-data closed-loop system (50) with ϕ satisfying (19) and $T_k \in [\mathcal{T}_1, \mathcal{T}_2]$ is globally asymptotically stable.

Proof. Considering the result of *Theorem 1*, the idea is to prove that (29) and (30) are satisfied, $\forall k \in \mathbb{N}$, considering $\mathcal{W}_0$ as given in (42) and a generalized Lure-type function (43).

It is straightforward to prove that the positivity of V is implied by the inequalities (53) and (54) using *Lemma 2* and *Lemma 5*. Note that by left and right multiplying (54) by $\begin{bmatrix} x \\ \phi \end{bmatrix}^T$ and $\begin{bmatrix} x \\ \phi \end{bmatrix}$, respectively, and considering the sector conditions (19) it follows that (49) is satisfied. Furthermore, as seen in Chapter 3, the functional $\mathcal{W}_0$ given in (42) satisfies the condition (29). Moreover, it is continuous at all sampling instants and differentiable over $[0, T_k)$. The rest of the proof consists in showing that (51)-(52) imply (30). With this aim, the expression of $\dot{W} = \frac{\mathrm{d}W}{\mathrm{d}\tau}$ is given as follows:

$$
\begin{aligned}
\dot{W}(\tau, x_k, T_k) &= 2 \begin{bmatrix} x_k(\tau) \\ \phi_k(\tau) \end{bmatrix}^T P \begin{bmatrix} \dot{x}_k(\tau) \\ \dot{\phi}_k(\tau) \end{bmatrix} - [(x_k^T(\tau)(\underline{\Delta} C)^T + \phi_k^T(\tau)(\underline{\Delta} D_\phi - I)^T)\Lambda C]\dot{x_k}(\tau) \\
&- [(x_k^T(\tau)(\underline{\Delta} C)^T + \phi_k^T(\tau)(\underline{\Delta} D_\phi - I)^T)\Lambda D_\phi]\dot{\phi}_k(\tau) \\
&- (x_k(\tau) - x_k(0))^T[F_x(x_k(\tau) - x_k(0)) + 2G_x x_k(0)] + (T_k - 2\tau) \begin{bmatrix} x_k(0) \\ \phi_k(0) \end{bmatrix}^T X \begin{bmatrix} x_k(0) \\ \phi_k(0) \end{bmatrix} \\
&+ (T_k - \tau)\dot{x}_k^T(\tau)[R_x \dot{x}_k(\tau) + 2F_x(x_k(\tau) - x_k(0)) + 2G_x x_k(0)] - \int_0^\tau \dot{x}_k^T(\theta) R_x \dot{x}_k(\theta) \mathrm{d}\theta \\
&- (\phi_k(\tau) - \phi_k(0))^T[F_\phi(\phi_k(\tau) - \phi_k(0)) + 2G_\phi \phi_k(0)] \\
&+ (T_k - \tau)\dot{\phi}_k^T(\tau)[R_\phi \dot{\phi}_k(\tau) + 2F_\phi(\phi_k(\tau) - \phi_k(0)) + 2G_\phi \phi_k(0)] - \int_0^\tau \dot{\phi}_k^T(\theta) R_\phi \dot{\phi}_k(\theta) \mathrm{d}\theta.
\end{aligned} \tag{56}
$$

Using the sector conditions defined in *Lemma 2* and *Lemma 3*, we have that

$$
\begin{aligned}
\dot{W}(\tau, x_k, T_k) < \dot{W}(\tau, x_k, T_k) &+ 2S_\Delta(U_1, \phi_k(\tau), y_k(\tau)) + 2S_\Gamma(U_2, \dot{\phi}_k(\tau), \dot{y}_k(\tau)) \\
&+ 2S_\Delta(U_3, \phi_k(0), y_k(0)),
\end{aligned} \tag{57}
$$

[1]The matrices $M_0, \ldots, M_6$ are not of the same dimension. The notations 0 and I correspond to the zero and identity matrices of appropriate dimensions.

or equivalently

$$\begin{aligned}
&\dot{W}(\tau, x_k, T_k) < \dot{W}(\tau, x_k, T_k) \\
&+ 2(\phi_k^T(\tau)(I - (\underline{\Delta} D_\phi)^T) - x_k^T(\tau)(\underline{\Delta} C)^T) U_1(\overline{\Delta} C x_k(\tau) + (\overline{\Delta} D_\phi - I)\phi_k(\tau)) \\
&+ 2(\dot{\phi}_k^T(\tau)(I - (\underline{\Gamma} D_\phi)^T) - \dot{x}_k^T(\tau)(\underline{\Gamma} C)^T) U_2(\overline{\Gamma} C \dot{x}_k(\tau) + (\overline{\Gamma} D_\phi - I)\dot{\phi}_k(\tau)) \\
&+ 2(\phi_k^T(0)(I - (\underline{\Delta} D_\phi)^T) - x_k^T(0)(\underline{\Delta} C)^T) U_3(\overline{\Delta} C x_k(0) + (\overline{\Delta} D_\phi - I)\phi_k(0)).
\end{aligned} \tag{58}$$

Consider the vector $\eta_k(\tau) = [x_k^T(\tau)\ \phi_k^T(\tau)\ \dot{x}_k^T(\tau)\ \dot{\phi}_k^T(\tau)\ x_k^T(0)\ \phi_k^T(0)]^T$, the vector $\zeta_k(\tau) = M_{135}\,\eta_k(\tau)$ and a matrix $Q_x \in \mathbb{R}^{(3n)\times n}$. Since R_x is assumed to be positive definite, it follows that $(\dot{x}_k(\theta) - R_x^{-1}Q_x^T\zeta_k(\tau))^T R_x(\dot{x}_k(\theta) - R_x^{-1}Q_x^T\zeta_k(\tau)) > 0$. Integrating this expression over $[0, \tau]$, the following inequality is obtained (BRIAT; SEURET, 2012a):

$$\int_0^\tau \dot{x}_k^T(\theta) R_x \dot{x}_k(\theta) \mathrm{d}\theta - 2\zeta_k^T(\tau) Q_x (x_k(\tau) - x_k(0)) + \tau \zeta_k^T(\tau) Q_x R_x^{-1} Q_x^T \zeta_k(\tau) \geq 0. \tag{59}$$

Consider now a new vector $\psi_k(\tau) = M_{246}\,\eta_k(\tau)$ and a matrix $Q_\phi \in \mathbb{R}^{(3m)\times m}$. Following the same reasoning as above, we have that:

$$\int_0^\tau \dot{\phi}_k^T(\theta) R_\phi \dot{\phi}_k(\theta) \mathrm{d}\theta - 2\psi_k^T(\tau) Q_\phi (\phi_k(\tau) - \phi_k(0)) + \tau \psi_k^T(\tau) Q_\phi R_\phi^{-1} Q_\phi^T \psi_k(\tau) \geq 0. \tag{60}$$

On the other hand, from (27), there exists a coupling relation between the components of the vector $\eta_k(\tau)$. Hence, $\forall L \in \mathbb{R}^{3(n+m)\times n}$ the following equality is satisfied:

$$\begin{aligned}
&\eta_k^T(\tau) L [A x_k(\tau) + B_\phi \phi_k(\tau) - \dot{x}_k(\tau) + B_u(K_x x_k(0) + K_\phi \phi_k(0))] \eta_k(\tau) \\
&= \eta_k^T(\tau) L M_0 \eta_k(\tau) = 0.
\end{aligned} \tag{61}$$

This null term can be added to (58). Hence, combining (58), (59), (60) and (61), one obtains that

$$\begin{aligned}
\dot{W} \leq \eta_k^T(\tau) [&\Pi_1 + (T_k - \tau)\Pi_2 + \tau(M_{135}^T Q_x R_x^{-1} Q_x^T M_{135} + M_{246}^T Q_\phi R_\phi^{-1} Q_\phi^T M_{246}) \\
&+ (T_k - 2\tau)\Pi_3] \eta_k(\tau).
\end{aligned} \tag{62}$$

Thus, to prove that $\dot{W} < 0$, it suffices to guarantee that

$$\Pi_1 + (T_k - \tau)\Pi_2 + \tau(M_{135}^T Q_x R_x^{-1} Q_x^T M_{135} + M_{246}^T Q_\phi R_\phi^{-1} Q_\phi^T M_{246}) + (T_k - 2\tau)\Pi_3 \prec 0. \tag{63}$$

As this matrix inequality is affine with respect to τ, and $\tau \in [0, T_k)$, a necessary and sufficient condition to satisfy it is given by

$$\begin{cases}
\Pi_1 + T_k(\Pi_2 + \Pi_3) \prec 0 & (64) \\
\Pi_1 - T_k\Pi_3 + T_k(M_{135}^T Q_x R_x^{-1} Q_x^T M_{135} + M_{246}^T Q_\phi R_\phi^{-1} Q_\phi^T M_{246}) \prec 0. & (65)
\end{cases}$$

Finally, as (64) and (65) are affine in T_k and $T_k \in [\mathcal{T}_1, \mathcal{T}_2]$, applying the same reasoning and Schur's Complement to (65), we conclude that $\Psi_1(\mathcal{T}_i) \prec 0$ and $\Psi_2(\mathcal{T}_i) \prec 0$, $i = 1,2$, are sufficient to ensure $\dot{W} < 0$. Hence, by virtue of *Theorem 4*, the satisfaction of conditions (51)-(54) ensures the global asymptotic convergence of the trajectories to the origin. □

Remark 4 (Adapted from (VALMORBIDA; DRUMMOND; DUNCAN, 2018))**.** *The use of Lemma 3 in the proof of Theorem 4, requires y to be differentiable. As $y(x) = Cx + D_\phi\phi(y(x))$, we have $\frac{\mathrm{d}y}{\mathrm{d}t} = C\frac{\mathrm{d}x}{\mathrm{d}t} + D_\phi\partial\phi(y)\frac{\mathrm{d}y}{\mathrm{d}t}$, which can be written as $(I - D_\phi\partial\phi(y))\frac{\mathrm{d}y}{\mathrm{d}t} = C\frac{\mathrm{d}x}{\mathrm{d}t}$. If Proposition 1 is satisfied, then $(I - D_\phi\partial\phi(y))$ is nonsingular for all $y \in \mathcal{Y}_0$ and $\frac{\mathrm{d}y}{\mathrm{d}t}$ exists, given by $\frac{\mathrm{d}y}{\mathrm{d}t} = (I - D_\phi\partial\phi(y))^{-1}C\frac{\mathrm{d}x}{\mathrm{d}t}$.*

Remark 5. *The conditions presented in Theorem 6 consider in its developments the use of the generalized Lure function V_{LG}. However, the LMIs can be easily modified to deal with special cases of this LF. This can be particularly useful for comparing results and giving an idea of the conservatism of each approach. With this aim, for the numerical examples presented in the next subsection, inequalities (53) and (54) are adapted or removed according to each LF: for V_Q, we substitute them by $P_{11} \succ 0$; for V_{QG}, we eliminate (53) and the term related to $\tilde{\Lambda}$ in (54); lastly, for V_L we substitute them respectively, by $\Lambda \succ 0$ and by $P_{11} \succ 0$. The terms of (55) are adjusted according to the following: for the functions V_Q and V_L, we modify the structure of the matrix P to $P = \begin{bmatrix} P_{11} & 0 \\ \star & 0 \end{bmatrix}$. Also, the terms related to Λ are removed for the functions V_Q and V_{QG} as these LFs does not have the Lure coefficients on its formulations.*

When the slope bounds ($\underline{\Gamma}$, $\overline{\Gamma}$) are unknown or ϕ is supposed to be continuous but with arbitrary slope, *i.e.*, only conditions (19a) and (19b) are satisfied, we cannot consider $\dot{\phi}$ in the developments. Nevertheless, stability conditions can be obtained by considering a quadratic function $V(x) = V_Q(x) = x^T P_{11} x$ and a functional

$$\mathcal{W}_0(\tau, x_k, T_k) = (T_k - \tau)\tau \begin{bmatrix} x_k(0) \\ \phi_k(0) \end{bmatrix}^T X \begin{bmatrix} x_k(0) \\ \phi_k(0) \end{bmatrix}$$
$$+ (T_k - \tau)\left\{ \int_0^\tau \dot{x}_k^T(\theta) R_x \dot{x}_k(\theta) \mathrm{d}\theta + (x_k(\tau) - x_k(0))^T [F_x(x_k(\tau) - x_k(0)) + 2G_x x_k(0)] \right\}, \tag{66}$$

with $F_x \in \mathbb{S}^n$, $G_x \in \mathbb{R}^{n\times n}$, $X \in \mathbb{S}^{n+m}$ and $R_x \in \mathbb{S}^n_{\succ 0}$. In this context, observe that stability conditions can only be derived from a Lure-Postnikov function V_L if we assume $D_\phi = 0$, that is $y = Cx$.

Then, considering $V(x) = x^T P_{11} x$ the following corollary can be stated, regarding the stability of the closed-loop system under aperiodic sampling and with nonlinearities that lies on a sector.

Corollary 1. *For given* $0 < \mathcal{T}_1 \leq \mathcal{T}_2$*, assume that there exist matrices* $P_{11} \in \mathbb{S}^n_{\succ 0}$*,* $U_h \in \mathbb{D}^m_{\succeq 0}$*,* $h = 1, \ldots, 2$*,* $F_x \in \mathbb{S}^n$*,* $G_x \in \mathbb{R}^{n\times n}$*,* $R_x \in \mathbb{S}^n_{\succ 0}$*,* $Q_x \in \mathbb{R}^{(3n)\times n}$*,* $X \in \mathbb{S}^{n+m}$*,* $L \in \mathbb{R}^{(3n+2m)\times n}$ *that satisfy, for* $i = 1, 2$ *:*

$$\Psi_1(\mathcal{T}_i) = \Pi_1 + \mathcal{T}_i\Pi_2 + \mathcal{T}_i\Pi_3 \prec 0 \tag{67}$$

$$\Psi_2(\mathcal{T}_i) = \begin{bmatrix} \Pi_1 - \mathcal{T}_i\Pi_3 & \mathcal{T}_i M_{134}^T Q_x \\ \star & -\mathcal{T}_i R_x \end{bmatrix} \prec 0 \tag{68}$$

with

$$\begin{aligned}
\Pi_1 &= \mathrm{He}\{M_1^T P_{11} M_3\} - M_{14}^T F_x M_{14} - \mathrm{He}\{M_{14}^T G_x M_4\} - \mathrm{He}\{M_{134}^T Q_x M_{14}\} + \mathrm{He}\{LM_0\} \\
&\quad + \mathrm{He}\{M_2^T(I - (\underline{\Delta}D_\phi)^T) - M_1^T(\underline{\Delta}C)^T)U_1(\overline{\Delta}CM_1 + (\overline{\Delta}D_\phi - I)M_2)\} \\
&\quad + \mathrm{He}\{M_5^T(I - (\underline{\Delta}D_\phi)^T) - M_4^T(\underline{\Delta}C)^T)U_2(\overline{\Delta}CM_4 + (\overline{\Delta}D_\phi - I)M_5)\} \\
\Pi_2 &= M_3^T R_x M_3 + \mathrm{He}\{M_3^T(F_x M_{14} + G_x M_4)\} \\
\Pi_3 &= M_{45}^T X M_{45},
\end{aligned} \tag{69}$$

where

$$\begin{aligned}
M_0 &= [A \;\; B_\phi \;\; -I \;\; B_u K_x \;\; B_u K_\phi] \\
M_1 &= [I \;\; 0 \;\; 0 \;\; 0 \;\; 0] \qquad M_2 = [0 \;\; I \;\; 0 \;\; 0 \;\; 0] \quad M_3 = [0 \;\; 0 \;\; I \;\; 0 \;\; 0] \\
M_4 &= [0 \;\; 0 \;\; 0 \;\; I \;\; 0] \qquad M_5 = [0 \;\; 0 \;\; 0 \;\; 0 \;\; I] \\
M_{14} &= M_1 - M_4 \qquad M_{45} = [M_4^T \;\; M_5^T]^T \;\; M_{134} = [M_1^T \;\; M_3^T \;\; M_4^T]^T.
\end{aligned}$$

Then the origin of the sampled-data closed-loop system (50), with ϕ *satisfying (19a), (19b) and* $T_k \in [\mathcal{T}_1, \mathcal{T}_2]$ *is globally asymptotically stable.*

Proof. The proof follows the same steps from the proof of *Theorem 2*, by considering the augmented vector $\eta_k(\tau) = [x_k^T(\tau)\ \phi_k^T(\tau)\ \dot{x}_k^T(\tau)\ x_k^T(0)\ \phi_k^T(0)]^T$, the function $V(x) = x^T P_{11} x$, the sector conditions from *Lemma 2* and Schur's Complement. □

4.2.1 Optimization Problems

From the conditions stated in *Theorem 6*, we can formulate three optimization problems, detailed as follows.

P1. Given $\mathcal{T}_1$, the sector and slope bounds, find the maximal $\mathcal{T}_2$ such that the global stability of the closed-loop system (50) is ensured.

P2. Given a nominal sampling time $\mathcal{T}_{nom}$, the sector and slope bounds, find a bound on the maximum symmetrical allowable jitter, denoted by σ, (*i.e.*, $\mathcal{T}_1 = \mathcal{T}_{nom} - \sigma$, $\mathcal{T}_2 = \mathcal{T}_{nom} + \sigma$), such that the global stability of the closed-loop system (50) is ensured.

P3. Given $\mathcal{T}_1$ and $\mathcal{T}_2$, compute the maximum sector and slope bounds given by the diagonal matrix Ω, such that the global stability of the closed-loop system (50) is ensured.

Note that, as (51), (52), (53), (54) are LMIs once $\mathcal{T}_1$, $\mathcal{T}_2$ and the sector bounds are fixed, these optimization problems can be straightforwardly solved by considering feasibility LMI problems and bisection techniques.

In the bisection algorithm, we interactively increase/decrease $\mathcal{T}_2$, σ or a parameter defining the sector and test the LMIs constraints with these variables fixed. For instance, for the maximization of $\mathcal{T}_2$, we start with a guess for $\mathcal{T}_2$ and if the LMI problem is feasible, we increase $\mathcal{T}_2$ of a certain amount. Otherwise, if it is infeasible, we decrease $\mathcal{T}_2$. Once for $\mathcal{T}_2$ of an iteration the problem is feasible (say $\mathcal{T}_2 = a$) and for the next one (or the previous one) it is not (say $\mathcal{T}_2 = b$), we can choose for the next iteration $\mathcal{T}_2 = (a+b)/2$. We stop the procedure when a certain toleration $e = a - b$ is achieved. Note that this procedure approaches the maximum $\mathcal{T}_2$ for which the LMIs are feasible.

Remark 6. *The numerical complexity of the conditions presented in Theorem 6 is related to the optimization problems P1-P3. The numerical complexity that LMI solvers are able to handle is an open topic, which is discussed in some references only when the authors find convergence problems. It usually depends on the considered solver (e.g., LMILAB or SeDuMi) and some optimization problem parameters such as the number of LMI conditions (n_l), maximum LMI order (n_o) and number of decision variables (n_v). Based on the LMI conditions (51), (52), (53), (54), these parameters can be computed as a function of the plant dimensions n of the state and m of the nonlinearity. Table 2 illustrates the numerical complexity of the method through the expressions of n_l, n_o and n_v.*

Table 2: Numerical complexity associated to the optimization problems P1-P3.

n_l	13
n_o	4(n+m)
n_v	n(9n+2)+m(6m+8)+5nm

4.2.2 Numerical Examples

Example 1: Consider the SISO system given in (VALMORBIDA; DRUMMOND; DUNCAN, 2018) that can be described in the form (18) with the following matrices

$$A = \begin{bmatrix} -0.5 & -6.2 & -0.105 & -1.2 \\ 1 & 0 & 0 & 0 \\ 0 & 1 & 0 & 0 \\ 0 & 0 & 1 & 0 \end{bmatrix}, B_u = \begin{bmatrix} 1 \\ 0 \\ 0 \\ 0 \end{bmatrix}, B_\phi = \begin{bmatrix} 0.5 \\ 0 \\ 0 \\ 0 \end{bmatrix}$$

$$C = \begin{bmatrix} 0 & 0.2 & 0 & 0 \end{bmatrix}, D_\phi = [0],$$

and the control law (20) with the following gains

$$K_x = \begin{bmatrix} 0.1 & 0.2 & 0.005 & 0.2 \end{bmatrix}, \quad K_\phi = [0.5],$$

with the bounds on ϕ given by $\underline{\delta} = 0$, $\overline{\delta} = \Omega$, $\underline{\gamma} = -\Omega$, $\overline{\gamma} = \Omega$. In what follows, we present comparative results considering different structures of the function V_{LG} (see Table 1), as presented in Table 1. Inequalities are adjusted to each function, as detailed in *Remark 5*. The obtained results for problems P1-P3 are shown in Table 3. For P1, we consider $\mathcal{T}_1 = 0.1$ ms and $\Omega = \frac{1}{\sqrt{2}}$. For P2, we fixed $\mathcal{T}_{nom} = 1.5$ s and $\Omega = \frac{1}{\sqrt{2}}$ and for P3 we defined $\mathcal{T}_1 = 0.1$ ms and $\mathcal{T}_2 = 2.0$ s. The numerical complexity for the solutions of the optimization problems is defined by $n_l = 13$, $n_o = 20$ and $n_v = 186$.

Table 3: Global analysis, Ex. 1 - Results for problems P1-P3.

Problem	Parameter	V_Q	V_{QG}	V_L	V_{LG}
P1	$\boldsymbol{\mathcal{T}_2}$	1.1151	1.1161	2.2121	2.6362
P2	$\boldsymbol{\sigma}$	1.0492	1.0496	1.0888	1.2260
P3	$\boldsymbol{\Omega}$	0.5955	0.5970	0.7842	1.1043

For the first problem, as shown in Table 3, using the generalized Lure function V_{LG} we achieve values for $\mathcal{T}_2$ that are greater 19.1%, 136.1% and 136.4% than the ones obtained with V_L, V_{QG} and V_Q, respectively. For P2, we guaranteed the stability for $\mathcal{T}_1 = 0.2740$ s and $\mathcal{T}_2 = 2.7260$ s, with σ greater 12.6%, 16.8 % and 16.8 % than the ones obtained with V_L, V_{QG} and V_Q, respectively. For the last feasibility problem, the sector bounds and the lower slope bound, represented by Ω, were 40.8%, 84.9% and 85.4% bigger than the ones obtained with V_L, V_{QG} and V_Q, respectively. This shows, as expected, a considerable conservatism reduction when a generalized Lure-type function is considered.

Observe that the value of $\mathcal{T}_2$ achieved by P2 with the function V_{LG} is greater than the one obtained from P1 with the same function, which evidences that the choice of $\mathcal{T}_1$ affects the maximal intersampling bound for which stability is preserved. Table 4 shows the influence on $\mathcal{T}_2$ for different values of $\mathcal{T}_1$, considering $\Omega = \frac{1}{\sqrt{2}}$ and the function V_{LG}.

Table 4: Global analysis, Ex. 1 - Influence of $\mathcal{T}_1$ on $\mathcal{T}_2$, considering the function V_{LG}.

$\boldsymbol{\mathcal{T}_1}$ (s)	0.5	1.0	2.0	3.0	4.0	5.0
$\boldsymbol{\mathcal{T}_2}$ (s)	2.9075	3.3161	3.9955	4.4764	4.8205	5.0739

From the results presented in Table 4, one sees that increasing $\mathcal{T}_1$ leads to greater $\mathcal{T}_2$ up to a certain limit, given by $\mathcal{T}_1 = \mathcal{T}_2 = 5.0889$ s, *i.e.*, the admissible sampling intervals for which stability is ensured, is reduced to the periodic case. Although this result is quite interesting, it is difficult to precise a link of this behavior with the matrices of the system. In addition, this phenomenon may have come from limitations of the derived sufficient stability conditions.

To show that the achieved results support the global stabilization of the closed-loop system (50), we simulate the system considering the result from P1, *i.e.*, $T_k \in [0.0001, 2.6362]$, and the nonlinearity

$$\phi(y(t)) = 0.1\sin(5y(t)) + 0.15y(t), \tag{70}$$

that satisfies (19) with $\underline{\delta} = 0$, $\overline{\delta} = \frac{1}{\sqrt{2}}$, $\underline{\gamma} = -\frac{1}{\sqrt{2}}$, $\overline{\gamma} = \frac{1}{\sqrt{2}}$. The control action and the states of the closed-loop system are presented in Fig. 9 and Fig. 10, respectively, for initial conditions $x(0) = [1\ 1\ 1\ 1]^T$. Fig. 11 illustrates the sequence of samplings instants used in the simulation through the lifted variable $\tau(t)$.

Figure 9: Global analysis, Ex. 1 - Control action of the closed-loop system.

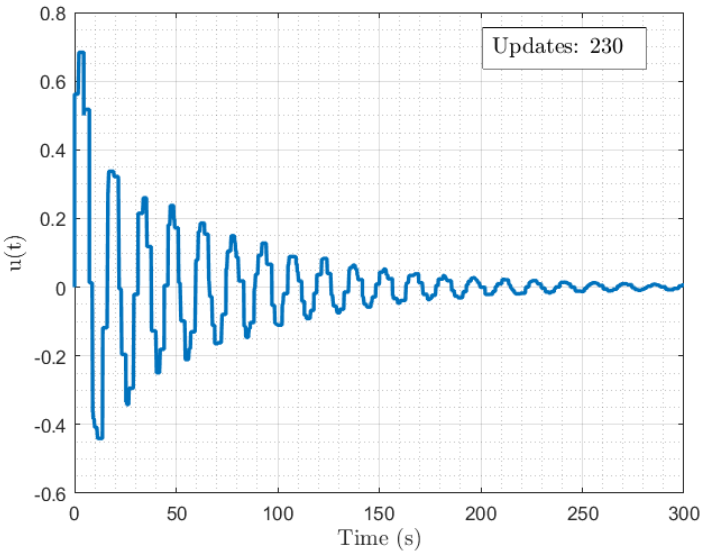

Font: Author.

Figure 10: Global analysis, Ex. 1 - States of the closed-loop system.

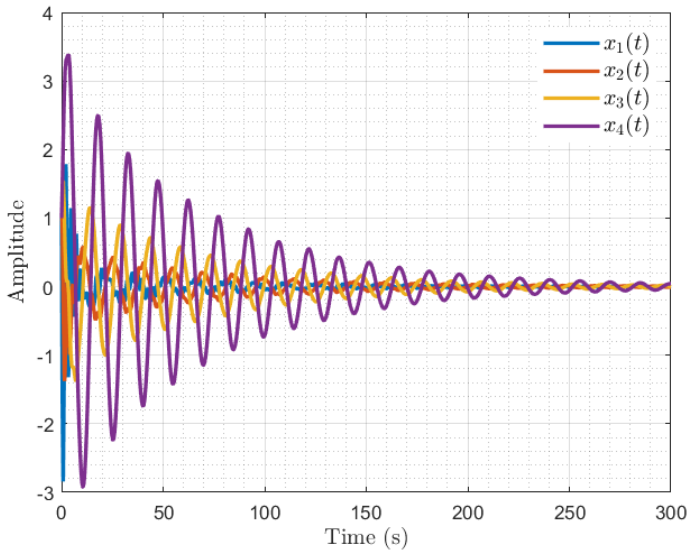

Font: Author.

Figure 11: Global analysis, Ex. 1 - Sequence of the sampling instants.

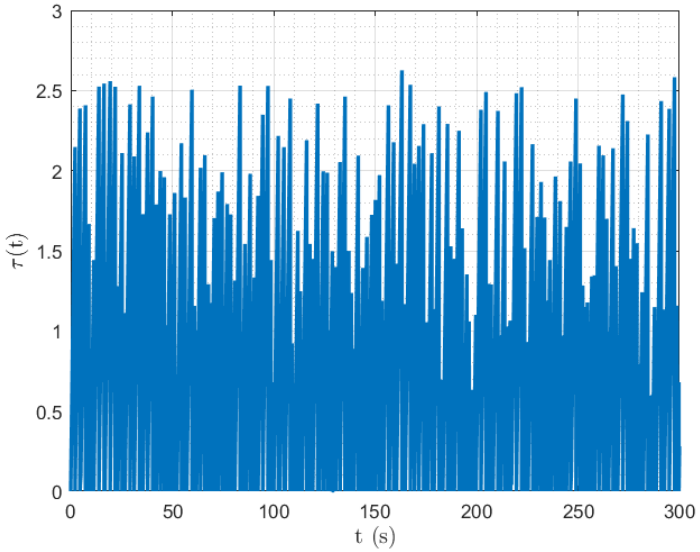

Font: Author.

It is easy to notice that when $t \to \infty$ the states and the control law converge to the origin, reinforcing the obtained results. To obtain the values of T_k, we used a pseudo-random algorithm (function *rand*$(\cdot)$ from MATLAB, with default seed) that generates its numbers from the standard uniform distribution over the defined interval.

Example 2: Consider system (18) given by the following matrices

$$A = \begin{bmatrix} -1.1 & -2 \\ 1 & 0 \end{bmatrix}, B_u = \begin{bmatrix} 1 \\ 0 \end{bmatrix}, B_\phi = \begin{bmatrix} 0.5 \\ 0 \end{bmatrix}, \; C = \begin{bmatrix} -0.95 & 1.50 \end{bmatrix}, \; D_\phi = [-0.5],$$

and the control law (20) with the following gains

$$K_x = \begin{bmatrix} 1 & 1 \end{bmatrix}, \; K_\phi = [0.5],$$

with the bounds on ϕ given by $\underline{\delta} = 0$, $\overline{\delta} = \Omega$, $\underline{\gamma} = 0$, $\overline{\gamma} = \Omega$. This system satisfies *Proposition 1*, that is, the algebraic loop in (50) is well-posed. The obtained results for problems P1-P3 are detailed in Table 5 by considering different LF structures. For P1, we consider $\mathcal{T}_1 = 0.5$ s and $\Omega = \frac{1}{\sqrt{2}}$. For P2, we fixed $\mathcal{T}_{nom} = 0.75$ s and $\Omega = \frac{1}{\sqrt{2}}$ and for P3 we defined $\mathcal{T}_1 = 0.5$ s and $\mathcal{T}_2 = 1.0$ s.

Table 5: Global analysis, Ex. 2 - Results for problems P1-P3.

Problem	Parameter	V_Q	V_{QG}	V_L	V_{LG}
P1	$\boldsymbol{\mathcal{T}_2}$	1.0308	1.0964	1.0308	1.5378
P2	$\boldsymbol{\sigma}$	0.2566	0.2702	0.2566	0.5542
P3	$\boldsymbol{\Omega}$	0.7141	0.7277	0.7141	0.9999

For the first problem, using the generalized Lure function V_{LG} we obtain the larger value of $\mathcal{T}_2$. We achieve values for $\mathcal{T}_2$ that are greater 40.2%, 49.1% and 49.1% than the

ones obtained with V_{QG}, V_Q and V_L, respectively. For P2, we guaranteed the stability for $\mathfrak{T}_1 = 0.1958$ s and $\mathfrak{T}_2 = 1.3042$ s, with σ greater 105.1%, 115.9% and 115.9% than the ones obtained with V_{QG}, V_L and V_Q, respectively. For the last feasibility problem, the upper sector and slope bounds, represented by Ω were 37.4%, 40.0% and 40.0% bigger than the ones obtained with V_{QG}, V_L and V_Q, respectively. We also observed that for some values of $\mathfrak{T}_1$ lesser than 0.43, the LMI restrictions were infeasible for V_Q, V_{QG} and V_L by solving P1. However, with the function V_{LG}, stability can be certified by considering smaller values of $\mathfrak{T}_1$. For instance, fixing $\mathfrak{T}_1 = 0.1$ ms, by virtue of *Theorem 6* we guaranteed stability for $\mathfrak{T}_2 = 1.2071$.

To show that the achieved results support the global stabilization of the closed-loop system (50), we simulate the system considering the result from P2, *i.e.*, $T_k \in [0.1958, 1.3042]$, and a saturation nonlinearity

$$\phi(y(t)) = \begin{cases} 0.5y(t), -0.5 \leq y(t) \leq 0.5 \\ 0.25, \quad y(t) > 0.5 \\ -0.25, \quad y(t) < -0.5 \end{cases} \tag{71}$$

which satisfies (19) with $\underline{\delta} = 0$, $\overline{\delta} = \frac{1}{\sqrt{2}}$, $\underline{\gamma} = 0$, $\overline{\gamma} = \frac{1}{\sqrt{2}}$. The control action and the states of the closed-loop system are presented in Figs. 12 and 13.

Figure 12 – Global analysis, Ex. 2 - Control action (left axis) and saturation nonlinearity behavior (right axis) of the closed-loop system.

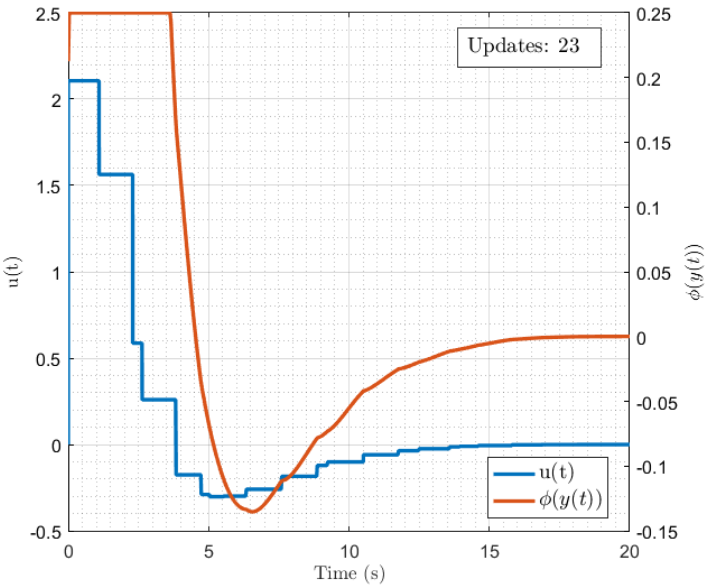

Font: Author.

Figure 13: Global analysis, Ex. 2 - States of the closed-loop system.

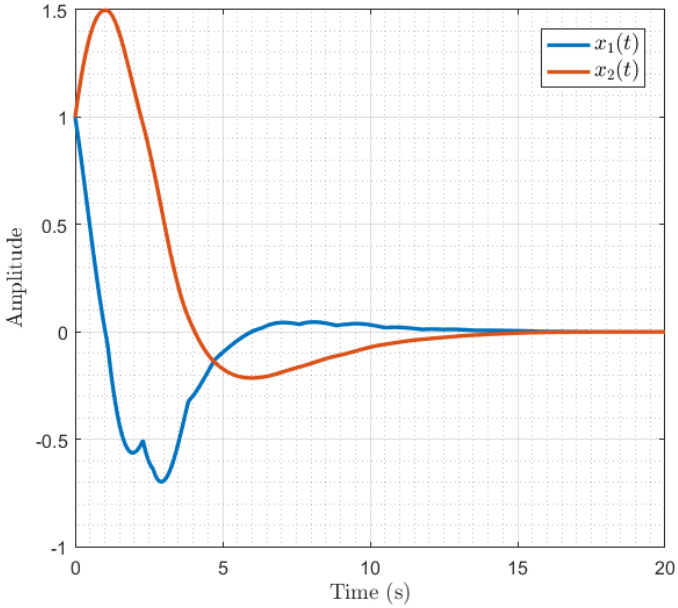

Font: Author.

Example 3: Aiming to compare our results with a different work on sampled-data Lure systems, consider the following system treated in (SEIFULLAEV; FRADKOV, 2015):

$$\begin{cases} \dot{x}_1(t) = -2x_1(t) + \sin(x_2(t)), \\ \dot{x}_2(t) = x_1(t) - x_2(t) + 2\sin(x_2(t)) + u(t) \\ y(t) \;\; = x_2(t) \\ u(t) \;\; = -Ky(t_k), \quad \forall t \in [t_k, t_{k+1}),\ t_{k+1} - t_k \leq \mathcal{T}_2. \end{cases}$$

This system can be rewritten in form (18)-(20) with the following matrices:

$$A = \begin{bmatrix} -2 & 1 \\ 1 & 1 \end{bmatrix}, B_u = \begin{bmatrix} 0 \\ 1 \end{bmatrix}, B_\phi = \begin{bmatrix} 1 \\ 2 \end{bmatrix}, C = \begin{bmatrix} 0 & 1 \end{bmatrix}, D_\phi = [0], K_x = \begin{bmatrix} 0 & -K \end{bmatrix}, K_\phi = [0],$$

and with $\phi(y(t)) = \sin(y(t)) - y(t)$, satisfying (19) with $\underline{\delta} = -1.2173$, $\overline{\delta} = 0$, $\underline{\gamma} = -2$ and $\overline{\gamma} = 0$. The maximum values of $\mathcal{T}_2$ (P1) obtained with *Theorem 6*, by considering V_{LG} and $\mathcal{T}_1 = 0.0001$ s and with Theorem 3 from (SEIFULLAEV; FRADKOV, 2015) are given in Fig. 14 for different gains K. It is important to mention that to make the results comparable, we set the decay rate in (SEIFULLAEV; FRADKOV, 2015) to zero.

From Fig. 14, one can easily note that our formulation leads to greater values of $\mathcal{T}_2$ than the ones obtained by (SEIFULLAEV; FRADKOV, 2015). The maximal values of $\mathcal{T}_2$ obtained with *Theorem 6* and with Theorem 3 from (SEIFULLAEV; FRADKOV, 2015) were $\mathcal{T}_2 = 1.3601$ s and $\mathcal{T}_2 = 0.8768$ s, with respective gains $K = 1.51$ and $K = 1.62$. This represents an increase of 55.1% on the upper intersampling bound. Observe that for $K < 1.51$ no feasible solution is obtained for conditions (51)-(54) neither for the ones

in (SEIFULLAEV; FRADKOV, 2015). Thus, our approach provides less conservative results in comparison to the above work on sampled-data Lure systems.

Figure 14: Global analysis, Ex. 3 - Dependence of the upper bound $\mathcal{T}_2$ on gain K.

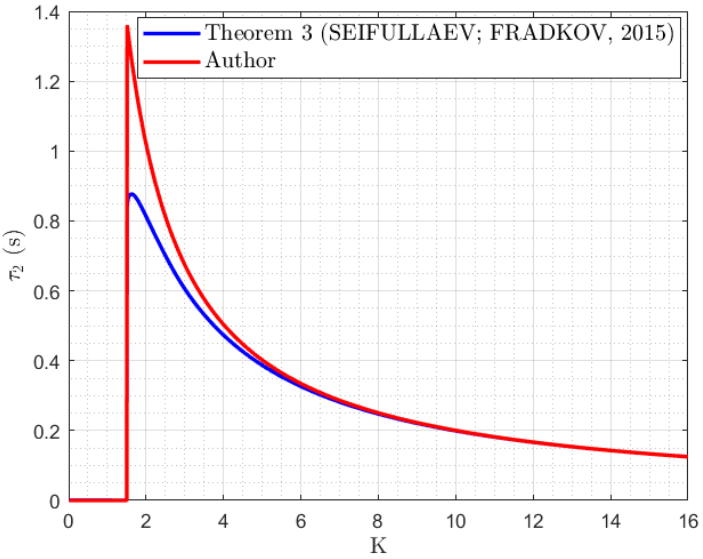

Font: Author.

To show that the results support asymptotic global stabilization of the origin, we simulate the closed-loop system by considering $K = 2$, $\mathcal{T}_1 = \mathcal{T}_2 = 1.0197$ s (although we prove stability for any $T_k \in [0.0001, 1.0197]$), and initial conditions $x(0) = [2\ 0]^T$, as illustrated in Fig. 15.

Figure 15 – Global analysis, Ex. 3 - Trajectories of the closed-loop system for $K = 2$ and $\mathcal{T}_1 = \mathcal{T}_2 = 1.0197$ s.

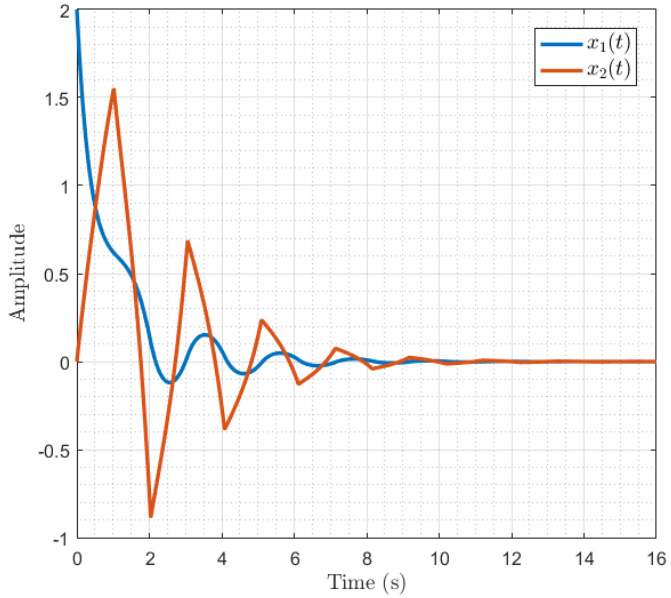

Font: Author.

4.3 Regional Results

When the nonlinearities does not satisfy the sector conditions for $\mathcal{Y}_0 = \mathbb{R}^m$, it is said that stability can be achieved only locally. In this context, the objective of this section consists in guaranteeing the asymptotic stability of the origin of the system (50) for nonlinearities satisfying the sector and slope bounded conditions (19b), (19c) in a region of validity $\mathcal{Y}_0 = \{y \in \mathbb{R}^m | y_j(x) \in [\underline{y}_j, \overline{y}_j], \forall j = 1, \ldots, m\}$, where $y_j(x) = C_j x + D_{\phi_j}\phi(y(x))$, $\underline{y}_j \in \mathbb{R}$, $\overline{y}_j \in \mathbb{R}$, $\underline{y}_j < 0 < \overline{y}_j$, $j = 1, \ldots, m$.

Afterwards, when the origin is asymptotically stable, we are often interested in determining how far from it the trajectory can be initialized and still converge to the origin as $t \to \infty$ (KHALIL, 2002), which gives rise to the definition of the region of attraction ($\mathcal{R}_a$). The region of attraction is defined as the set of all $x \in \mathbb{R}^n$, such that $\Phi(t, x)$ is defined for all $t \geq 0$ and $\lim_{t\to\infty} \Phi(t, x) = 0$, where $\Phi(t, x)$ are the solutions of (50) that starts at initial state x at time $t = 0$. Determining the exact region of attraction by analytical means may be a hard or even an impossible task. However, one can use Lyapunov's theory to determine an estimate of the region of attraction by finding levels sets $\mathcal{L}(V, \rho) = \{x \in \mathbb{R}^n | \ V(x) \leq \rho\}$ of a function V such that they are positively invariant and included in a domain $\mathcal{D}_x \subseteq \mathcal{X}_0 \subset \mathbb{R}^n$ where the sector and slope bounds hold (for this, note that a mapping of the region $\mathcal{Y}_0 \subset \mathbb{R}^m$ to $\mathcal{X}_0 \subset \mathbb{R}^n$ is required).

On this basis, the rationale under the development of the conditions here presented is based on *Theorem 5*, which provides sufficient conditions to assess the asymptotic stability of the origin of the sampled-data Lure system (50) in a local context. Recalling its results in a simplified way, we consider a function $W(\tau, x_k, T_k) = V(x_k(\tau)) + \mathcal{W}_0(\tau, x_k, T_k)$, where V is a continuously differentiable function and $\mathcal{W}_0$ is a continuous-time positive definite functional which is equal to zero at the sequence of samplings. If $\dot{W}(\tau, x_k, T_k) < 0$ along the solutions of the system, than the continuous-time trajectories starting at $x(t_k) \in \partial\mathcal{L}(V, \rho) \subset \mathcal{D}_x$ moves from one Lyapunov surface $V(x) = \rho$ to an inner Lyapunov surface with a smaller ρ at the instant t_{k+1} without leaving $\mathcal{L}(V, \rho)$. This is achieved thanks to the positivity of the functional and the fact that the function V is strictly decreasing at the sampling instants (but not necessarily between two successive sampling instants). This implies that $\mathcal{L}(V, \rho)$ is a positively invariant set but not continuously contractive.

In other words, we have that the satisfaction of conditions from *Theorem 5* implies that any trajectories starting in $\mathcal{L}(V, \rho)$ remains in $\mathcal{L}(V, \rho)$ for all $t \geq 0$ and approaches the origin as $t \to \infty$. Thus, if we include the level sets in a domain of validity $\mathcal{D}_x \subseteq \mathcal{X}_0$, then $\mathcal{L}(V, \rho)$ may be seen as an estimate of the region of attraction of the origin, that is, $\mathcal{L}(V, \rho) \subset \mathcal{R}_a \subset \mathbb{R}^n$. In what follows, we will present conditions to guarantee the inclusion $\mathcal{L}(V, c) \subset \mathcal{D}_x = \mathcal{X}_0$, starting from the case where the domain $\mathcal{X}_0$ corresponds to an asymmetric validity region.

4.3.1 Asymmetric Validity Regions

When $\underline{y}_j$ is not equal to $\overline{y}_j$, we have an asymmetric region of validity for the sector and slope restrictions. The region $\mathcal{Y}_0$ can be mapped in space $\mathbb{R}^n$ by $\mathcal{X}_0$ given in (24), which can be equivalently described as follows:

$$\mathcal{X}_0 = \{x \in \mathbb{R}^n | (y_j(x) - \underline{y}_j)(y_j(x) - \overline{y}_j) \leq 0, j = 1, \ldots, m\}. \tag{72}$$

Note that $y(x) \in \mathcal{Y}_0$ if and only if $x \in \mathcal{X}_0$.

In the following lemma, we provide conditions that guarantee generic inclusions for the level set $\mathcal{L}(V, \rho)$ of a function V in $\mathcal{X}_0$, as defined in (72).

Lemma 6. *(VALMORBIDA; DRUMMOND; DUNCAN, 2018). If there exist scalars* $\sigma_j > 0$ *such that the following inequalities are satisfied*

$$-\sigma_j(y_j(x) - \underline{y}_j)(y_j(x) - \overline{y}_j) \geq (\rho - V(x)), \tag{73}$$

for $j = 1, \ldots, m$*, then* $\mathcal{L}(V, \rho) \subset \mathcal{X}_0$ *holds, with* $\mathcal{X}_0$ *given by (72).*

Proof. If the above inequality holds, then for all x satisfying $(\rho - V(x)) \geq 0$, *i.e.*, $\forall x \in \mathcal{L}(V, \rho)$, the inequality $\sigma_j(y_j(x) - \underline{y}_j)(y_j(x) - \overline{y}_j) \leq 0$ holds, which as $\sigma_j > 0$ ensures that $x \in \mathcal{X}_0$. □

The following lemma provides LMI conditions to check the inclusion of the level set of the generalized Lure function $V_{LG}(x)$ expressed by $\mathcal{L}(V_{LG}, \rho)$ in the set (72).

Lemma 7. *If there exist matrices* $P \in \mathbb{S}^{n+m}$, $\tilde{\Lambda} \in \mathbb{D}^m_{\geq 0}$, $S_{c,j} \in \mathbb{D}^m_{\geq 0}$ *and positive scalars* σ_j *and* ρ*, such that the following inequalities are satisfied*

$$\begin{bmatrix} -(\sigma_j \underline{y}_j \overline{y}_j + \rho) & \sigma_j \frac{\underline{y}_j + \overline{y}_j}{2} C_j & \sigma_j \frac{\underline{y}_j + \overline{y}_j}{2} D_{\phi_j} & 0 \\ \star & P_{11} - \frac{1}{2} C^T (\overline{\Delta} - \underline{\Delta}) \tilde{\Lambda} C & P_{12} - \frac{1}{2} C^T (\overline{\Delta} - \underline{\Delta}) \tilde{\Lambda} D_\phi & \sigma_j C_j^T \\ \star & \star & P_{22} - \frac{1}{2} D_\phi^T (\overline{\Delta} - \underline{\Delta}) \tilde{\Lambda} D_\phi & \sigma_j D_{\phi_j}^T \\ \star & \star & \star & \sigma_j \end{bmatrix}$$
$$+ \mathrm{He} \left\{ \frac{1}{2} \begin{bmatrix} 0 \\ (\underline{\Delta} C)^T \\ (\underline{\Delta} D_\phi - I)^T \\ 0 \end{bmatrix} S_{c,j} \begin{bmatrix} 0 & \overline{\Delta} C & (\overline{\Delta} D_\phi - I) & 0 \end{bmatrix} \right\} \succeq 0, \tag{74}$$

for $j = 1, \ldots, m$*, then* $\mathcal{L}(V_{LG}, \rho) \subset \mathcal{X}_0$*, with* $\mathcal{X}_0$ *given by (72).*

Proof. From *Lemma 6* and the generalized Lure function $V_{LG}(x)$ defined in (43), inequalities (73) becomes

$$-\sigma_j \underline{y}_j \overline{y}_j - \rho + \sigma_j (\underline{y}_j + \overline{y}_j) y_j(x) - \sigma_j y_j^2(x) + V_{QG}(x) + \sum_{i=1}^{m} \lambda_i \int_0^{y_i} (\phi_i(s) - \underline{\delta}_i s) \mathrm{d}s \geq 0, \tag{75}$$

$j = 1, \ldots, m$. Consider that $\lambda_i \geq -\tilde{\lambda}_i$ is satisfied $\forall i$. From (48), we obtain a lower bound for the Lure-Postnikov terms, given by the following relation:

$$\sum_{i=1}^{m} \lambda_i \int_0^{y_i} (\phi_i(s) - \underline{\delta}_i s) \mathrm{d}s \geq -\frac{1}{2} y^T (\overline{\Delta} - \underline{\Delta}) \tilde{\Lambda} y \geq 0. \tag{76}$$

Hence, provided the inequalities

$$-\sigma_j \underline{y}_j \overline{y}_j - \rho + \sigma_j (\underline{y}_j + \overline{y}_j) y_j(x) - \sigma_j y_j^2(x) + V_{QG}(x) - \frac{1}{2} y^T (\overline{\Delta} - \underline{\Delta}) \tilde{\Lambda} y \geq 0 \tag{77}$$

hold, we have that (75) holds. Note that the substitution of the lower bound (77) in (73) correspond to the inclusion of an outer approximation of the level set $\mathcal{L}(V_{LG}, \rho)$ in $\mathcal{X}_0$, that is, if the outer approximation is included in $\mathcal{X}_0$, then $\mathcal{L}(V_{LG}, \rho)$ will also be included in $\mathcal{X}_0$. Expanding the terms $y_j(x) = C_j x + D_{\phi_j} \phi(y(x))$, rewriting (77) in a matrix format and relaxing for all x and ϕ which satisfies the sector conditions through adding the term $-S_\Delta(S_{c,j}, \phi, y)$ (as defined in *Lemma 5*) on the left side of (77), we have that the following inequalities provide sufficient conditions to verify (77):

$$\begin{bmatrix} I \\ x \\ \phi \end{bmatrix}^T \Psi \begin{bmatrix} I \\ x \\ \phi \end{bmatrix} - S_\Delta(S_{c,j}, \phi, y) = \begin{bmatrix} I \\ x \\ \phi \end{bmatrix}^T \tilde{\Psi} \begin{bmatrix} I \\ x \\ \phi \end{bmatrix} \geq 0, \tag{78}$$

with $\tilde{\Psi}$ given by:

$$\begin{aligned} \tilde{\Psi} = &\begin{bmatrix} -(\sigma_j \underline{y}_j \overline{y}_j + \rho) & \sigma_j \frac{\underline{y}_j + \overline{y}_j}{2} C_j & \sigma_j \frac{\underline{y}_j + \overline{y}_j}{2} D_{\phi_j} \\ \star & P_{11} - \frac{1}{2} C^T (\overline{\Delta} - \underline{\Delta}) \tilde{\Lambda} C & P_{12} - \frac{1}{2} C^T (\overline{\Delta} - \underline{\Delta}) \tilde{\Lambda} D_\phi \\ \star & \star & P_{22} - \frac{1}{2} D_\phi^T (\overline{\Delta} - \underline{\Delta}) \tilde{\Lambda} D_\phi \end{bmatrix} \\ &- \sigma_j \begin{bmatrix} 0 & 0 & 0 \\ 0 & C_j^T C_j & C_j^T D_{\phi_j} \\ 0 & \star & D_{\phi_j}^T D_{\phi_j} \end{bmatrix} + \mathrm{He} \left\{ \frac{1}{2} \begin{bmatrix} 0 \\ (\underline{\Delta} C)^T \\ (\underline{\Delta} D_\phi - I)^T \end{bmatrix} S_{c,j} \begin{bmatrix} 0 & \overline{\Delta} C & (\overline{\Delta} D_\phi - I) \end{bmatrix} \right\}. \end{aligned} \tag{79}$$

A sufficient condition to ensure (78) is that $\tilde{\Psi} \succeq 0$. Applying Schur's Complement on $\tilde{\Psi} \succeq 0$ it is straightforward to obtain (74), which ensures that (78) be satisfied, hence guaranteeing that $\mathcal{L}(V_{LG}, \rho) \subset \mathcal{X}_0$. □

Remark 7. *Aiming the comparison with other candidate functions V, to include the level sets $\mathcal{L}(V_Q, \rho)$ and $\mathcal{L}(V_L, \rho)$ in (72), we adapt the inequalities (74) from Lemma 7 by considering $P = \begin{bmatrix} P_{11} & 0 \\ \star & 0 \end{bmatrix}$ and $\tilde{\Lambda} = 0$. Observe that the conditions for the function V_L are reduced to the inclusion of the level set $\mathcal{L}(V_Q, \rho)$ in $\mathcal{X}_0$. Note that $\mathcal{L}(V_Q, \rho)$ is an outer approximation of $\mathcal{L}(V_L, \rho)$. To guarantee the inclusion of the level set $\mathcal{L}(V_{QG}, \rho)$ in (72), it suffices to consider $\tilde{\Lambda} = 0$. For the special case where $D_{\phi_j} = 0$, inequalities (74)*

to guarantee the inclusion of the level sets $\mathcal{L}(V_Q, \rho)$ and $\mathcal{L}(V_L, \rho)$ in $\mathcal{X}_0$, are simplified by the following ones:

$$\begin{bmatrix} -(\sigma_j \underline{y}_j \overline{y}_j + \rho) & \sigma_j \frac{\underline{y}_j + \overline{y}_j}{2} C_j & 0 \\ \star & P_{11} & \sigma_j C_j^T \\ \star & \star & \sigma_j \end{bmatrix} \succeq 0. \tag{80}$$

In the sequence, we will present the inclusion of level sets in a domain which represents symmetric validity regions.

4.3.2 Symmetric Validity Regions

If the validity region defined by the variables $\underline{y}_j$ and $\overline{y}_j$ is symmetric, *i.e.*, $\underline{y}_j = \overline{y}_j$, then simplified set inclusions can be considered. In this case, $\mathcal{X}_0$ can be generically defined as follows:

$$\mathcal{X}_0 = \{x \in \mathbb{R}^n \,|\, |y_j(x)| \leq \overline{y}_j, j = 1, \ldots, m\}, \tag{81}$$

In the following lemma, we provide conditions that guarantee generic inclusions for the level set $\mathcal{L}(V, \rho)$ of a function V in $\mathcal{X}_0$, as defined in (81).

Lemma 8. *If there exist a scalar $\rho > 0$ such that the following inequalities are satisfied*

$$y_j(x)^T \rho \, \overline{y}_j^{-2} \, y_j(x) < V(x), \tag{82}$$

for $j = 1, \ldots, m$, then $\mathcal{L}(V, \rho) \subset \mathcal{X}_0$ holds, with $\mathcal{X}_0$ given by (81).

Proof. If $x \in \mathcal{L}(V, \rho)$ then $V(x) \leq \rho$. Thus, from (82), one has $\rho \geq y_j(x)^T \rho \overline{y}_j^{-2} y_j(x)$, that is, $y_j(x)^T y_j(x) \leq \overline{y}_j^2$, which implies that $x \in \mathcal{X}_0$. □

The following lemma provides the inclusion of the level set of the generalized Lure function $V_{LG}(x)$ expressed by $\mathcal{L}(V_{LG}, \rho)$ in the set (81).

Lemma 9. *If there exist matrices $P \in \mathbb{S}^{n+m}$, $\tilde{\Lambda} \in \mathbb{D}^m_{\succeq 0}$, $S_{c,j} \in \mathbb{D}^m_{\succeq 0}$ and a positive scalar ρ such that the following inequalities are satisfied*

$$\begin{bmatrix} P_{11} - \frac{1}{2} C^T (\overline{\Delta} - \underline{\Delta}) \tilde{\Lambda} C & P_{12} - \frac{1}{2} C^T (\overline{\Delta} - \underline{\Delta}) \tilde{\Lambda} D_\phi & \rho C_j^T \\ \star & P_{22} - \frac{1}{2} D_\phi^T (\overline{\Delta} - \underline{\Delta}) \tilde{\Lambda} D_\phi & \rho D_{\phi_j}^T \\ \star & \star & \rho \overline{y}_j^2 \end{bmatrix}$$
$$+ \mathrm{He} \left\{ \frac{1}{2} \begin{bmatrix} (\underline{\Delta} C)^T \\ (\underline{\Delta} D_\phi - I)^T \\ 0 \end{bmatrix} S_{c,j} \begin{bmatrix} \overline{\Delta} C & (\overline{\Delta} D_\phi - I) & 0 \end{bmatrix} \right\} \succeq 0, \tag{83}$$

for $j = 1, \ldots, m$, then $\mathcal{L}(V_{LG}, \rho) \subset \mathcal{X}_0$, with $\mathcal{X}_0$ given by (81).

Proof. From (81), we have $|y_j(x)|^2 \leq \overline{y}_j^2$. Expanding this terms by considering $y_j(x) = C_j x + D_{\phi_j}\phi(y(x))$ and then multiplying both sides of the resulting inequality by ρ, we have that $|y_j(x)|^2 \leq \overline{y}_j^2$ is equivalent to

$$\rho(x^T C_j^T + \phi^T D_{\phi_j}^T)\rho^{-1}\overline{y}_j^{-2}(C_j x + D_{\phi_j}\phi)\rho \leq \rho. \tag{84}$$

Applying Schur's Complement to the terms on the third row and third column of the matrix on the left of (83), then pre- and post-multiplying the resulting inequality, respectively by $\text{diag}(x^T, \phi^T, I)$ and its transpose, respectively, one obtains:

$$\begin{aligned}\begin{bmatrix} x \\ \phi \end{bmatrix}^T \begin{bmatrix} P_{11} & P_{12} \\ \star & P_{22} \end{bmatrix} \begin{bmatrix} x \\ \phi \end{bmatrix} - \frac{1}{2} y^T(\overline{\Delta} - \underline{\Delta})\tilde{\Lambda} y - S_\Delta(S_{c,j}, \phi, y) \\ \geq \rho(x^T C_j^T + \phi^T D_{\phi_j}^T)\rho^{-1}\overline{y}_j^{-2}(C_i x + D_{\phi_j}\phi)\rho. \end{aligned} \tag{85}$$

Suppose that (85) is satisfied. As $S_\Delta(S_{c,j}, \phi, y) \geq 0$, one has

$$\begin{bmatrix} x \\ \phi \end{bmatrix}^T \begin{bmatrix} P_{11} & P_{12} \\ \star & P_{22} \end{bmatrix} \begin{bmatrix} x \\ \phi \end{bmatrix} - \frac{1}{2} y^T(\overline{\Delta} - \underline{\Delta})\tilde{\Lambda} y \geq \rho(x^T C_j^T + \phi^T D_{\phi_j}^T)\rho^{-1}\overline{y}_j^{-2}(C_j x + D_{\phi_j}\phi)\rho. \tag{86}$$

From (76), we can thus conclude that

$$\begin{bmatrix} x \\ \phi \end{bmatrix}^T \begin{bmatrix} P_{11} & P_{12} \\ \star & P_{22} \end{bmatrix} \begin{bmatrix} x \\ \phi \end{bmatrix} + \sum_{i=1}^{m} \lambda_i \int_0^{y_i} (\phi_i(s) - \underline{\delta}_i s)\mathrm{d}s > y_j(x)^T \rho \overline{y}_j^{-2} y_j(x). \tag{87}$$

Hence, if $x \in \mathcal{L}(V_{LG}, \rho)$, one has $y_j(x)^T \rho \overline{y}_j^{-2} y_j(x) \leq \rho$, that is, $y_j(x)^T y_j(x) \leq \overline{y}_j^2$, which implies that $x \in \mathcal{X}_0$. □

Remark 8. *Aiming the comparison with other candidate functions, to include the level sets $\mathcal{L}(V_Q, \rho)$ and $\mathcal{L}(V_L, \rho)$ in (81), we adapt the inequalities (83) from Lemma 9 by considering $P = \begin{bmatrix} P_{11} & 0 \\ \star & 0 \end{bmatrix}$ and $\tilde{\Lambda} = 0$. Observe that the conditions for the function V_L are reduced to the inclusion of the level set $\mathcal{L}(V_Q, \rho)$ in $\mathcal{X}_0$. Note that $\mathcal{L}(V_Q, \rho)$ is an outer approximation of $\mathcal{L}(V_L, \rho)$. To guarantee the inclusion of the level set $\mathcal{L}(V_{QG}, \rho)$ in (81), it suffices to consider $\tilde{\Lambda} = 0$. For the special case where $D_{\phi_j} = 0$, inequalities (83) to guarantee the inclusion of the level sets $\mathcal{L}(V_Q, \rho)$ and $\mathcal{L}(V_L, \rho)$ in $\mathcal{X}_0$, are replaced by:*

$$\begin{bmatrix} P_{11} & \rho C_j^T \\ \star & \rho \overline{y}_j^2 \end{bmatrix} \succeq 0. \tag{88}$$

From the given inclusion conditions, we present below the main result of this section, which provides conditions to guarantee asymptotic convergence of the trajectories of the closed-loop Lure system (50) to the origin in a regional context.

4.3.3 Main Results

The following theorem presents sufficient conditions to assess the asymptotic stability of the origin of the sampled-data closed-loop system (50) in a regional context, under aperiodic sampling satisfying $T_k \in [\mathcal{T}_1, \mathcal{T}_2]$. In this case, the sector nonlinearity ϕ is supposed to satisfy (19) only for $y \in \mathcal{Y}_0$, or equivalently for $x \in \mathcal{X}_0$, as defined in (72).

Theorem 7. *For given $0 < \mathcal{T}_1 \leq \mathcal{T}_2$, assume that there exist matrices $P \in \mathbb{S}^{n+m}$, $\Lambda \in \mathbb{D}^m$, $\tilde{\Lambda} \in \mathbb{D}^m_{\succeq 0}$, $U_h \in \mathbb{D}^m_{\succeq 0}$, $h = 0, \ldots, 3$, $F_x \in \mathbb{S}^n_{\succ 0}$, $F_\phi \in \mathbb{S}^m_{\succ 0}$, $R_x \in \mathbb{S}^n_{\succ 0}$, $R_\phi \in \mathbb{S}^m_{\succ 0}$, $Q_x \in \mathbb{R}^{(3n)\times n}$, $Q_\phi \in \mathbb{R}^{(3m)\times m}$, $X \in \mathbb{S}^{n+m}_{\succ 0}$, $L \in \mathbb{R}^{3(n+m)\times n}$ that satisfy, for $i = 1, 2$:*

$$\Psi_1(\mathcal{T}_i) = \Pi_1 + \mathcal{T}_i\Pi_2 + \mathcal{T}_i\Pi_3 \prec 0 \tag{89}$$

$$\Psi_2(\mathcal{T}_i) = \begin{bmatrix} \Pi_1 - \mathcal{T}_i\Pi_3 & \mathcal{T}_i M_{135}^T Q_x & \mathcal{T}_i M_{246}^T Q_\phi \\ \star & -\mathcal{T}_i R_x & 0 \\ \star & \star & -\mathcal{T}_i R_\phi \end{bmatrix} \prec 0 \tag{90}$$

$$\Lambda \succeq -\tilde{\Lambda} \tag{91}$$

$$P - \frac{1}{2}\begin{bmatrix} C^T \\ D_\phi^T \end{bmatrix}(\overline{\Delta} - \underline{\Delta})\tilde{\Lambda}\begin{bmatrix} C & D_\phi \end{bmatrix} + \mathrm{He}\left\{\frac{1}{2}\begin{bmatrix} (\underline{\Delta}C)^T \\ (\underline{\Delta}D_\phi - I)^T \end{bmatrix} U_0 \begin{bmatrix} \overline{\Delta}C & (\overline{\Delta}D_\phi - I) \end{bmatrix}\right\} \succ 0, \tag{92}$$

with

$$\begin{aligned}
\Pi_1 &= \mathrm{He}\{M_{12}^T P M_{34}\} - M_{15}^T F_x M_{15} - M_{26}^T F_\phi M_{26} \\
&\quad - \mathrm{He}\left\{\frac{1}{2}(M_1^T(\underline{\Delta}C)^T + M_2^T(\underline{\Delta}D_\phi - I)^T)\Lambda C M_3\right\} \\
&\quad - \mathrm{He}\left\{\frac{1}{2}(M_1^T(\underline{\Delta}C)^T + M_2^T(\underline{\Delta}D_\phi - I)^T)\Lambda D_\phi M_4\right\} \\
&\quad + \mathrm{He}\{M_2^T(I - (\underline{\Delta}D_\phi)^T) - M_1^T(\underline{\Delta}C)^T)U_1(\overline{\Delta}CM_1 + (\overline{\Delta}D_\phi - I)M_2)\} \\
&\quad + \mathrm{He}\{M_4^T(I - (\underline{\Gamma}D_\phi)^T) - M_3^T(\underline{\Gamma}C)^T)U_2(\overline{\Gamma}CM_3 + (\overline{\Gamma}D_\phi - I)M_4)\} \\
&\quad + \mathrm{He}\{M_6^T(I - (\underline{\Delta}D_\phi)^T) - M_5^T(\underline{\Delta}C)^T)U_3(\overline{\Delta}CM_5 + (\overline{\Delta}D_\phi - I)M_6)\} \\
&\quad - \mathrm{He}\{M_{135}^T Q_x M_{15}\} - \mathrm{He}\{M_{246}^T Q_\phi M_{26}\} + \mathrm{He}\{LM_0\} \\
\Pi_2 &= M_3^T R_x M_3 + \mathrm{He}\{M_3^T F_x M_{15}\} + \mathrm{He}\{M_4^T F_\phi M_{26}\} + M_4^T R_\phi M_4 \\
\Pi_3 &= M_{56}^T X M_{56},
\end{aligned} \tag{93}$$

where

$$\begin{aligned}
M_0 &= [A \;\; B_\phi \;\; -I \;\; 0 \;\; B_u K_x \;\; B_u K_\phi] \\
M_1 &= [I \;\; 0 \;\; 0 \;\; 0 \;\; 0 \;\; 0] \qquad M_2 = [0 \;\; I \;\; 0 \;\; 0 \;\; 0 \;\; 0] \quad M_3 = [0 \;\; 0 \;\; I \;\; 0 \;\; 0 \;\; 0] \\
M_4 &= [0 \;\; 0 \;\; 0 \;\; I \;\; 0 \;\; 0] \qquad M_5 = [0 \;\; 0 \;\; 0 \;\; 0 \;\; I \;\; 0] \quad M_6 = [0 \;\; 0 \;\; 0 \;\; 0 \;\; 0 \;\; I] \\
M_{15} &= M_1 - M_5 \qquad M_{26} = M_2 - M_6 \\
M_{12} &= [M_1^T \;\; M_2^T]^T \qquad M_{34} = [M_3^T \;\; M_4^T]^T \qquad M_{56} = [M_5^T \;\; M_6^T]^T \\
M_{135} &= [M_1^T \;\; M_3^T \;\; M_5^T]^T \quad M_{246} = [M_2^T \;\; M_4^T \;\; M_6^T]^T.
\end{aligned}$$

Then, the corresponding trajectories of the closed-loop system, (50), with ϕ satisfying (19) and $T_k \in [\mathcal{T}_1, \mathcal{T}_2]$ converge asymptotically to the origin for all initial conditions belonging to $\mathcal{L}(V_{LG}, \rho) \subset \mathcal{X}_0$.

Proof. The proof follows the same steps as demonstrated in *Theorem 6*. The inequalities (89)-(92) ensures the positivity of V_{LG} and that $\dot{W}(\tau, x_k, T_k) < 0$. However, by virtue of *Theorem 5*, in this case we need the functional $\mathcal{W}_0$ to be positive definite. With this aim, we consider in the developments a particular structure of the functional $\mathcal{W}_0$ defined in (42), with $G_x = 0$, $G_\phi = 0$ and we assume $X \succ 0$, $F_x \succ 0$ and $F_\phi \succ 0$, which implies the positivity of the crossed terms between $x_k(\tau)$ and $x_k(0)$ and between $\phi_k(\tau)$ and $\phi_k(0)$, guaranteeing, by consequence, the positivity of the functional. □

Remark 9. *The inclusion of the level set $\mathcal{L}(V_{LG}, \rho) \subset \mathcal{X}_0$ is ensured by inequalities (74) from Lemma 7 for the case where the validity region is asymmetric ($\mathcal{X}_0$ as in (72)), or by inequalities (83) from Lemma 9 for the symmetric case ($\mathcal{X}_0$ as in (81)). For comparison results with different structures of V, the reader can refer to Remark 5.*

4.3.4 Optimization Problems

From the above conditions, we can formulate the following optimization problems.

P4. Given $\mathcal{T}_1$, the sector and slope bounds and the domain of validity of the sector conditions $\mathcal{X}_0$, find the maximal $\mathcal{T}_2$ and obtain an estimate of the region of attraction for which the stability of the closed-loop system (50) is ensured.

P5. Given a nominal sampling time $\mathcal{T}_{nom}$, the sector and slope bounds and the domain of validity of the sector conditions $\mathcal{X}_0$, find a bound on the maximum symmetrical allowable jitter, denoted by σ, (*i.e.*, $\mathcal{T}_1 = \mathcal{T}_{nom} - \sigma$, $\mathcal{T}_2 = \mathcal{T}_{nom} + \sigma$) and obtain an estimate of the region of attraction for which the stability of the closed-loop system (50) is ensured.

P6. Given $\mathcal{T}_1$, $\mathcal{T}_2$ and the domain of validity of the sector conditions $\mathcal{X}_0$, compute the maximum sector and slope bounds given by the diagonal matrix Ω and obtain an estimate of the region of attraction for which the stability of the closed-loop system (50) is ensured.

As seen in the previous chapter, inequalities (89), (90), (91) and (92) are LMIs by fixing $\mathcal{T}_1$, $\mathcal{T}_2$ and the parameters defining the sector and slope bounds. Moreover, inequalities (74) and (83) are also LMIs, which allow us to evaluate the conditions from *Theorem 7* through feasibility LMI problems and bisection techniques. A procedure to solve problems P4-P6 is given by the following steps:

Step 1/3 - Solve the corresponding optimization problem:

$$\begin{cases} \max\ \mathcal{T}_2\ (\text{or } \sigma,\ \text{or } \Omega) \\ \text{subject to } (89), (90), (91), (92). \end{cases} \tag{94}$$

Step 2/3 - From the matrices obtained in Step 1, determine the maximum level set of the Lyapunov function such that $\mathcal{L}(V_{LG}, \rho) \subset \mathcal{X}_0$. This can be accomplished through the following optimization problem:

$$\begin{cases} \max \rho \\ \text{subject to } (74). \text{ (Asymmetric case)} \\ \qquad\qquad (83). \text{ (Symmetric case)} \end{cases} \tag{95}$$

Step 3/3 - If the obtained level set does not touch at least one of the boundaries of the validity region $\mathcal{X}_0$, then increase ρ until this condition is satisfied. Therefore, this new level set defines an estimate of the region of attraction.

Observe that first step basically consists in solving similar LMIs to the global case, with a difference of the positivity assumptions in some matrices of the functional $\mathcal{W}_0$. In the second step, we search for the maximum level set that is included in $\mathcal{X}_0$. However, it does not necessarily touches the boundaries delimited by the validity region. Note that the inclusion conditions from *Lemma 7* and *Lemma 9* uses in its developments a lower bound for $V_{LG}(x)$ to incorporate its integral terms and then ensure the inclusion of the level sets in $\mathcal{X}_0$. This lower bound implies that an outer approximation of $\mathcal{L}(V_{LG}, \rho)$ is actually contained in $\mathcal{X}_0$. From these facts, the third step becomes necessary, which searches, for example, for a new level set of V_{LG} that in fact gives a better idea about the estimate of the region of attraction.

4.3.5 Numerical Examples

Example 1: Consider Lure system (18) with the following matrices:

$$A = \begin{bmatrix} -8 & -3 \\ 1 & 0 \end{bmatrix}, B_u = \begin{bmatrix} 2 \\ 0 \end{bmatrix}, B_\phi = \begin{bmatrix} 0.5 \\ 0 \end{bmatrix} C = \begin{bmatrix} 0.1 & 0.1 \end{bmatrix}, D_\phi = \begin{bmatrix} 0 \end{bmatrix},$$

and the control law (20) with the following gains

$$K_x = \begin{bmatrix} -1 & 1 \end{bmatrix}, \quad K_\phi = [0.25].$$

Suppose that the system is fed back by the nonlinearity $\phi(y) = \ln(1 + y)$ with sector and slope bounds that support the set inclusion $\mathcal{X}_0$ as in (72) only in the interval $[\underline{y}, \overline{y}]$, with $-1 < \underline{y} < 0$ and $0 < \overline{y} < \infty$, where the sector and slope bounds are defined by $\underline{\delta} = \frac{\ln(1+\overline{y})}{\overline{y}}$, $\overline{\delta} = \frac{\ln(1+\underline{y})}{\underline{y}}$, $\underline{\gamma} = \frac{1}{1+\overline{y}}$ and $\overline{\gamma} = \frac{1}{1+\underline{y}}$.

We take $\underline{y} = -0.99$ and $\overline{y} = 2$ and use the corresponding bounds to perform the local analysis, *i.e.*, $\underline{\delta} = 0.5493$, $\overline{\delta} = 4.6517$, $\underline{\gamma} = 0.3333$ and $\overline{\gamma} = 100$. The obtained results for problems P4-P6 are detailed in Table 6 by considering different structures of function V (see Table 1). For P4, we fixed $\mathfrak{T}_1 = 0.1$ ms. For P5, we defined $\mathfrak{T}_{nom} = 0.75$ s and for P6 we defined $\mathfrak{T}_1 = 0.1$ ms and $\mathfrak{T}_2 = 0.8$ s, but we change the sector conditions to $\underline{\delta} = \underline{\gamma} = 0$, $\overline{\delta} = \Omega$ and $\overline{\gamma} = 100$ ($\underline{y}$ and $\overline{y}$ were kept).

Table 6: Regional analysis, Ex. 1 - Results for problems P4-P6.

Problem	Parameter	V_Q	V_{QG}	V_L	V_{LG}
P4	$\boldsymbol{\mathfrak{T}_2}$	0.9543	0.9640	0.9543	1.0046
P5	$\boldsymbol{\sigma}$	0.2043	0.2140	0.2043	0.2546
P6	$\boldsymbol{\Omega}$	7.2321	8.3597	7.2321	8.7868

For P4, using the generalized Lure function V_{LG} we obtain the larger value of $\mathfrak{T}_2$. For P5, we guaranteed the stability for $\mathfrak{T}_1 = 0.4954$ s and $\mathfrak{T}_2 = 1.0046$ s, with σ greater 18.9%, 24.6% and 24.6% than the ones obtained with V_{QG}, V_L and V_Q, respectively. For the last problem, the upper sector bound represented by Ω was 5.1%, 21.4% and 21.4% bigger than the ones obtained with V_{QG}, V_L and V_Q, respectively. The estimate of the region of attraction concerning problem P4 and different structures of V is presented in Fig. 16, along with the boundaries of the region of validity of the sector conditions given by the lines $x_2 = -x_1 + 20$ and $x_2 = -x_1 - 9.9$.

Figure 16 – Regional analysis, Ex. 1 - Estimate of the region of attraction for P4 with different structures of V.

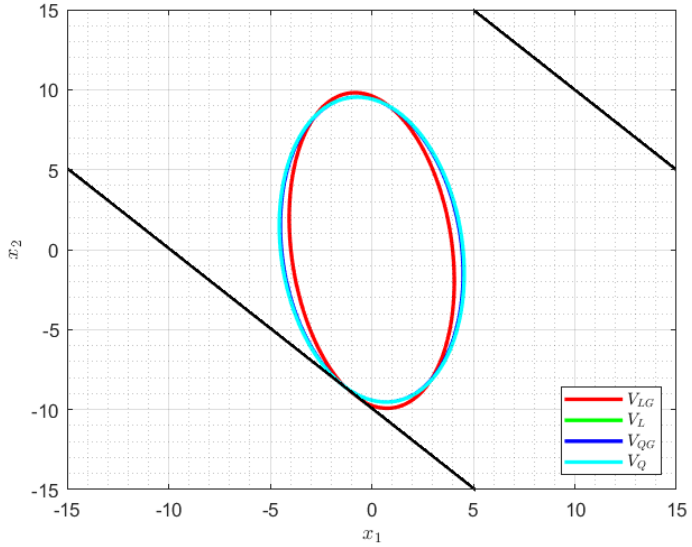

Font: Author.

The obtained level set for the function V_{LG} was $\rho = 92254.92$, with the matrices

$$P = \begin{bmatrix} 6576.65 & 558.61 & -0.0467 \\ 558.61 & 1134.12 & 0.0000 \\ -0.0467 & 0.0000 & -0.0148 \end{bmatrix}, \quad \Lambda = -5990.38, \quad \tilde{\Lambda} = 6950.39.$$

In the sequence, we simulate the closed-loop system (50) by considering the solution obtained for P4 with V_{LG} and $T_k \in [0.0001, 1.0046]$. Aiming to show that stability is guaranteed for the obtained region, different trajectories starting on the boundary of $\mathcal{L}(V_{LG}, \rho)$ are depicted in Fig. 17. To obtain the values of T_k, we used a pseudo-random algorithm (function *rand*$(\cdot)$ from MATLAB, with default seed) that generates its numbers from the standard uniform distribution over the defined interval.

Figure 17: Regional analysis, Ex. 1 - Trajectories of the closed-loop system for P4.

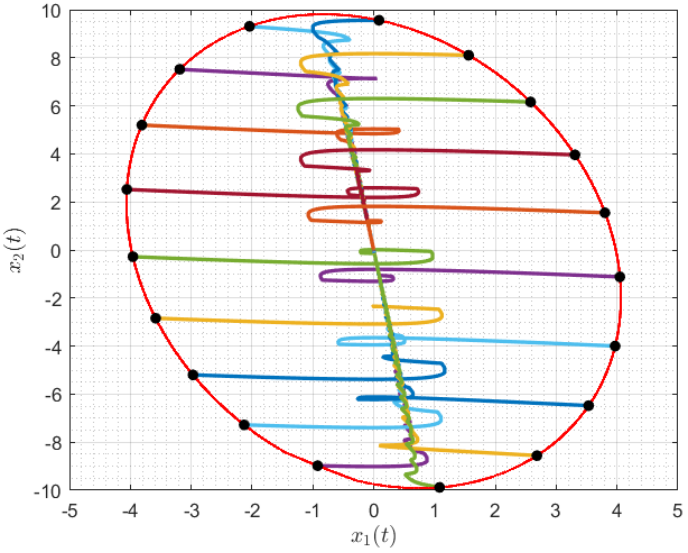

Font: Author.

Observe that with the function V_{LG} we could guarantee stability for a larger $\mathcal{T}_2$ for almost the same region. Moreover, when the system is initialized with conditions inside this region, the trajectories converge to the origin and do not leave $\mathcal{L}(V_{LG}, \rho)$, as expected. The resulting effect of the sampled-data control can be noted in the pattern of the trajectories of the system when the states get closer to the origin.

Example 2: Consider the following MIMO system, taken from (VALMORBIDA; DRUMMOND; DUNCAN, 2018):

$$\begin{cases} \dot{x}_1 &= -x_2 + \ln(1+y_1) + 2\frac{y_2}{1+y_2} \\ \dot{x}_2 &= x_1 - 0.65x_2 + \ln(1+y_1) + \frac{y_2}{1+y_2} \\ y_1 &= 0.1(x_1 + x_2) - 0.2\frac{y_2}{1+y_2} \\ y_2 &= 0.1(x_2 - x_1) \end{cases}.$$

This system can be put in the form (18) with the sampled-data control law (20) by choosing a realization for the closed-loop system, with $\phi_1(y_1) = \ln(1 + y_1)$, $\phi_2(y_2) = \frac{y_2}{1+y_2}$, as detailed below:

$$A = \begin{bmatrix} 0.5 & 1.5 \\ 0.5 & 1.35 \end{bmatrix}, B_u = \begin{bmatrix} 1 & 0.5 \\ 0.5 & 1 \end{bmatrix}, B_\phi = \begin{bmatrix} 1 & 1.25 \\ -0.5 & 1 \end{bmatrix}, C = \begin{bmatrix} 0.1 & 0.1 \\ -0.1 & 0.1 \end{bmatrix},$$
$$D_\phi = \begin{bmatrix} 0 & -0.2 \\ 0 & 0 \end{bmatrix}, K_x = \begin{bmatrix} -1 & -2 \\ 1 & -1 \end{bmatrix}, \quad K_\phi = \begin{bmatrix} -1 & 1 \\ 2 & -0.5 \end{bmatrix}.$$

This system satisfies *Proposition 1*, *i.e.*, the algebraic loop is well-posed. The nonlinearities present sector and slope bounds that, as presented in (VALMORBIDA; DRUMMOND; DUNCAN, 2018), hold only in the intervals demonstrated in Table 7.

Table 7 – Regional analysis, Ex. 2 - Local sector and slope bounds for $\ln(1+y_i)$ and $\frac{y_i}{1+y_i}$.

$\phi(y_i)$	$\underline{\delta}$	$\overline{\delta}$	$\underline{\gamma}$	$\overline{\gamma}$
$\ln(1 + y_i)$	$\frac{\ln(1+\overline{y}_i)}{\overline{y}_i}$	$\frac{\ln(1+\underline{y}_i)}{\underline{y}_i}$	$\frac{1}{1+\overline{y}_i}$	$\frac{1}{1+\underline{y}_i}$
$\frac{y_i}{1+y_i}$	$\frac{1}{1+\overline{y}_i}$	$\frac{1}{1+\underline{y}_i}$	$\frac{1}{(1+\overline{y}_i)^2}$	$\frac{1}{(1+\underline{y}_i)^2}$

Note that for both nonlinearities, (19) holds with $\mathcal{Y} = (-1, \infty)$, thus $\mathcal{Y}_0 = [\underline{y}_i, \overline{y}_i]$ is defined for $-1 < \underline{y}_i < 0$ and $0 < \overline{y}_i$. Suppose that we are interested in the interval $y_1 \in [-0.4, 50]$, $y_2 \in [-0.5, 50]$, which define the sector and slope bounds for the nonlinearities according to Table 7. The obtained results for problems P4-P6 are detailed in Table 8 by considering different structures of V. For P4, we fixed $\mathfrak{T}_1 = 0.1$ ms. For P5, we defined $\mathfrak{T}_{nom} = 0.1$ s and for P6 we defined $\mathfrak{T}_1 = 0.1$ ms and $\mathfrak{T}_2 = 0.1$ s, but we change the sector conditions to $\underline{\delta}_i = \underline{\gamma}_i = 0$, $\overline{\delta}_i = \Omega$ and $\overline{\gamma}_i = 5$, $\forall i$ ($\underline{y}_i$ and $\overline{y}_i$ were kept for all i).

Table 8: Regional analysis, Ex. 2 - Results for problems P4-P6.

Problem	Parameter	V_Q	V_{QG}	V_L	V_{LG}
P4	$\boldsymbol{\mathfrak{T}_2}$	0.1298	0.1361	0.1302	0.1943
P5	$\boldsymbol{\sigma}$	0.0298	0.0361	0.0302	0.0943
P6	$\boldsymbol{\Omega}$	1.5164	1.6472	1.5187	2.1627

For P4, using the generalized Lure function, we achieve values for $\mathfrak{T}_2$ that are greater 42.7%, 49.2% and 49.6% than the ones obtained with V_{QG}, V_L and V_Q, respectively. For P5, we guaranteed stability for $\mathfrak{T}_1 = 0.0057$ s and $\mathfrak{T}_2 = 0.1943$ s, with σ greater 161.2%, 212.2% and 216.4% than the ones obtained with V_{QG}, V_L and V_Q, respectively. For the last feasibility problem, the upper sector bounds, represented by Ω were 31.2%, 42.4% and 42.6% bigger than the ones obtained with V_{QG}, V_L and V_Q, respectively. The estimates of the region of attraction concerning obtained from the solution of P5 for different structures of V are presented in Fig. 18, along with the boundaries of the region of validity.

Figure 18 – Regional analysis, Ex. 2 - Estimate of the region of attraction for P5 with different structures of V.

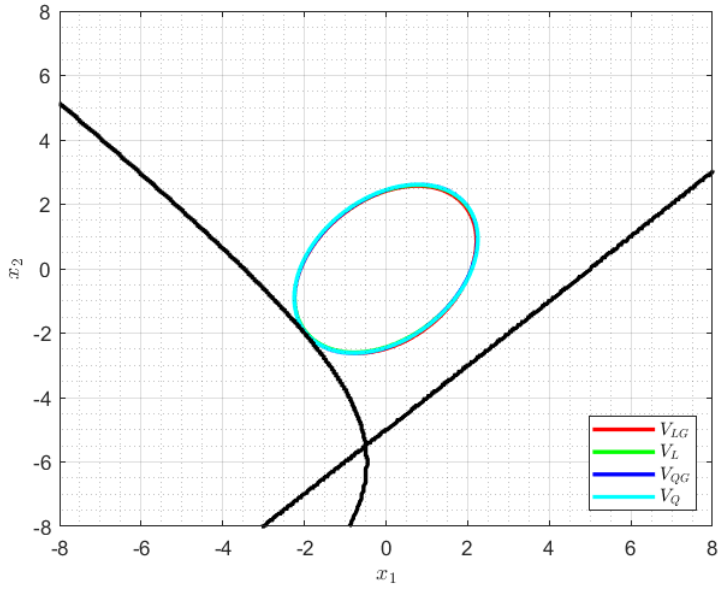

Font: Author.

The obtained level set for the function V_{LG} was $\rho = 0.8650$, with the matrices

$$P = \begin{bmatrix} 0.2208 & -0.0707 & -0.0103 & -0.0427 \\ -0.0707 & 0.1766 & -0.0025 & -0.0363 \\ -0.0103 & -0.0025 & 0.0542 & 0.0210 \\ -0.0427 & -0.0363 & 0.0210 & 0.2470 \end{bmatrix},$$

$$\Lambda = \begin{bmatrix} -1.3979 & 0 \\ 0 & -4.6468 \end{bmatrix}, \quad \tilde{\Lambda} = \begin{bmatrix} 2.2889 & 0 \\ 0 & 5.3729 \end{bmatrix}.$$

In this case, the validity region of y_2 is bounded by the lines $x_2 = -5 + x_1$ (shown in Fig. 18) and $x_2 = 500 + x_1$. On the other hand, the presence of the algebraic loop affects y_1 (see the matrix D_ϕ), which implies that an analytical expression for the bounds of the validity region of y_1 cannot be directly obtained. To overcome this problem, we make a grid on the states x_1 and x_2 (that is, we test the possible combination of the states with a sufficient spacing and range) and then we solve the implicit function $y(t) = Cx(t) + D_\phi\phi(y(t))$ for y through iterative methods. If the obtained values for y_1 are equal (or almost equal, given some tolerance) to its respective lower and upper limits given by -0.4 and 50, then we save the corresponding states that generates these outputs. This way, we map $\mathcal{Y}_0$ to $\mathcal{X}_0$, which allow us to visualize the validity region in the plane of states. One of these bounds corresponding to $y_1 = -0.4$ can be seen Fig. 18, given by the curve depicted in black. The other bound coming from the algebraic loop cannot be seen by the graph due to the scale.

Also, from Fig. 18, observe that the estimate of the region of attraction were almost the same for every function V, but we emphasize that with the function V_{LG} we guaranteed

stability for a larger jitter (see Table 8). This is justified by the fact that the function V_{LG} relaxes the positivity requirement on the Lure coefficients.

Aiming to show that stability is guaranteed for the computed estimate of the region of attraction, in the sequence we simulate the closed-loop system (50) by considering the solution obtained for P5 with V_{LG} and $T_k \in [0.0057, 0.1943]$. Once again, when the system is initialized with conditions on the boundary, we observe that the trajectories converge to the origin, which is corroborated by the obtained results.

Figure 19: Regional analysis, Ex. 2 - Trajectories of the closed-loop system for P5.

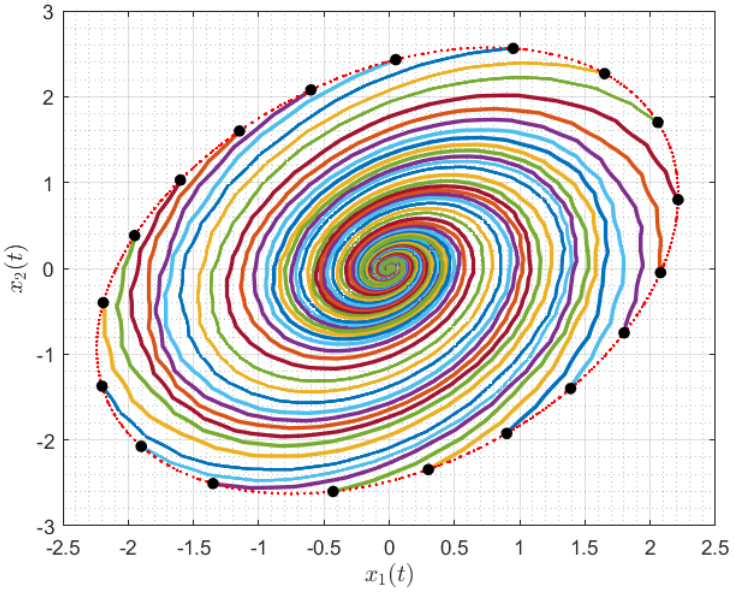

Font: Author.

Example 3: Consider system (18) given by the following matrices:

$$A = \begin{bmatrix} -2 & 1 \\ 1 & 1 \end{bmatrix}, B_u = \begin{bmatrix} 1 & 0 \\ 0 & 1 \end{bmatrix}, B_\phi = \begin{bmatrix} 1 & 0 \\ 0 & 2 \end{bmatrix} C = \begin{bmatrix} 0 & 1 \\ 1 & 0 \end{bmatrix}, D_\phi = \begin{bmatrix} 0 & 0 \\ 0 & 0 \end{bmatrix},$$

and the control law (20) with the following gains

$$K_x = \begin{bmatrix} -1 & -2 \\ -0.5 & -2 \end{bmatrix}, \quad K_\phi = \begin{bmatrix} 0 & 1 \\ -0.5 & 1 \end{bmatrix}.$$

Suppose that this system is fed back by the nonlinearities $\phi(y_1) = \sin(y_1)$, $\phi(y_2) = \sin(y_2)$. This nonlinearities lie in a sector given by $\underline{\delta}_1 = \underline{\delta}_2 = 0$, $\overline{\delta}_1 = \overline{\delta}_2 = 1$, with slope bounds $\underline{\gamma}_1 = \underline{\gamma}_2 = -1$ and $\overline{\gamma}_1 = \overline{\gamma}_2 = 1$, provided that y_1, $y_2 \in [-\pi, \pi]$. In this case, the obtained results for problems P4-P6 are detailed in Table 9 by considering different structures of V. For P4, we fixed $\mathcal{T}_1 = 0.1$ ms. For P5, we defined $\mathcal{T}_{nom} = 0.25$ s and for P6 we defined $\mathcal{T}_1 = 0.1$ ms and $\mathcal{T}_2 = 0.2$ s, but we change the sector conditions to $\underline{\delta}_i = 0$, $\underline{\gamma}_i = -\Omega$, $\overline{\delta}_i = \overline{\gamma}_i = \Omega$, $\forall i$ ($\underline{y}_i$ and $\overline{y}_i$ were kept $\forall i$).

Table 9: Regional analysis, Ex. 3 - Results for problems P4-P6.

Problem	Parameter	V_Q	V_{QG}	V_L	V_{LG}
P4	$\mathfrak{T}_2$	0.3403	0.3464	0.3437	0.4052
P5	σ	0.0904	0.0965	0.1513	0.1553
P6	Ω	1.2902	1.3063	1.3750	1.4397

Using the generalized Lure function V_{LG}, for P4 we achieve values for $\mathfrak{T}_2$ that are greater 16.9%, 17.8% and 19.0% than the ones obtained with V_{QG}, V_L and V_Q, respectively. For P5, we guaranteed the stability for $\mathfrak{T}_1 = 0.0947$ s and $\mathfrak{T}_2 = 0.4053$ s, with σ greater 2.6%, 60.9% and 71.7% than the ones obtained with V_L, V_{QG} and V_Q, respectively. For the last problem, the sector and slope bounds represented by Ω were 4.7%, 10.2% and 11.5% bigger than the ones obtained with V_L, V_{QG} and V_Q, respectively. The estimates of the region of attraction corresponding to the solution of P6 for the different functions V are presented in Fig. 20, along with the boundaries of the region of validity. The obtained level set for the function V_{LG} was $\rho = 0.4550$, with the matrices

$$P = \begin{bmatrix} 0.1233 & -0.0040 & -0.0161 & 0.0175 \\ -0.0040 & 0.0478 & -0.0013 & -0.0227 \\ -0.0161 & -0.0013 & 0.0022 & 0.0070 \\ 0.0175 & -0.0227 & 0.0070 & 0.0140 \end{bmatrix},$$

$$\Lambda = \begin{bmatrix} -0.0340 & 0 \\ 0 & 0.0501 \end{bmatrix}, \quad \tilde{\Lambda} = \begin{bmatrix} 0.0386 & 0 \\ 0 & 0.0379 \end{bmatrix}.$$

Figure 20 – Regional analysis, Ex. 3 - Estimate of the region of attraction for P6 with different structures of V.

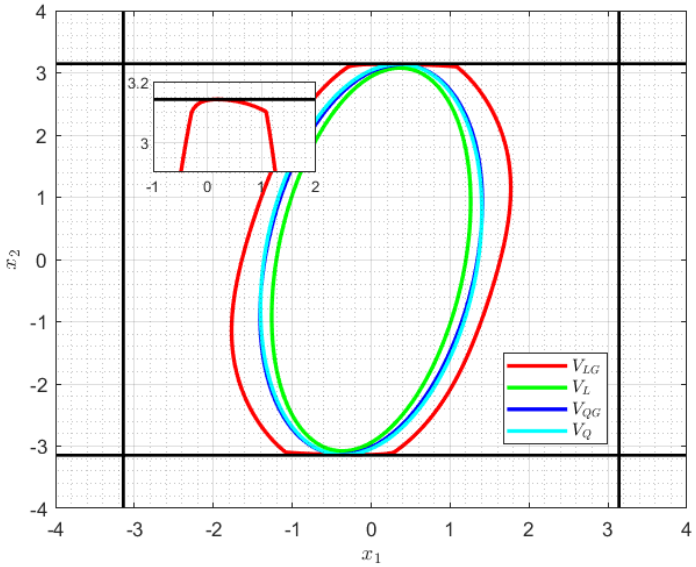

Font: Author.

In this case, the validity region in $\mathbb{R}^n$ can be described as $\mathcal{X}_0 = \{x \in \mathbb{R}^2 | -\pi \leq x_i \leq \pi, i = 1, 2\}$, as shown in Fig. 20. Observe that with the function V_{LG}, we enlarge the estimate of the region of attraction in comparison to the other functions. Furthermore, we increase the sector and slope admissible bounds.

To show that stability is guaranteed for the obtained region, we simulate the closed-loop system (50), as presented in Fig. 21, by considering the solution of P6 with V_{LG}, $T_k \in [0.0001, 0.2]$ and the nonlinearities $\phi(y_1) = 1.4\sin(y_1)$ and $\phi(y_2) = 1.4\sin(y_2)$, which satisfies the sector conditions for $\underline{\delta}_1 = \underline{\delta}_2 = 0$, $\overline{\delta}_1 = \overline{\delta}_2 = 1.4$, $\underline{\gamma}_1 = \underline{\gamma}_2 = -1.4$ and $\overline{\gamma}_1 = \overline{\gamma}_2 = 1.4$.

Figure 21: Regional analysis, Ex. 3 - Trajectories of the closed-loop system for P6.

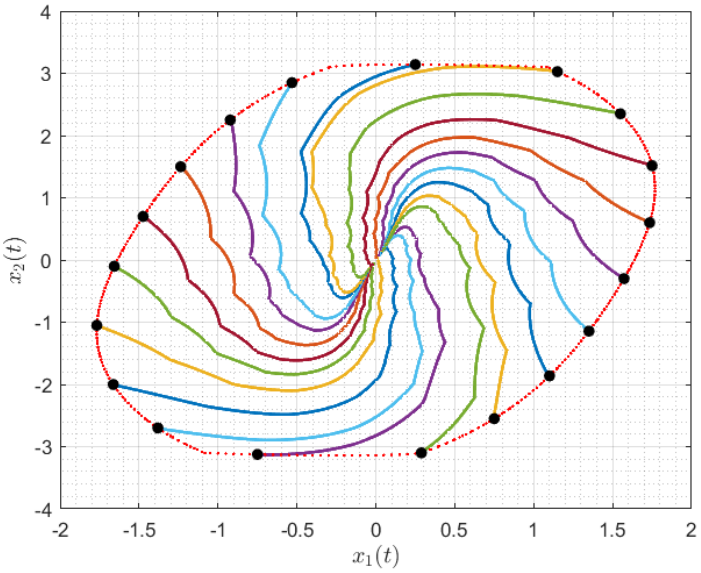

Font: Author.

As observed, all the trajectories starting at the boundary of the obtained estimate of the region of attraction converge to the origin.

4.4 Final Comments

The main contribution of this chapter was the proposition of new methods for stability analysis of sampled-data Lure systems. Conditions in the form of LMIs were derived to ensure that the generic conditions provided by *Theorem 4* and *Theorem 5* are satisfied, thus guaranteeing the global or regional convergence of the trajectories of the continuous-time system to the origin.

Optimization problems are stated for global and regional contexts. In the first one, we aim to maximize the admissible intersampling intervals or the maximal sector bounds, such that stability holds globally. In the latter, the solution of these optimization problems also provide an estimate of the region of attraction of the origin for the continuous-time

trajectories of the closed-loop system. Numerical examples are provided for both contexts with a comparative result with (SEIFULLAEV; FRADKOV, 2015) on the global analysis.

The obtained results are significantly better with the function V_{LG} in comparison to those achieved with other functions V. Regarding the local analysis, for instance, it has been shown that the reduction in conservatism provided by V_{LG}, in addition to improving the maximal $\mathcal{T}_2$, σ or Ω can also lead to better estimates of the region of attraction in some cases, which highlights the potentialities of the method.

5 SYNTHESIS OF STABILIZING CONTROLLERS

5.1 Introduction

In this chapter, the synthesis of a controller for system (18), given by the control law (20) is tackled. The global and regional results from the Chapter 4 underpin the developments presented here, aiming at obtaining sufficient conditions for the constraints of *Theorem 4* and *Theorem 5*, respectively, in the form of matrix inequalities from which solutions the gains K_x and K_ϕ can be computed.

The main obstacle to achieve this goal is to manipulate the stability conditions presented in the last chapter in an appropriate manner to provide optimization problems in SDP formulation. As it will be seen, LMI constraints can only be obtained by considering some particular structures of the involved variables. Furthermore, some of this variables need to be fixed. To overcome this problem, we propose a Particle Swarm Optimization (PSO) algorithm to test the feasibility of the LMIs while searching for the best combination of the variables that need to be fixed according to each optimization problem.

5.2 Global Results

To obtain global synthesis conditions, some extra assumptions need to be made. Let us consider without loss of generalization (as a loop transformation can always be done) $\underline{\Delta} = 0$. Besides, assume that the nonlinearities are monotonically increasing, that is, $\underline{\Gamma} = 0$. We also consider a Lure function $V_R : \mathbb{R}^n \to \mathbb{R}^+$, recalled as follows, which is a particular case of function V_{LG} given in (43) with $\underline{\delta}_i = 0$ and $\lambda_i > 0, \forall i, i = 1, \ldots, m$.

$$V_R(x) = V_{QG}(x) + \sum_{i=1}^{m} \lambda_i \int_0^{y_i} \phi_i(s)\,\mathrm{d}s, \quad \lambda_i > 0, \tag{96}$$

The positivity of V_R is guaranteed by the following lemma:

Lemma 10. *Consider $V_R(x)$ in (96), where ϕ satisfies (19a)-(19b) with $\underline{\delta}_i = 0$, $\forall i$. If there exist a matrix $L \in \mathbb{D}^m_{\succeq 0}$ such that*

$$\begin{bmatrix} P_{11} & P_{12} \\ P_{12}^T & P_{22} \end{bmatrix} + \mathrm{He}\left\{ \frac{1}{2} \begin{bmatrix} 0 \\ -I \end{bmatrix} L^{-1} \begin{bmatrix} \overline{\Delta} C & (\overline{\Delta} D_\phi - I) \end{bmatrix} \right\} \succ 0, \tag{97}$$

then $V_R(x) > 0, \forall x \in \mathbb{R}^n, x \neq 0$.

Proof. Note that (97) implies that

$$V_{QG}(x) > S_\Delta(L^{-1}, \phi_k(\tau), y_k(\tau)) \geq 0. \tag{98}$$

Hence, from *Lemma 2*, and the fact that $\sum_{i=1}^{m} \lambda_i \int_0^{y_i} \phi_i(s)\mathrm{d}s \geq 0$, $\forall x \in \mathbb{R}^n$, we conclude that $V_R(x) > 0, \forall x \in \mathbb{R}^n$. □

The following theorem provides conditions to obtain gains K_x and K_ϕ that ensure the asymptotic stability of the origin of the closed-loop system under aperiodic sampling.

Theorem 8. *If there exist matrices* $\tilde{P} \in \mathbb{S}^{n+m}$, $\tilde{Y} \in \mathbb{R}^{n\times n}$, $\tilde{U} \in \mathbb{D}^m_{\succeq 0}$, $\tilde{F}_x \in \mathbb{S}^n$, $\tilde{G}_x \in \mathbb{R}^{n\times n}$, $\tilde{F}_\phi \in \mathbb{S}^m$, $\tilde{G}_\phi \in \mathbb{R}^{m\times m}$, $\tilde{R}_x \in \mathbb{S}^n_{\succ 0}$, $\tilde{R}_\phi \in \mathbb{S}^m_{\succ 0}$, $\tilde{Q}_x \in \mathbb{R}^{3(n+m)\times n}$, $\tilde{Q}_\phi \in \mathbb{R}^{3(n+m)\times m}$, $\tilde{X} \in \mathbb{S}^{n+m}$, $\tilde{K}_x \in \mathbb{R}^{q\times n}$, $\tilde{K}_\phi \in \mathbb{R}^{q\times m}$, $\overline{\Lambda} \in \mathbb{D}^m_{\succeq 0}$ *and positive scalars* ε, β, *that satisfy, for* $i = 1,2$*:*

$$\tilde{\Psi}_1(\mathcal{T}_i) = \tilde{\Pi}_1 + \mathcal{T}_i\tilde{\Pi}_2 + \mathcal{T}_i\tilde{\Pi}_3 \prec 0 \tag{99}$$

$$\tilde{\Psi}_2(\mathcal{T}_i) = \begin{bmatrix} \tilde{\Pi}_1 - \mathcal{T}_i\tilde{\Pi}_3 & \mathcal{T}_i\tilde{Q}_x & \mathcal{T}_i\tilde{Q}_\phi \\ \star & -\mathcal{T}_i\tilde{R}_x & 0 \\ \star & \star & -\mathcal{T}_i\tilde{R}_\phi \end{bmatrix} \prec 0 \tag{100}$$

$$\begin{bmatrix} 2\tilde{P}_{11} & 2\tilde{P}_{12} - \tilde{Y}^T C^T \overline{\Delta} \\ \star & 2\tilde{P}_{22} + 2(I - \overline{\Delta}D_\phi)\tilde{U} \end{bmatrix} \succ 0, \tag{101}$$

with

$$\begin{aligned}
\tilde{\Pi}_1 &= \mathrm{He}\left\{M_{12}^T\tilde{P}M_{34}\right\} - M_{15}^T\tilde{F}_xM_{15} - \mathrm{He}\{M_{15}^T\tilde{G}_xM_5\} + \mathrm{He}\left\{\frac{1}{2}M_2^T\overline{\Lambda}C\tilde{Y}M_3\right\} \\
&\quad + \mathrm{He}\left\{\frac{1}{2}M_2^T\overline{\Lambda}D_\phi\tilde{U}M_4\right\} - (M_2 - \beta M_6)^T\tilde{F}_\phi(M_2 - \beta M_6) \\
&\quad - \mathrm{He}\{\beta(M_2 - \beta M_6)^T\tilde{G}_\phi M_6\} + \mathrm{He}\left\{M_2^T(\overline{\Delta}C\tilde{Y}M_1 + (\overline{\Delta}D_\phi - I)\tilde{U}M_2)\right\} \\
&\quad + \mathrm{He}\left\{M_4^T(\overline{\Gamma}C\tilde{Y}M_3 + (\overline{\Gamma}D_\phi - I)\tilde{U}M_4)\right\} \\
&\quad + \mathrm{He}\left\{M_6^T(\overline{\Delta}C\tilde{Y}M_5 + (\overline{\Delta}D_\phi - I)\beta\tilde{U}M_6)\right\} - \mathrm{He}\{\tilde{Q}_xM_{15}\} - \mathrm{He}\{\tilde{Q}_\phi(M_2 - \beta M_6)\} \\
&\quad + \mathrm{He}\{(\varepsilon M_1^T + M_3^T)(A\tilde{Y}M_1 + B_\phi\tilde{U}M_2 - \tilde{Y}M_3 + B_u\tilde{K}_xM_5 + B_u\beta\tilde{K}_\phi M_6)\} \\
\tilde{\Pi}_2 &= M_3^T\tilde{R}_xM_3 + \mathrm{He}\{M_3^T(\tilde{F}_xM_{15} + \tilde{G}_xM_5)\} \\
&\quad + M_4^T\tilde{R}_\phi M_4 + \mathrm{He}\{M_4^T[\tilde{F}_\phi(M_2 - \beta M_6) + \tilde{G}_\phi\beta M_6]\} \\
\tilde{\Pi}_3 &= M_{56}^T\tilde{X}M_{56},
\end{aligned} \tag{102}$$

where[1]

$$
\begin{aligned}
M_1 &= [I\ 0\ 0\ 0\ 0\ 0] \qquad M_2 = [0\ I\ 0\ 0\ 0\ 0] \quad M_3 = [0\ 0\ I\ 0\ 0\ 0]\\
M_4 &= [0\ 0\ 0\ I\ 0\ 0] \qquad M_5 = [0\ 0\ 0\ 0\ I\ 0] \quad M_6 = [0\ 0\ 0\ 0\ 0\ I]\\
M_{15} &= M_1 - M_5 \qquad M_{26} = M_2 - M_6\\
M_{12} &= [M_1^T\ M_2^T]^T \qquad M_{34} = [M_3^T\ M_4^T]^T \qquad M_{56} = [M_5^T\ M_6^T]^T\\
M_{135} &= [M_1^T\ M_3^T\ M_5^T]^T \quad M_{246} = [M_2^T\ M_4^T\ M_6^T]^T\\
M_0 &= [A\ B_\phi\ -I\ 0\ B_uK_x\ B_uK_\phi]
\end{aligned} \tag{103}
$$

Then, the gains $K_x = \tilde{K}_x\tilde{Y}^{-1}$ *and* $K_\phi = \tilde{K}_\phi\tilde{U}^{-1}$ *ensures that the origin of the sampled-data closed-loop system (50) with* ϕ *satisfying (19) with* $\underline{\Delta} = \underline{\Gamma} = 0$ *and* $T_k \in [\mathcal{T}_1, \mathcal{T}_2]$ *is globally asymptotically stable.*

Proof. Considering the result of *Theorem 8*, the idea is to prove that (30) is satisfied, $\forall k \in \mathbb{N}$, considering a functional $\mathcal{W}_0$ as given in (42) and a Lure-type function (96) provided that (99) and (100) are verified. With this aim, the expression of $\dot{W}$ is obtained as follows:

$$
\begin{aligned}
\dot{W}(\tau, x_k, T_k) &= 2\begin{bmatrix} x_k(\tau) \\ \phi_k(\tau) \end{bmatrix}^T P \begin{bmatrix} \dot{x}_k(\tau) \\ \dot{\phi}_k(\tau) \end{bmatrix} + [\phi_k^T(\tau)\Lambda C]\dot{x}_k(\tau) + [\phi_k^T(\tau)\Lambda D_\phi]\dot{\phi}_k(\tau)\\
&- (x_k(\tau) - x_k(0))^T[F_x(x_k(\tau) - x_k(0)) + 2G_x x_k(0)]\\
&+ (T_k - \tau)\dot{x}_k^T(\tau)[R_x\dot{x}_k(\tau) + 2F_x(x_k(\tau) - x_k(0)) + 2G_x x_k(0)] - \int_0^\tau \dot{x}_k^T(\theta)R_x\dot{x}_k(\theta)\mathrm{d}\theta\\
&+ (T_k - 2\tau)\begin{bmatrix} x_k(0) \\ \phi_k(0) \end{bmatrix}^T X \begin{bmatrix} x_k(0) \\ \phi_k(0) \end{bmatrix} - (\phi_k(\tau) - \phi_k(0))^T[F_\phi(\phi_k(\tau) - \phi_k(0)) + 2G_\phi\phi_k(0)]\\
&+ (T_k - \tau)\dot{\phi}_k^T(\tau)[R_\phi\dot{\phi}_k(\tau) + 2F_\phi(\phi_k(\tau) - \phi_k(0)) + 2G_\phi\phi_k(0)] - \int_0^\tau \dot{\phi}_k^T(\theta)R_\phi\dot{\phi}_k(\theta)\mathrm{d}\theta.
\end{aligned} \tag{104}
$$

Using the sector conditions defined in *Lemma 1* and *Lemma 2*, and considering $U_1 = U_2 = U$ and $U_3 = \beta^{-1}U$ (see the proof of *Theorem 6*), we have that

$$
\begin{aligned}
\dot{W}(\tau, x_k, T_k) \leq \dot{W}(\tau, x_k, T_k) &+ 2S_\Delta(U, \phi_k(\tau), y_k(\tau))\\
&+ 2S_\Gamma(U, \dot{\phi}_k(\tau), \dot{y}_k(\tau)) + 2S_\Delta(\beta^{-1}U, \phi_k(0), y_k(0)),
\end{aligned} \tag{105}
$$

or, equivalently,

$$
\begin{aligned}
\dot{W}(\tau, x_k, T_k) \leq \dot{W}(\tau, x_k, T_k) &+ 2\phi_k^T(\tau)U(\overline{\Delta}Cx_k(\tau) + (\overline{\Delta}D_\phi - I)\phi_k(\tau))\\
&+ 2\dot{\phi}_k^T(\tau)U(\overline{\Gamma}C\dot{x}_k(\tau) + (\overline{\Gamma}D_\phi - I)\dot{\phi}_k(\tau))\\
&+ 2\phi_k^T(0)\beta^{-1}U(\overline{\Delta}Cx_k(0) + (\overline{\Delta}D_\phi - I)\phi_k(0)).
\end{aligned} \tag{106}
$$

[1]The matrices M_i are not of the same dimension. The notations 0 and I correspond to the zero and identity matrices of appropriate dimension.

Consider the vector $\eta_k(\tau) = [x_k^T(\tau)\ \phi_k^T(\tau)\ \dot{x}_k^T(\tau)\ \dot{\phi}_k^T(\tau)\ x_k^T(0)\ \phi_k^T(0)]^T$, the vectors $\zeta_k(\tau) = M_{135}\,\eta_k(\tau)$, $\psi_k(\tau) = M_{246}\,\eta_k(\tau)$ and matrices $Q_x \in \mathbb{R}^{(3n)\times n}$ and $Q_\phi \in \mathbb{R}^{(3m)\times m}$. It follows that

$$\int_0^\tau \dot{x_k}^T(\theta) R_x \dot{x_k}(\theta) \mathrm{d}\theta - 2\zeta_k^T(\tau) Q_x (x_k(\tau) - x_k(0)) + \tau \zeta_k^T(\tau) Q_x R_x^{-1} Q_x^T \zeta_k(\tau) \geq 0, \tag{107}$$

$$\int_0^\tau \dot{\phi}_k^T(\theta) R_\phi \dot{\phi}_k(\theta) \mathrm{d}\theta - 2\psi_k^T(\tau) Q_\phi (\phi_k(\tau) - \phi_k(0)) + \tau \psi_k^T(\tau) Q_\phi R_\phi^{-1} Q_\phi^T \psi_k(\tau) \geq 0. \tag{108}$$

On the other hand, from (27), and considering $L = \varepsilon M_1^T Y^T + M_3^T Y^T$ it follows that

$$2(x_k^T(\tau)\varepsilon Y^T + \dot{x}_k^T(\tau) Y^T)(A x_k(\tau) + B_\phi \phi_k(\tau) - \dot{x}_k(\tau) + B_u(K_x x_k(0) + K_\phi \phi_k(0)) = 0, \tag{109}$$

along the trajectories of (27) for any matrix $Y \in \mathbb{R}^{n\times n}$, where ε is a positive free scalar. This null term can be added to (106). Hence, combining (106), (107), (108) and (109), one obtains that

$$\begin{aligned} \dot{W} \leq \eta_k^T(\tau)[&\Pi_1 + (T_k - \tau)\Pi_2 + \tau(M_{135}^T Q_x R_x^{-1} Q_x^T M_{135} + M_{246}^T Q_\phi R_\phi^{-1} Q_\phi^T M_{246}) \\ &+ (T_k - 2\tau)\Pi_3]\eta_k(\tau), \end{aligned} \tag{110}$$

with

$$\begin{aligned} \Pi_1 = {} & \mathrm{He}\{M_{12}^T P M_{34}\} - M_{15}^T F_x M_{15} - \mathrm{He}\{M_{15}^T G_x M_5\} + \mathrm{He}\left\{\frac{1}{2} M_2^T \Lambda C M_3\right\} \\ & + \mathrm{He}\left\{\frac{1}{2} M_2^T \Lambda D_\phi M_4\right\} - M_{26}^T F_\phi M_{26} - \mathrm{He}\{M_{26}^T G_\phi M_6\} \\ & + \mathrm{He}\{M_2^T U(\overline{\Delta} C M_1 + (\overline{\Delta} D_\phi - I) M_2)\} + \mathrm{He}\{M_4^T U(\overline{\Gamma} C M_3 + (\overline{\Gamma} D_\phi - I) M_4)\} \\ & + \mathrm{He}\{M_6^T \beta^{-1} U(\overline{\Delta} C M_5 + (\overline{\Delta} D_\phi - I) M_6)\} - \mathrm{He}\{M_{135}^T Q_x M_{15}\} \\ & - \mathrm{He}\{M_{246}^T Q_\phi M_{26}\} + \mathrm{He}\{(M_1^T \varepsilon Y^T + M_3^T Y^T) M_0\} \\ \Pi_2 = {} & M_3^T R_x M_3 + \mathrm{He}\{M_3^T (F_x M_{15} + G_x M_5)\} + \mathrm{He}\{M_4^T (F_\phi M_{26} + G_\phi M_6)\} \\ & + M_4^T R_\phi M_4 \\ \Pi_3 = {} & M_{56}^T X M_{56}. \end{aligned} \tag{111}$$

Suppose that Y is nonsingular and define the matrices $\tilde{Y} = Y^{-1}$, $\tilde{U} = U^{-1}$ and $\Xi = \mathrm{diag}\{\tilde{Y}, \tilde{U}, \tilde{Y}, \tilde{U}, \tilde{Y}, \beta\tilde{U}\}$. Consider now the vector $\tilde{\eta}_k(\tau) = \Xi^{-1}\eta_k(\tau)$. Rewriting (110), using $\tilde{\eta}_k$ leads to

$$\begin{aligned} \dot{W} \leq \tilde{\eta}_k^T(\tau)[&\Xi^T \Pi_1 \Xi + (T_k - \tau)\Xi^T \Pi_2 \Xi \\ &+ \tau \Xi^T (M_{135}^T Q_x R_x^{-1} Q_x^T M_{135} + M_{246}^T Q_\phi R_\phi^{-1} Q_\phi^T M_{246})\Xi + (T_k - 2\tau)\Xi^T \Pi_3 \Xi]\tilde{\eta}_k(\tau). \end{aligned} \tag{112}$$

From the definition of the matrices in (103), note that

$$
\begin{aligned}
&M_1\Xi = \tilde{Y}M_1, \qquad M_2\Xi = \tilde{U}M_2, \qquad M_3\Xi = \tilde{Y}M_3,\\
&M_4\Xi = \tilde{U}M_4, \qquad M_5\Xi = \tilde{Y}M_5, \qquad M_6\Xi = \beta\tilde{U}M_6,\\
&M_{15}\Xi = \tilde{Y}M_{15}, \qquad M_{26}\Xi = \tilde{U}M_2 - \beta\tilde{U}M_6,\\
&M_{135}\Xi = \tilde{Y}M_{135}, \qquad M_{246}\Xi = \tilde{U}M_{246},\\
&M_{12}\Xi = \begin{bmatrix}\tilde{Y} & 0\\ 0 & \tilde{U}\end{bmatrix} M_{12},\ M_{34}\Xi = \begin{bmatrix}\tilde{Y} & 0\\ 0 & \tilde{U}\end{bmatrix} M_{34},\ M_{56}\Xi = \begin{bmatrix}\tilde{Y} & 0\\ 0 & \beta\tilde{U}\end{bmatrix} M_{56},\\
&M_0\Xi = A\tilde{Y}M_1 + B_\phi\tilde{U}M_2 - \tilde{Y}M_3 + B_uK_x\tilde{Y}M_5 + B_u\beta K_\phi\tilde{U}M_6.
\end{aligned}
$$

Consider the following change of variables: $\tilde{P} = \begin{bmatrix}\tilde{Y} & 0\\ 0 & \tilde{U}\end{bmatrix}^T \begin{bmatrix}P_{11} & P_{12}\\ P_{12}^T & P_{22}\end{bmatrix} \begin{bmatrix}\tilde{Y} & 0\\ 0 & \tilde{U}\end{bmatrix}$, $\tilde{F}_x = \tilde{Y}^T F_x \tilde{Y}$, $\tilde{G}_x = \tilde{Y}^T G_x \tilde{Y}$, $\tilde{F}_\phi = \tilde{U}^T F_\phi \tilde{U}$, $\tilde{G}_\phi = \tilde{U}^T G_\phi \tilde{U}$, $\tilde{Q}_x = \Xi^T M_{135}^T Q_x \tilde{Y}$, $\tilde{Q}_\phi = \Xi^T M_{246}^T Q_\phi \tilde{U}$, $\tilde{R}_x = \tilde{Y}^T R_x \tilde{Y}$, $\tilde{R}_\phi = \tilde{U}^T R_\phi \tilde{U}$, $\tilde{X} = \begin{bmatrix}\tilde{Y} & 0\\ 0 & \beta\tilde{U}\end{bmatrix}^T \begin{bmatrix}X_{11} & X_{12}\\ X_{12}^T & X_{22}\end{bmatrix} \begin{bmatrix}\tilde{Y} & 0\\ 0 & \beta\tilde{U}\end{bmatrix}$, $\overline{\Lambda} = \tilde{U}\Lambda$, $\tilde{K}_x = K_x\tilde{Y}$ and $\tilde{K}_\phi = K_\phi\tilde{U}$. Then, (112) can be re-written as follows

$$
\dot{W} \leq \tilde{\eta}_k^T(\tau)[\tilde{\Pi}_1 + (T_k - \tau)\tilde{\Pi}_2 + \tau(\tilde{Q}_x\tilde{R}_x^{-1}\tilde{Q}_x^T + \tilde{Q}_\phi\tilde{R}_\phi^{-1}\tilde{Q}_\phi^T) + (T_k - 2\tau)\tilde{\Pi}_3]\tilde{\eta}_k(\tau), \tag{113}
$$

where $\tilde{\Pi}_1$, $\tilde{\Pi}_2$, $\tilde{\Pi}_3$ are defined in (102). Hence, we can conclude that if

$$
\tilde{\Pi}_1 + (T_k - \tau)\tilde{\Pi}_2 + \tau(\tilde{Q}_x\tilde{R}_x^{-1}\tilde{Q}_x^T + \tilde{Q}_\phi\tilde{R}_\phi^{-1}\tilde{Q}_\phi^T) + (T_k - 2\tau)\tilde{\Pi}_3 \prec 0, \tag{114}
$$

then $\dot{W} < 0$. As (114) is affine with respect to τ, a necessary and sufficient condition to satisfy it $\forall\tau \in [0, T_k)$, is given by

$$
\begin{cases}
\tilde{\Pi}_1 + T_k(\tilde{\Pi}_2 + \tilde{\Pi}_3) \prec 0 & (115)\\
\tilde{\Pi}_1 - T_k\tilde{\Pi}_3 + T_k(\tilde{Q}_x\tilde{R}_x^{-1}\tilde{Q}_x^T + \tilde{Q}_\phi\tilde{R}_\phi^{-1}\tilde{Q}_\phi^T) \prec 0. & (116)
\end{cases}
$$

Finally, as (115) and (116) are affine in T_k and $T_k \in [\mathfrak{T}_1, \mathfrak{T}_2]$, applying the same reasoning and the Schur's Complement to (116), we conclude that $\tilde{\Psi}_1(\mathfrak{T}_i) \prec 0$ and $\tilde{\Psi}_2(\mathfrak{T}_i) \prec 0$, $i = 1, 2$ guarantee that (114) is verified $\forall\tau \in [0, T_k)$, $\forall T_k \in [\mathfrak{T}_1, \mathfrak{T}_2]$ provided that $\tilde{Y}$ and $\tilde{U}$ are nonsingular matrices. This is implicitly ensured by (99) and (100). Note that as (115) is ensured by (99), it follows that

$$
M_3[\tilde{\Pi}_1 + T_k(\tilde{\Pi}_2 + \tilde{\Pi}_3)]M_3^T \tag{117}
$$

This leads to a term $-\tilde{Y} - \tilde{Y}^T + T_k\tilde{R}_x \prec 0$ in the diagonal of (115), which implies that $-\tilde{Y} - \tilde{Y}^T$ is negative definite, and thus $\tilde{Y}$ is a nonsingular matrix. Moreover, $\tilde{U}$ is nonsingular by assumption. To conclude the proof, we must ensure the positivity of V. Left- and right-multiplying (97) by a factor of 2, and then left- and right- multiplying

the expression by $\begin{bmatrix} \tilde{Y} & 0 \\ 0 & \tilde{U} \end{bmatrix}^T$ and its transpose, respectively, one obtains (101). Hence, from *Lemma 10*, we conclude that (101) ensures that V_R is positive definite, $\forall x \in \mathbb{R}^n$. Furthermore, from (96) and (97) it is possible to show that there exist μ_1 and μ_2 satisfying (28) for $p = 2$. The proof is therefore complete, as (99)-(101) implies that conditions of *Theorem 8* are satisfied. □

Remark 10. *We may consider an additional condition to improve the time response of the closed-loop system in terms of the decay rate of the function V_R at the sampling instants. This may be done by replacing (30) by the following (PALMEIRA et al., 2016):*

$$\dot{W}(\tau, x_k, T_k) + \mu V_R(x_k(0)) < 0, \tag{118}$$

with $\mu \in [0, 1/\mathcal{T}_2)$. Integrating the above expression over the interval $[0, T_k]$ leads to

$$V_R(x_{k+1}(0)) < (1 - T_k\mu)V_R(x_k(0)) < (1 - \mathcal{T}_1\mu)V_R(x_k(0)), \tag{119}$$

which guarantees that the states at the sampling instants converge to the origin with a decay rate at least of $\nu = 1 - \mathcal{T}_1\mu$. Note that to satisfy (118), it is sufficient to replace (99) and (100), respectively, by the following matrix inequalities

$$\tilde{\Psi}_1(\mathcal{T}_i) = \tilde{\Pi}_1 + \mathcal{T}_i\tilde{\Pi}_2 + \mathcal{T}_i\tilde{\Pi}_3 + \mu M_5^T \tilde{P}_{11} M_5 \prec 0, \tag{120}$$

$$\tilde{\Psi}_2(\mathcal{T}_i) = \begin{bmatrix} \tilde{\Pi}_1 - \mathcal{T}_i\tilde{\Pi}_3 + \mu M_5^T \tilde{P}_{11} M_5 & \mathcal{T}_i\tilde{Q}_x & \mathcal{T}_i\tilde{Q}_\phi \\ \star & -\mathcal{T}_i\tilde{R}_x & 0 \\ \star & \star & -\mathcal{T}_i\tilde{R}_\phi \end{bmatrix} \prec 0. \tag{121}$$

Note that conditions (120) and (121) ensure that $V_R(x(t_k)) < \mu^k V_R(x(0))$.

Remark 11. *The conditions presented in Theorem 8 consider in its developments the use of the function V_R. However, the conditions can be easily modified to deal with special cases of this function. With this aim, for the numerical examples presented in subsection 5.2.2, inequality (101) is substituted, respectively, by $\tilde{P}_{11} \succ 0$ for V_Q and for V_L. For the functions V_Q and V_{QG}, which does not have the Lure-Postnikov coefficients, the terms related on $\overline{\Lambda}$ in (102) are eliminated.*

5.2.1 Optimization Problems

From the conditions stated in *Theorem 8*, we can formulate the following optimization problems:

P7. Given $\mathcal{T}_1$, the sector and slope bounds, compute the gains K_x and K_ϕ in order to maximize $\mathcal{T}_2$, for which the global stabilization of the origin of the closed-loop system (50) is ensured.

P8. Given a nominal sampling period $\mathcal{T}_{nom}$, the sector and slope upper bounds, compute the gains K_x and K_ϕ in order to find a bound on the maximum symmetrical allowable jitter, denoted by σ (*i.e.*, $\mathcal{T}_1 = \mathcal{T}_{nom} - \sigma$, $\mathcal{T}_2 = \mathcal{T}_{nom} + \sigma$), for which the global stabilization of the origin of the closed-loop system (50) is ensured.

P9. Given $\mathcal{T}_1$ and $\mathcal{T}_2$, compute the gains K_x and K_ϕ in order to maximize the sector and slope upper bounds given by the diagonal matrix Ω, for which the global stabilization of the origin of the closed-loop system (50) is ensured.

P10. Given $\mathcal{T}_1$, $\mathcal{T}_2$, the sector and slope bounds, compute the gains K_x and K_ϕ in order to improve the temporal response by maximizing μ, for which the global stabilization of the origin of the closed-loop system (50) is ensured and the decay rate at the sampling instants is maximized.

Problems P7 and P8 can be seen as a network design problem, as the network designer will consider the maximum allowable sampling time or jitter as a constraint in the network scheduling. Problem P9 is useful for systems where nonlinearities are not completely known, thus providing a certain security margin for which stability of the system can be guaranteed. In the last problem, the network constraints and the nonlinearities are completely known and the designer wishes to obtain gains to improve the time response of the closed-loop trajectories.

Observe that the conditions from *Theorem 8* are quasi-LMIs, since there exist nonlinearities which comes from the product between ε, β and $\overline{\Lambda}$ and the other decision variables. On the other hand, for a given μ and fixed ε, β and $\overline{\Lambda}$, the matrix inequalities (101), (120), (121), become LMIs. In addition, for P7 we should test, in an iterative way, the feasibility for $\mathcal{T}_2$ given, while for P8, P9 and P10 we should consider, respectively, σ, Ω and μ given.

We point that finding an optimal solution for the combination of these parameters may be a challenging task. Grid-based solutions, for instance, are poor from an efficiency perspective. An alternative to deal with this problem is to use a BMI solver, however according to (CHIU, 2016), the existing BMI solution methods can suffer from drawbacks, some of which are enumerated as follows: 1) In some methods, the decision variables are expressed solely in a vector, when a matrix form is more convenient in control problems; 2) Solution methods are originally designed to fit particular problem structures. Applying developed methods to other problem structures, if not impossible, requires extra efforts to reformulate the problem; 3) Prior derivations such as approximations or decompositions must be performed before algorithms are applied (*e.g.* linearize the BMI constraints and then solve a sequence of SDPs), and these derivations can be burdensome and sometimes heuristic and 4) only local optimization is performed while BMI problems inherently have multiple local optima. Moreover, few MATLAB toolboxes for BMI problems are available online and when found, they deal with particular problems (as discussed in the

second drawback). In this work, we propose a new approach for solving the optimization problems through the use of a Particle Swarm Optimization algorithm, which has been shown to be suitable to handle the limitations imposed by the synthesis conditions.

Although the PSO algorithm is an heuristic one and do not guarantee optimality for the solutions, some good practices seen in many BMI solvers can also be applied to improve the results. For instance, efforts can be directed to choose adequate initial values for the search variables, which is important for convergence to an optimal or suboptimal solution. Furthermore, reducing the ranges of the problem variables as much as possible, is frequently the key to tight an objective function bounding. Hereupon, we emphasize that we do not intend to exhaust the discussion about the numerical method, since there exist different levels of complexity and computational costs involved and a good tradeoff between them is usually desired.

5.2.1.1 Particle Swarm Optimization Algorithm

To solve the problems stated previously, we will use the PSO algorithm. This algorithm was originally introduced by KENNEDY; EBERHART (1995), inspired by artificial life, bird flocking, fish schooling, and swarming theory (social/nature behavior). It comprehends a population-solution based method, which can be applied to continuous, nondifferentiable, nonlinear, multidimensional search space problems (BANSAL *et al.*, 2011).

The choice of this heuristic stands on (BANSAL *et al.*, 2011), (KENNEDY; EBERHART, 1995): 1) code efficiency, as it can be executed in a few lines of code. Moreover, considering that time of execution of a solution for a set of LMIs can be already computationally expense, in the PSO algorithm the optimization function is evaluated only once, differently from other evolutionary algorithms such as the genetic one, where the optimization function is evaluated after applying some operations *e.g.* elitism, tournament, and others; 2) ease to implement; 3) robustness in the control parameters of the algorithm, *i.e.*, the solution does not deteriorate too much under slightly different parameter choices; 4) stability, since the explosion of the variables can be controlled and the algorithm can be parameterized in such a way that the particle system consistently converges on local optima with a sufficient number of iterations (CLERC; KENNEDY, 2002); 5) allows to reach all space of solutions over the defined interval, as it has real codification; 6) has the ability to perform a local search in the neighbourhood of the incumbent solution, which is the best feasible solution so far, and 7) combines individual and collective experience throughout iterations.

The main idea behind the PSO algorithm is to search the space of solutions by adjusting trajectories of individual vectors, called "particles", as they are conceptualized moving points into a multidimensional space (CLERC; KENNEDY, 2002). The jth particle of the swarm l in a n_d-dimensional search space, is represented by $\overline{M}_j(l) = [m_{j1}\ m_{j2}\ \ldots\ m_{jn_d}]$,

$\overline{M}(l) = [\overline{M}_1^T(l)\ \overline{M}_2^T(l)\ \ldots\ \overline{M}_{n_p}^T(l)]^T$, where n_p is the number of particles in each swarm. The velocity of each particle in swarm l is denoted by $\overline{S}_j(l) = [s_{j1}\ s_{j2}\ \ldots\ s_{jn_d}]$ and $\overline{S}(l) = [\overline{S}_1^T(l)\ \overline{S}_2^T(l)\ \ldots\ \overline{S}_{n_p}^T(l)]^T$. The previously best position visited by the jth particle is represented by $\overline{E}_j(l) = [e_{j1}\ e_{j2}\ \ldots\ e_{jn_d}]$ and $\overline{E}(l) = [\overline{E}_1^T(l)\ \overline{E}_2^T(l)\ \ldots\ \overline{E}_{n_p}^T(l)]^T$, while the best particle among all the others in the swarm (classified according to a fitness function) receives the index g, that is, $\overline{G}(l) = \overline{E}_g(l) = [e_{g1}\ e_{g2}\ \ldots\ e_{gn_d}]$. Particles evolve through iterations according to the following velocity and position equations:

$$s_{jd}(l+1) = \omega s_{jd}(l) + c_1 r_1(e_{jd}(l) - e_{jd}(l)) + c_2 r_2(e_{gd}(l) - m_{jd}(l)) \tag{122}$$

$$m_{jd}(l+1) = m_{jd}(l) + s_{jd}(l+1), \tag{123}$$

where $d = 1, 2 \ldots, n_d$, $j = 1, 2 \ldots, n_p$, $l = 1, 2, \ldots, n_{sw}$, with n_{sw} being the maximum number of swarms. These parameters are kept constant during the execution of the code. Velocity is updated in (122) which depends on its previous weighted velocity, the distances of its current position from its own best position experience and the best swarm position experience. Then, particle uses the obtained velocity and goes toward a new position, as indicated in (123).

The positive scalar ω is the inertia weight parameter, conceived by (SHI; EBERHART, 1998) to balance exploration *i.e.*, the capability to a particle search new areas into the variables space far from the incumbent solution, and exploitation, that is, the hability to search the surrounding area nearby the incumbent solution. As ω multiplies the velocity term, large inertia weights give emphasis to global search, while small inertia weights favors local search. Thus, there exists a trade-off. According to (BANSAL *et al.*, 2011), a constant inertia weight is a good strategy to minimize errors, compared to other weighting techniques.

Components c_1 and c_2 are positive constant values corresponding, respectively, to the cognitive and social scaling parameters. Usually, it is adopted $c_1 = c_2$, as (KENNEDY; EBERHART, 1995) afirms that this combination seems to result in the most effective search of the problem domain. Parameters r_1 and r_2 are random numbers uniformly distributed in the interval [0,1] and independently generated. The term $(e_{jd} - m_{jd})$ is the cognition part of the particle, which represents its individual experience (autobiographical memory), whereas $(e_{gd} - m_{jd})$ is the social part, representing the swarm or collective experience (KENNEDY, 1997).

For optimization problems P7, P8, P9 and P10, the particles are defined by $[\varepsilon, \beta, \tilde{\Lambda}, \mathcal{T}_2]$, $[\varepsilon, \beta, \tilde{\Lambda}, \sigma]$, $[\varepsilon, \beta, \tilde{\Lambda}, \Omega]$, $[\varepsilon, \beta, \tilde{\Lambda}, \mu]$, respectively. To evaluate the performance of the particles $\overline{X}_j$, we must assign to each optimization problem a fitness function $f(\cdot)$ in order to identify which particle has the best solution among all. The fitness function tests the feasibility of the LMIs (99)-(101) for the input particle, where each element of the particle corresponds to an optimization parameter. Two possible outcomes are assigned to the fitness function for the problems P7-P10, as detailed in Table 10.

Table 10: Global Synthesis - Outputs of the fitness function for each optim. problem.

Problem	Fitness Function	Feasible	Infeasible
P7	$f_1([\varepsilon, \beta, \overline{\Lambda}, \Im_2])$	$f_1 = \Im_2$	$f_1 = -1$
P8	$f_2([\varepsilon, \beta, \overline{\Lambda}, \sigma])$	$f_2 = \sigma$	$f_2 = -1$
P9	$f_3([\varepsilon, \beta, \overline{\Lambda}, \Omega])$	$f_3 = \Omega$	$f_3 = -1$
P10	$f_4([\varepsilon, \beta, \overline{\Lambda}, \mu])$	$f_4 = \mu$	$f_4 = -1$

The explanation is therefore simple: if the LMIs are feasible for a given particle, f_1, f_2, f_3 and f_4 will return, respectively, $\Im_2$, σ, Ω and μ. Otherwise, the respective functions will return -1, as we do not admit negative solutions from the above variables. In other words, for infeasible particle solutions, we just penalize in the objective function, without discarding the particle, as it may be closer to an optimal or suboptimal solution.

Remark 12. *In the case of multivariable control input, aiming to reduce the number of optimization parameters, one may assume equal values for the elements on the diagonal matrix $\overline{\Lambda}$, with the drawback of increasing the conservativeness for the optimization problem.*

Next we will present our PSO algorithm implementation, given by Algorithm 1. At a first moment, we define the maximum and minimum position and velocities limits over the search space for each optimization variable and the parameters of the PSO algorithm. Then, the initial population of positions and velocities are generated in lines 2-7, where $\underline{m}_d$ and $\overline{m}_d$ are, respectively, the lower and upper position limits for the dth optimization variable, $\underline{m}_d \geq 0$, $\forall d$, whereas $\underline{s}_d$ and $\overline{s}_d$ are, respectively, the minimum and maximum initial velocities for the dth optimization variable, $\underline{s}_d \leq 0$, $\overline{s}_d \geq 0$, $\forall d$. The function rand() generates a random number uniformly distributed in the interval [0,1].

We will start with swarm (1). In line 8, the best position ever visited it will simply be the current/initial position of the particle. Then, we evaluate the fitness function for each particle inside population $\overline{E}(1)$ according to the desired optimization problem (f_1, f_2, f_3 or f_4), and obtain the particle index associated with the best fitness value. In possession of the index g, we update the global best position. Next step consists in evolving the swarms until it reaches n_{sw}, which will be the stopping criterion. Note that in lines 16-21 we implemented an explicit position control of variables to restrict the search space. We do not restrict velocities limits. Then, we evaluate the fitness function for the new particle and if the result is better than its previous value, we update the particle's best own position experience. These steps are repeated for all optimization variables (particle elements) and all particles in the swarm. Once finished, we update the global best position experience and move on to the next swarm. At the end of the process, the best solution encountered by the algorithm in the variables space is given by $\overline{G}(l+1)$.

It should be noticed that we cannot ensure that the whole search space of solutions will be covered, thus we cannot guarantee optimality, as any other heuristic technique.

Algorithm 1 Particle Swarm Optimization

Define $\underline{m}_d$, $\overline{m}_d$, $\underline{s}_d$, $\overline{s}_d$, $\forall d$, ω, c_1, c_2;

▷ Random initialization of the particle population, within the admissible intervals.

for $d = 1$ to n_d **do**

  for $j = 1$ to n_p **do**

    $m_{jd} = \underline{m}_d + (\overline{m}_d - \underline{m}_d) \cdot \mathrm{rand}()$

    $s_{jd} = \underline{s}_d + (\overline{s}_d - \underline{s}_d) \cdot \mathrm{rand}()$

  end

end

▷ Update of the particle's and global best position, through solving the LMIs for $\overline{E}(1)$.

$\overline{E}(1) = \overline{M}(1)$;

$g = [\mathrm{index}]\max(f(\overline{E}(1)))$;

$\overline{G}(1) = \overline{E}_g(1))$;

▷ Start of the iterative process.

for $l = 1$ to n_{sw} **do**

  for $j = 1$ to n_p **do**

    for $d = 1$ to n_d **do**

      Generate random numbers r_1, r_2;

      Evaluate (122) and then evaluate (123);

      ▷ Position control.

      if $m_{jd}(l+1) < \underline{m}_d$ **then**

        $m_{jd}(l+1) = \underline{m}_d$;

      end

      if $m_{jd}(l+1) > \overline{m}_d$ **then**

        $m_{jd}(l+1) = \overline{m}_d$;

      end

    end

    ▷ Check particle improvement. Solve the LMIs for the particle.

    if $f(\overline{M}_j(l+1)) > f(\overline{M}_j(l))$ **then**

      $\overline{E}_j(l+1) = \overline{M}_j(l+1)$;

    else

      $\overline{E}_j(l+1) = \overline{E}_j(l)$;

    end

  end

  ▷ Update the global best position.

  $g = [\mathrm{index}]\max(f(\overline{E}(l+1)))$;

  $\overline{G}(l+1) = \overline{E}_g(l+1))$;

end

▷ Solution is given by $\overline{G}(l+1)$.

However, the algorithm can be seen as an efficient way of finding at least suboptimal solutions to P7-P10.

5.2.2 Numerical Examples

Example 1: Consider system (18) given by the following matrices:

$$A = \begin{bmatrix} -0.5 & -6.2 & -0.105 & -1.2 \\ 1 & 0 & 0 & 0 \\ 0 & 1 & 0 & 0 \\ 0 & 0 & 1 & 0 \end{bmatrix}, B_u = \begin{bmatrix} 1 \\ 0 \\ 0 \\ 0 \end{bmatrix}, B_\phi = \begin{bmatrix} 0.5 \\ 0 \\ 0 \\ 0 \end{bmatrix},$$
$$C = \begin{bmatrix} 0 & 0.2 & 0 & 0 \end{bmatrix}, \; D_\phi = [0],$$

and the bounds on ϕ given by $\underline{\delta} = \underline{\gamma} = 0$, $\overline{\delta} = \overline{\gamma} = \Omega$. Regarding the PSO algorithm, a possible way to select the weighting parameters ω, c_1 and c_2 is presented in (CLERC; KENNEDY, 2002). In that way, we may choose $\omega = \chi$, $c_1 = \chi\varphi_1$ and $c_2 = \chi\varphi_2$, where χ is defined by (124), with $0 \leq h \leq 1$ and $\varphi = \varphi_1 + \varphi_2 \geq 4$. Arbitrarily, we choose $h = 1$, $\varphi_1 = 2.05$ and $\varphi_2 = 2.05$, which are common values used in the literature.

$$\chi = \frac{2h}{|2 - \varphi - \sqrt{\varphi^2 - 4\varphi}|}. \tag{124}$$

Computing these coefficients, one obtains $\omega = 0.7298$, $c_1 = c_2 = 1.4962$. The number of particles and the number of swarms were defined as $n_p = 100$, $n_{sw} = 75$. For this example, we defined the range of the search variables in the interval $\varepsilon \in [0.01, 2]$, $\beta \in [0.01, 10000]$ and $\overline{\Lambda} \in [0, 100]$ for P7, P8 and P9. For P10, we defined the interval $\varepsilon \in [0.01, 3]$, $\beta \in [0.01, 50000]$ and $\overline{\Lambda} \in [0, 10]$. Initial velocities $\underline{s}_d$, $\overline{s}_d$ were set until 5% of the maximal value of the interval for each optimization variable.

The results for P7 are detailed in Table 11, by considering $\mathcal{T}_1 = 0.1$ ms and $\Omega = \frac{1}{\sqrt{2}}$. In Table 11, the result "∞^*" means that for the tests that we made, we increased $\mathcal{T}_2$ and found no upper bound. However, there should exist control updates that bring the control input (and by consequence the states) to zero. Moreover, observe that there exists a tradeoff between μ, the maximal intersampling time and the sector bounds. For $\mu = 0$, the additional degree of freedom provided by the variable $\overline{\Lambda}$ significantly improved the results for V_R and V_L in comparison to V_{QG} and V_Q, but when some performance was required, no improvement was observed.

Table 11: Global synthesis, Ex. 1 - Maximum $\mathfrak{T}_2$ for different μ and function V.

	Parameter	V_Q	V_{QG}	V_L	V_R
$\mu = 0$	β	5690.95	4933.76	242.91	75.6818
	ε	0.3755	0.3772	1.4571	0.4047
	$\overline{\Lambda}$	-	-	7.7201	16.9366
	$\boldsymbol{\mathfrak{T}_2}$	**4.8038**	**4.8055**	$\boldsymbol{\infty^*}$	$\boldsymbol{\infty^*}$
$\mu = 0.5$	β	2652.89	5430.09	1226.91	1790.05
	ε	1.3739	1.3767	1.3745	1.3793
	$\overline{\Lambda}$	-	-	0.0000	0.0000
	$\boldsymbol{\mathfrak{T}_2}$	**0.7440**	**0.7444**	**0.7440**	**0.7444**
$\mu = 1.0$	β	6238.01	7435.78	3818.39	6648.50
	ε	1.8041	1.8065	1.8068	1.8018
	$\overline{\Lambda}$	-	-	0.0000	0.0000
	$\boldsymbol{\mathfrak{T}_2}$	**0.4651**	**0.4655**	**0.4651**	**0.4655**

The results for P8 are detailed in Table 12, by considering $\mathfrak{T}_{nom} = 3.5$ s and $\Omega = \frac{1}{\sqrt{2}}$. Note that for $\mu = 0$, we guarantee stability for a small enough sampling time and for $\mathfrak{T}_2 = 7.0$ s. In the cases of $\mu = 0.01$ and $\mu = 0.05$, the results of σ with the function V_R were better than the ones obtained with V_Q, V_{QG} and V_L, showing that the variable $\overline{\Lambda}$ improved the solutions.

Table 12: Global synthesis, Ex. 1 - Maximum σ for different μ and function V.

	Parameter	V_Q	V_{QG}	V_L	V_R
$\mu = 0$	β	2875.62	8123.71	205.95	131.65
	ε	0.3891	0.3910	1.8371	0.3460
	$\overline{\Lambda}$	-	-	6.5099	10.7621
	$\boldsymbol{\sigma}$	**1.3697**	**1.3709**	**3.5000**	**3.5000**
$\mu = 0.01$	β	3503.05	3384.47	5653.58	2253.67
	ε	0.3365	0.3346	0.3419	0.3435
	$\overline{\Lambda}$	-	-	1.6102	5.9785
	$\boldsymbol{\sigma}$	**1.1439**	**1.1450**	**1.1555**	**1.1712**
$\mu = 0.05$	β	9789.44	1708.08	293.29	6925.21
	ε	0.3155	0.3123	0.3141	0.3166
	$\overline{\Lambda}$	-	-	0.0000	0.9585
	$\boldsymbol{\sigma}$	**0.6196**	**0.6232**	**0.6196**	**0.6252**

For P9, we defined $\mathfrak{T}_1 = 0.1$ ms and $\mathfrak{T}_2 = 4.5\,s$. The results are depicted in Table 13. Considering $\mu = 0$, with the V_R function we obtained Ω greater 17.9%, 10.8% and 17.9% than the ones obtained with V_Q, V_{QG} and V_L, respectively. For $\mu = 0.015$, the percentage increase of the results of Ω get even better, 32.8%, 28.1% and 23.7% than the ones with V_Q, V_{QG} and V_L, respectively.

Table 13: Global synthesis, Ex. 1 - Maximum Ω for different μ and function V.

	Parameter	V_Q	V_{QG}	V_L	V_R
$\mu = 0$	β	32.92	5064.21	33.4892	443.78
	ε	0.3229	0.3172	0.3172	0.3286
	$\overline{\Lambda}$	-	-	0.0000	7.2131
	Ω	**2.8029**	**2.9824**	**2.8029**	**3.3056**
$\mu = 0.01$	β	39.50	5864.74	43.9983	5722.05
	ε	0.3137	0.3108	0.3158	0.3158
	$\overline{\Lambda}$	-	-	0.6022	4.6237
	Ω	**1.5170**	**1.5958**	**1.5321**	**1.8106**
$\mu = 0.015$	β	71.66	7593.90	652.09	1340.88
	ε	0.3119	0.3132	0.3148	0.3144
	$\overline{\Lambda}$	-	-	0.8848	3.6167
	Ω	**0.7209**	**0.7471**	**0.7735**	**0.9575**

Finally, the obtained results for P10 are presented in Table 14, with $\mathfrak{T}_1 = 0.1$ ms, $\mathfrak{T}_2 = 0.3$ s and $\Omega = \frac{1}{\sqrt{2}}$. The combination of parameters that yields in greater μ were $\beta = 40448.16$, $\varepsilon = 2.5793$ and $\overline{\Lambda} = 0$, achieved with the V_R function.

Table 14: Global synthesis, Ex. 1 - Maximum μ for different function V.

Parameter	V_Q	V_{QG}	V_L	V_R
β	10685.48	32455.55	27510.29	40448.16
ε	2.5780	2.5756	2.5770	2.5793
$\overline{\Lambda}$	-	-	0.0000	0.0000
μ	**1.6478**	**1.6494**	**1.6478**	**1.6494**

Let us consider the results from P9 (Table 13, V_R function). The gains obtained with performance constraint $\mu = 0$, $\mu = 0.01$ and $\mu = 0.015$ are given in Table 15.

Table 15: Global synthesis, Ex.1 - Gains obtained from P9 with the function V_R.

	K_x	K_ϕ
$\mu = 0$	[-0.0881 0.0666 -0.4888 0.2561]	[-0.0031]
$\mu = 0.01$	[-0.1272 0.0766 -0.7085 0.4139]	10^{-5}·[5.9588]
$\mu = 0.015$	[-0.1410 0.0833 -0.7841 0.4786]	10^{-5}·[4.5509]

Note that as μ grows, the magnitude of the gains K_x also increase, without change on the signal, which is justified due to the fact that the performance restrictions are imposed over the states of the system. On the other hand, the gains K_ϕ tends to a small value, for this example. We simulate now the system considering the result from P9, *i.e.*, $T_k \in$

$[0.0001,4.5]$, and the piecewise affine nonlinearity defined below

$$\phi(y(t)) = \begin{cases} 0.2\, y(t), & \text{sgn}(y(t))y(t) \leq 0.1 \\ 0.5\, y(t) - 0.03\, \text{sgn}(y(t)), & 0.1 < \text{sgn}(y(t))y(t) \leq 0.5 \\ 0.9575\, y(t) - 0.25875\, \text{sgn}(y(t)), & \text{sgn}(y(t))y(t) > 0.5, \end{cases} \tag{125}$$

that satisfies (19) with sector and slope restrictions $\underline{\delta} = \underline{\gamma} = 0$, $\overline{\delta} = \overline{\gamma} = 0.9575$. The control action $u(t)$ and the nonlinearity input $y(t)$ are presented in Figs. 22 and 23 for the different values of μ, by considering $x(0) = [10\ 10\ -10\ 10]^T$. Note that for higher μ, the rate of convergence of the trajectories to the origin is increased at the cost of a higher control action.

Figure 22: Global synthesis, Ex. 1 - Control action of the closed-loop system.

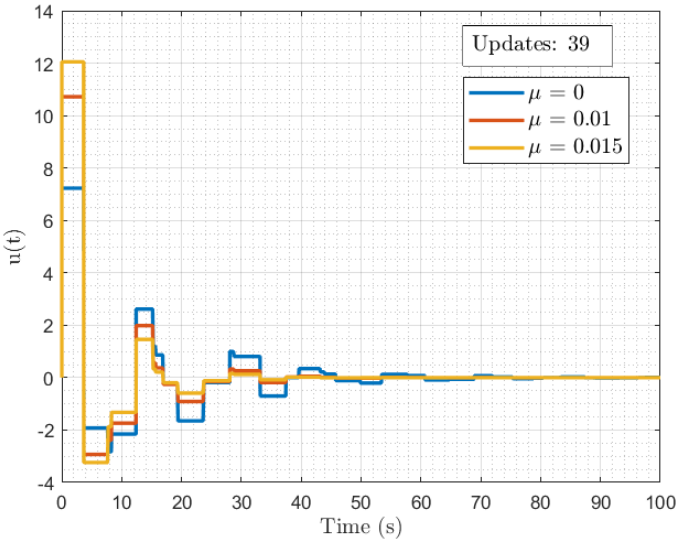

Font: Author.

Figure 23: Global synthesis, Ex. 1 - Nonlinearity input of the closed-loop system.

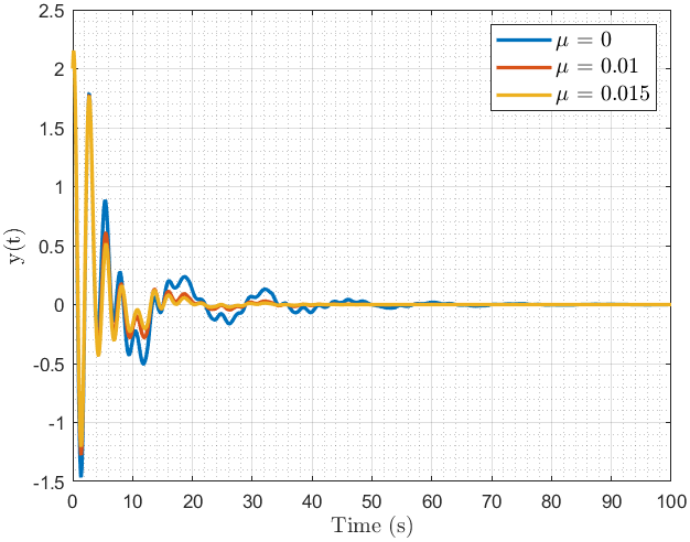

Font: Author.

To qualitatively characterize the solutions obtained with the PSO algorithm, Fig. 24 shows the evolution of the solutions (left axis) given by the fitness function associated to the optimization problem P8 (see Table 10), with $\mu = 0.01$ and $V_R(x)$ and the number of feasible particles and infeasible particles (right axis) along the swarms or iterations. In this case, a new random particle population initialization was considered.

Figure 24: Evolution of solutions and particles over iterations.

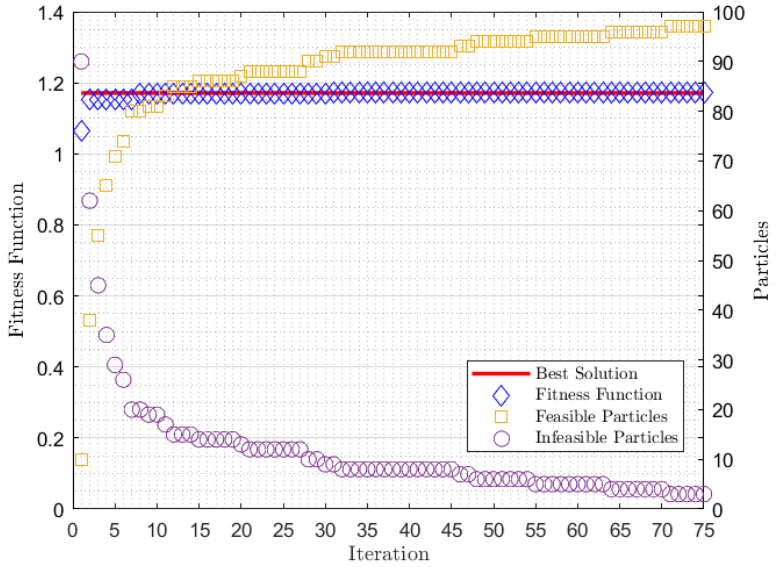

Font: Author.

From Fig. 24, we have that the best solution found by the algorithm was $\sigma = 1.1712$ s, which was equal to the one given in Table 12. This indicates that the solution may be near to the optimal one from the given range of the search variables in the interval $\varepsilon \in [0.01, 2]$, $\beta \in [0.01, 10000]$, $\overline{\Lambda} \in [0, 100]$ and $\sigma \in [0.01, 2]$. Observe that in the first swarm approximately 90% of the particles presents an infeasible solution, while in the end of the process almost all solutions are feasible, which shows the stability of the PSO algorithm. Furthermore, note that along the process it is interesting to have infeasible solutions, and do not discard the corresponding particles, since their solutions may be near to an optimal one. Indeed, this characteristics of the algorithm allows the search space of the variables to be better explored.

Example 2: Consider system (18) given by the following matrices

$$A = \begin{bmatrix} -1.1 & -2 \\ 1 & 0 \end{bmatrix}, B_u = \begin{bmatrix} 1 \\ 0 \end{bmatrix}, B_\phi = \begin{bmatrix} 0.5 \\ 0 \end{bmatrix}, \; C = \begin{bmatrix} -0.95 & 1.50 \end{bmatrix}, \; D_\phi = [-0.5],$$

and the bounds on ϕ given by $\underline{\delta} = \underline{\gamma} = 0$, $\overline{\delta} = \overline{\gamma} = \Omega$. This system satisfies *Proposition 1*, *i.e.*, the algebraic loop is well-posed. The parameters chosen for the PSO algorithm were $\omega = 0.7298$ and $c_1 = c_2 = 1.4962$. Also, we defined $n_p = 100$, $n_{sw} = 75$ and the search

space over $\varepsilon \in [0.01, 2]$, $\beta \in [0.01, 50000]$ and $\overline{\Lambda} \in [0, 100]$. Initial velocities $\underline{s}_d$, $\overline{s}_d$ were set until 5% of the maximal value of the interval for each optimization variable.

The results for P7 are detailed in Table 16, by considering $\mathcal{T}_1 = 0.5$ s and $\Omega = \frac{1}{\sqrt{2}}$. Observe that we guarantee stability for any $\mathcal{T}_2$ (as an upper bound could not be found) for all the functions, but we emphasize that there should exist other control updates that leads the control input to zero. Moreover, the functions V_R and V_{QG} leads to the same results for the optimization problems with $\mu = 0.5$ and $\mu = 1.0$, which are slightly greater than those obtained with V_L and V_Q.

Table 16: Global synthesis, Ex. 2 - Maximum $\mathcal{T}_2$ for different μ and function V.

	Parameter	V_Q	V_{QG}	V_L	V_R
$\mu = 0$	β	14788.22	22837.86	19947.38	38163.67
	ε	0.6627	1.6798	0.6982	1.4332
	$\overline{\Lambda}$	-	-	0.0000	0.0000
	$\boldsymbol{\mathcal{T}_2}$	$\boldsymbol{\infty^*}$	$\boldsymbol{\infty^*}$	$\boldsymbol{\infty^*}$	$\boldsymbol{\infty^*}$
$\mu = 0.5$	β	18984.67	9677.81	25830.82	7880.04
	ε	1.3740	1.3762	1.3736	1.3802
	$\overline{\Lambda}$	-	-	0.0000	0.0000
	$\boldsymbol{\mathcal{T}_2}$	**1.3877**	**1.4035**	**1.3877**	**1.4035**
$\mu = 1.0$	β	5201.66	14374.22	22428.28	4800.50
	ε	1.8992	1.8077	1.9018	1.8023
	$\overline{\Lambda}$	-	-	0.0000	0.0000
	$\boldsymbol{\mathcal{T}_2}$	**0.7550**	**0.7665**	**0.7550**	**0.7665**

The results for P8 are detailed in Table 17, by considering $\mathcal{T}_{nom} = 3.0$ s and $\Omega = \frac{1}{\sqrt{2}}$. Note that for $\mu = 0$ we guarantee stability for a small enough sampling time and for $\mathcal{T}_2 = 6.0$ s. For $\mu = 0.15$, the results of σ with the functions V_R and V_{QG} were 2.4% greater than the ones obtained with V_L and V_Q. For $\mu = 0.20$, this percentage increases to 7.8%.

Table 17: Global synthesis, Ex. 2 - Maximum σ for different μ and function V.

	Parameter	V_Q	V_{QG}	V_L	V_R
$\mu = 0$	β	14585.99	11735.03	23643.86	7816.50
	ε	1.2598	0.2179	0.0863	0.2375
	$\overline{\Lambda}$	-	-	0.0000	0.0000
	$\boldsymbol{\sigma}$	**3.0000**	**3.0000**	**3.0000**	**3.0000**
$\mu = 0.15$	β	48784.82	47169.81	41525.35	46850.01
	ε	1.4179	1.3885	1.4190	1.3898
	$\overline{\Lambda}$	-	-	0.0000	0.0000
	$\boldsymbol{\sigma}$	**1.8386**	**1.8844**	**1.8386**	**1.8844**
$\mu = 0.20$	β	13500.08	33601.56	12972.28	24318.98
	ε	1.4161	1.3873	1.4168	1.3885
	$\overline{\Lambda}$	-	-	0.0000	0.0000
	$\boldsymbol{\sigma}$	**0.5305**	**0.5722**	**0.5305**	**0.5722**

For P9, we defined $\mathfrak{T}_1 = 0.1$ ms and $\mathfrak{T}_2 = 4.0$ s, which results are depicted in Table 18. Observe that for this intersampling interval and $\mu = 0$, we ensure stability for nonlinearties with sector and slope bound restrictions in $[0, \infty^*]$, since an upper bound was not found. The quadratic terms that depend on the nonlinearities in the functions V_{QG} and V_L improved substantially the results for $\mu = 0.15$ and for $\mu = 0.18$ in comparison to the ones obtained with V_Q and V_L, respectively, in a order of 29.6% and 15.5%.

Table 18: Global synthesis, Ex. 2 - Maximum Ω for different μ and function V.

	Parameter	V_Q	V_{QG}	V_L	V_R
$\mu = 0$	β	22959.92	46584.06	25268.30	44978.74
	ε	0.1999	1.3943	0.5353	2.0000
	$\overline{\Lambda}$	-	-	34.0958	26.6681
	$\boldsymbol{\Omega}$	$\boldsymbol{\infty^*}$	$\boldsymbol{\infty^*}$	$\boldsymbol{\infty^*}$	$\boldsymbol{\infty^*}$
$\mu = 0.15$	β	11566.76	36910.01	50000.00	45534.47
	ε	1.2623	1.1996	1.2623	1.1996
	$\overline{\Lambda}$	-	-	0.0000	0.0000
	$\boldsymbol{\Omega}$	**3.0714**	**3.9817**	**3.0714**	**3.9817**
$\mu = 0.18$	β	13124.27	47084.42	23086.02	38293.34
	ε	1.4368	1.3993	1.4370	1.4002
	$\overline{\Lambda}$	-	-	0.0000	0.0000
	$\boldsymbol{\Omega}$	**0.6088**	**0.7033**	**0.6088**	**0.7033**

Finally, for P10, the results are presented in Table 19, with $\mathfrak{T}_1 = 0.1$ ms, $\mathfrak{T}_2 = 1.2071$ s and $\Omega = \frac{1}{\sqrt{2}}$. Again, the results with the function V_{QG} and V_R were less conservative than the ones with V_Q and V_L. The variable $\overline{\Lambda}$ did not help to improve the solutions.

Table 19: Global synthesis, Ex. 2 - Maximum μ for different function V.

Parameter	V_Q	V_{QG}	V_L	V_R
β	6055.11	48338.96	16014.40	19884.33
ε	1.4250	1.4173	1.4250	1.4160
$\overline{\Lambda}$	-	-	0.0000	0.0000
$\boldsymbol{\mu}$	**0.5864**	**0.5925**	**0.5864**	**0.5925**

The results show that the function V_R leads to greater values of $\mathfrak{T}_2$, σ, Ω and μ in all cases, for being less conservative. The function V_{QG} performed better than V_Q and V_L due to the quadratic terms on the nonlinearities in all cases. In this examples, the variable $\overline{\Lambda}$ did not contribute to improve the solutions, *i.e.*, the Lure terms in V_L and V_R did not provide an improvement in relation to the results obtained with V_Q and V_{QG}.

Let us now consider the results from P7 (Table 16, V_R function). The gains obtained with performance constraint $\mu = 0.5$ and $\mu = 1.0$ are given in Table 20.

Table 20: Global synthesis, Ex.2 - Gains obtained from P7 with the function V_R.

	K_x	K_ϕ
$\mu = 0.5$	[-0.3237 0.1440]	[-0.0845]
$\mu = 1.0$	[-1.1079 -0.3397]	[-0.2931]

Differently from the gains shown in the previous example, in this case there was signal change on an element of the gain K_x and on the magnitude of the gains K_ϕ when increasing μ. As the gains for $\mu = 0$ depend on the fixed $\mathcal{T}_2$, and as a maximal $\mathcal{T}_2$ could not be determined, this case will not be considered for presentation purposes.

To show that asymptotic stability holds for these cases, we choose the intersampling interval in the range $T_k \in [0.5, 0.7765]$, which is the result for $\mu = 1$. The control action and the nonlinearity input for different values of μ are presented in Figs. 25 and 26, by considering $x(0) = [-10\ 5]^T$ and the piecewise linear nonlinearity defined below

$$\phi(y(t)) = \begin{cases} 0.2\ y(t), & \text{sgn}(y(t))y(t) \leq 1 \\ 0.4\ y(t) - 0.2\ \text{sgn}(y(t)), & 1 < \text{sgn}(y(t))y(t) \leq 3 \\ \dfrac{1}{\sqrt{2}}\ y(t) - \dfrac{3-\sqrt{2}}{\sqrt{2}}\ \text{sgn}(y(t)), & \text{sgn}(y(t))y(t) > 3, \end{cases} \tag{126}$$

which satisfies (19) with sector and slope restrictions $\underline{\delta} = \underline{\gamma} = 0$, $\overline{\delta} = \overline{\gamma} = \frac{1}{\sqrt{2}}$.

Figure 25: Global synthesis, Ex. 2 - Control action of the closed-loop system.

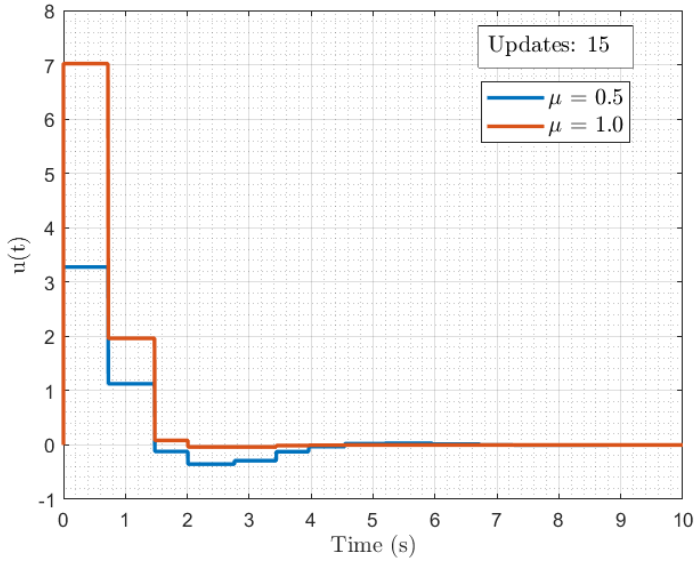

Font: Author.

Figure 26: Global synthesis, Ex. 2 - Nonlinearity input of the closed-loop system.

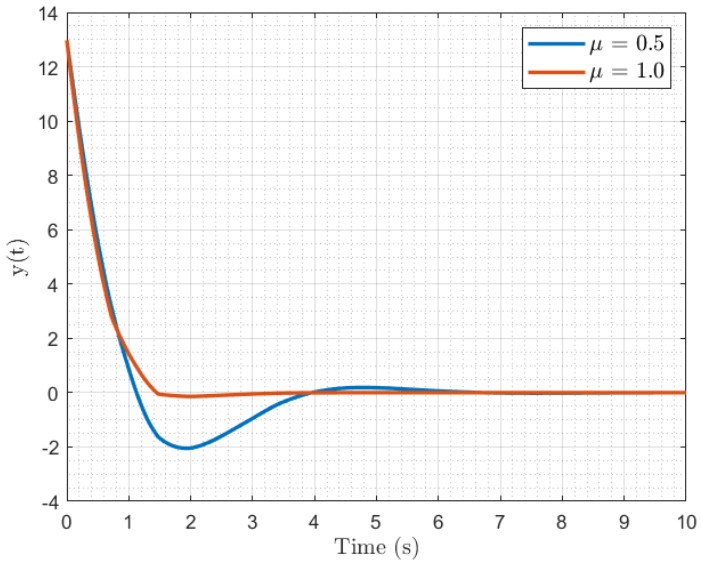

Font: Author.

As noted in the same way in the previous example, with $\mu = 1$ we have that trajectories converge to the origin in approximately 1.5 s, about 3 times lesser than with $\mu = 0.5$. However, the magnitude of the control action is increased.

We highlight that from the obtained gains K_x and K_ϕ via synthesis procedures, one can apply the analysis methods with the intent to obtain less conservative bounds for $\mathcal{T}_2$, σ or Ω. This is motivated by the fact that some assumptions and changes of variables are required to derive the stabilization conditions, such as $U_1 = U_2 = U$, $U_3 = \beta^{-1}U$ and $L = \varepsilon M_1^T Y^T + M_3^T Y^T$, which introduces conservatism in the synthesis methods (for more details, see the proof of *Theorem 8*). Applying this reasoning with the gains obtained from P7 as given in Table 20, we then solve P1 considering the generalized Lure function $V_{LG}(x)$. In this case, for $K_x = [-0.3237\ 0.1440]$ and $K_\phi = [-0.0845]$ we obtained $\mathcal{T}_2 = 16.8406$ s and for $K_x = [-1.1079\ -0.3397]$ and $K_\phi = [-0.2931]$, we obtained $\mathcal{T}_2 = 1.5878$ s, which are greater than the values presented in Table 16, respectively, $\mathcal{T}_2 = 1.4035$ s and $\mathcal{T}_2 = 0.7665$ s.

5.3 Regional Results

In this section, we present conditions in the form of quasi-LMIs to guarantee the stabilization of the origin of the sampled-data closed-loop system (50) in a local context, under aperiodic sampling satisfying $T_k \in [\mathcal{T}_1, \mathcal{T}_2]$ and subject to nonlinearities that verify the sector and slope restrictions (19) provided $y \in \mathcal{Y}_0$, or equivalently $x \in \mathcal{X}_0$, with $\mathcal{X}_0$ as defined in (24). Moreover, as in the global case, we assume that $\underline{\Delta} = \underline{\Gamma} = 0$. For this, we consider the function $V_R(x)$ (96) used in the global synthesis and a particular structure of the functional (42) with $G_x = 0$, $G_\phi = 0$, $X \succ 0$, $F_x \succ 0$ and $F_\phi \succ 0$, which ensures its

positivity as done in the regional analysis.

In this context, the following theorem provides conditions to obtain gains K_x and K_ϕ that ensure the asymptotic stability of the origin of the closed-loop system.

Theorem 9. *If there exist matrices $\tilde{P} \in \mathbb{S}^{n+m}$, $\tilde{Y} \in \mathbb{R}^{n\times n}$, $\tilde{U} \in \mathbb{D}^m_{\succeq 0}$, $\tilde{F}_x \in \mathbb{S}^n_{\succ 0}$, $\tilde{F}_\phi \in \mathbb{S}^m_{\succ 0}$, $\tilde{R}_x \in \mathbb{S}^n_{\succ 0}$, $\tilde{R}_\phi \in \mathbb{S}^m_{\succ 0}$, $\tilde{Q}_x \in \mathbb{R}^{3(n+m)\times n}$, $\tilde{Q}_\phi \in \mathbb{R}^{3(n+m)\times m}$, $\tilde{X} \in \mathbb{S}^{n+m}_{\succ 0}$, $\tilde{K}_x \in \mathbb{R}^{q\times n}$, $\tilde{K}_\phi \in \mathbb{R}^{q\times m}$, $\overline{\Lambda} \in \mathbb{D}^m_{\succeq 0}$ and positive scalars ε, β, that satisfy, for $i = 1,2$:*

$$\tilde{\Psi}_1(\mathcal{T}_i) = \tilde{\Pi}_1 + \mathcal{T}_i\tilde{\Pi}_2 + \mathcal{T}_i\tilde{\Pi}_3 \prec 0 \tag{127}$$

$$\tilde{\Psi}_2(\mathcal{T}_i) = \begin{bmatrix} \tilde{\Pi}_1 - \mathcal{T}_i\tilde{\Pi}_3 & \mathcal{T}_i\tilde{Q}_x & \mathcal{T}_i\tilde{Q}_\phi \\ \star & -\mathcal{T}_i\tilde{R}_x & 0 \\ \star & \star & -\mathcal{T}_i\tilde{R}_\phi \end{bmatrix} \prec 0 \tag{128}$$

$$\begin{bmatrix} 2\tilde{P}_{11} & 2\tilde{P}_{12} - \tilde{Y}^T C^T \overline{\Delta} \\ \star & 2\tilde{P}_{22} + 2(I - \overline{\Delta}D_\phi)\tilde{U} \end{bmatrix} \succ 0, \tag{129}$$

with

$$\begin{aligned}
\tilde{\Pi}_1 &= \mathrm{He}\left\{M_{12}^T\tilde{P}M_{34}\right\} - M_{15}^T\tilde{F}_xM_{15} + \mathrm{He}\left\{\frac{1}{2}M_2^T\overline{\Lambda}C\tilde{Y}M_3\right\} + \mathrm{He}\left\{\frac{1}{2}M_2^T\overline{\Lambda}D_\phi\tilde{U}M_4\right\} \\
&\quad - (M_2 - \beta M_6)^T\tilde{F}_\phi(M_2 - \beta M_6) + \mathrm{He}\left\{M_2^T(\overline{\Delta}C\tilde{Y}M_1 + (\overline{\Delta}D_\phi - I)\tilde{U}M_2)\right\} \\
&\quad + \mathrm{He}\left\{M_4^T(\overline{\Gamma}C\tilde{Y}M_3 + (\overline{\Gamma}D_\phi - I)\tilde{U}M_4)\right\} \\
&\quad + \mathrm{He}\left\{M_6^T(\overline{\Delta}C\tilde{Y}M_5 + (\overline{\Delta}D_\phi - I)\beta\tilde{U}M_6)\right\} - \mathrm{He}\{\tilde{Q}_xM_{15}\} - \mathrm{He}\{\tilde{Q}_\phi(M_2 - \beta M_6)\} \\
&\quad + \mathrm{He}\{(\varepsilon M_1^T + M_3^T)(A\tilde{Y}M_1 + B_\phi\tilde{U}M_2 - \tilde{Y}M_3 + B_u\tilde{K}_xM_5 + B_u\beta\tilde{K}_\phi M_6)\} \\
\tilde{\Pi}_2 &= M_3^T\tilde{R}_xM_3 + \mathrm{He}\{M_3^T\tilde{F}_xM_{15}\} + M_4^T\tilde{R}_\phi M_4 + \mathrm{He}\{M_4^T\tilde{F}_\phi(M_2 - \beta M_6)\} \\
\tilde{\Pi}_3 &= M_{56}^T\tilde{X}M_{56},
\end{aligned} \tag{130}$$

where[2]

$$\begin{aligned}
&M_1 = [I\ \ 0\ \ 0\ \ 0\ \ 0\ \ 0] \quad M_2 = [0\ \ I\ \ 0\ \ 0\ \ 0\ \ 0] \quad M_3 = [0\ \ 0\ \ I\ \ 0\ \ 0\ \ 0] \\
&M_4 = [0\ \ 0\ \ 0\ \ I\ \ 0\ \ 0] \quad M_5 = [0\ \ 0\ \ 0\ \ 0\ \ I\ \ 0] \quad M_6 = [0\ \ 0\ \ 0\ \ 0\ \ 0\ \ I] \\
&M_{15} = M_1 - M_5 \quad M_{12} = [M_1^T\ \ M_2^T]^T \quad M_{34} = [M_3^T\ \ M_4^T]^T \quad M_{56} = [M_5^T\ \ M_6^T]^T.
\end{aligned}$$

Then, the gains $K_x = \tilde{K}_x\tilde{Y}^{-1}$ and $K_\phi = \tilde{K}_\phi\tilde{U}^{-1}$ ensures that the origin of the sampled-data closed-loop system (50) with ϕ satisfying (19) with $\underline{\Delta} = \underline{\Gamma} = 0$ and $T_k \in [\mathcal{T}_1, \mathcal{T}_2]$ is locally asymptotically stable for all initial conditions inside $\mathcal{L}(V_R, \rho) \subset \mathcal{X}_0$, with V_R as defined in (96) with $P = \begin{bmatrix} \tilde{Y} & 0 \\ 0 & \tilde{U} \end{bmatrix}^{-T} \tilde{P} \begin{bmatrix} \tilde{Y} & 0 \\ 0 & \tilde{U} \end{bmatrix}^{-1}$ and $\Lambda = \tilde{U}^{-1}\overline{\Lambda}$.

[2]The matrices M_i are not of the same dimension. The notations 0 and I correspond to the zero and identity matrices of appropriate dimension.

Proof. The proof follows the same steps from the proofs of *Theorem 8* and *Theorem 5*. Note, however, that the assumptions on the functional imply that $\tilde{G}_x = 0$, $\tilde{G}_\phi = 0$ and that $\tilde{F}_x$, $\tilde{F}_\phi$ and $\tilde{X}$ are positive definite matrices, thus ensuring the positivity of the functional. □

Remark 13. *Inspired in Lemma 7, the inclusion of the level set $\mathcal{L}(V_R, \rho) \subset \mathcal{X}_0$ is ensured if there exist matrices $P \in \mathbb{S}^{n+m}$, $S_{c,j} \in \mathbb{D}^m_{\succeq 0}$ and positive scalars σ_j and ρ, such that the following inequalities are satisfied*

$$\begin{bmatrix} -(\sigma_j \underline{y}_j \overline{y}_j + \rho) & \sigma_j \frac{\underline{y}_j + \overline{y}_j}{2} C_j & \sigma_j \frac{\underline{y}_j + \overline{y}_j}{2} D_{\phi_j} & 0 \\ \star & P_{11} & P_{12} & \sigma_j C_j^T \\ \star & \star & P_{22} & \sigma_j D_{\phi_j}^T \\ \star & \star & \star & \sigma_j \end{bmatrix} + \mathrm{He}\left\{ \frac{1}{2} \begin{bmatrix} 0 \\ (\underline{\Delta} C)^T \\ (\underline{\Delta} D_\phi - I)^T \\ 0 \end{bmatrix} S_{c,j} \begin{bmatrix} 0 & \overline{\Delta} C & (\overline{\Delta} D_\phi - I) & 0 \end{bmatrix} \right\} \succeq 0, \tag{131}$$

for $j = 1, \ldots, m$. On the other hand, if the validity region is symmetric, i.e., for $\mathcal{X}_0$ given by (81) then, inspired from Lemma 9, the inclusion $\mathcal{L}(V_R, \rho) \subset \mathcal{X}_0$ is ensured if the following inequalities are satisfied

$$\begin{bmatrix} P_{11} & P_{12} & \rho C_j^T \\ \star & P_{22} & \rho D_{\phi_j}^T \\ \star & \star & \rho \overline{y}_j^2 \end{bmatrix} + \mathrm{He}\left\{ \frac{1}{2} \begin{bmatrix} (\underline{\Delta} C)^T \\ (\underline{\Delta} D_\phi - I)^T \\ 0 \end{bmatrix} S_{c,j} \begin{bmatrix} \overline{\Delta} C & (\overline{\Delta} D_\phi - I) & 0 \end{bmatrix} \right\} \succeq 0, \tag{132}$$

for $j = 1, \ldots, m$. Observe that in both cases the conditions for the function V_R are reduced to the inclusion of the level set $\mathcal{L}(V_{QG}, \rho)$ in $\mathcal{X}_0$, as discussed in Remark 7 and Remark 8, respectively. In fact, $\mathcal{L}(V_{QG}, \rho)$ is an outer approximation of $\mathcal{L}(V_R, \rho)$.

5.3.1 Optimization Problems

From the above conditions, we can formulate the following optimization problems.

P11. Given $\mathcal{T}_1$, the sector and slope bounds and the domain of validity of the sector conditions $\mathcal{X}_0$, compute the gains K_x and K_ϕ in order to maximize $\mathcal{T}_2$ and obtain an estimate of the region of attraction for which the stability of the closed-loop system (50) is ensured.

P12. Given a nominal sampling time $\mathcal{T}_{nom}$, the sector and slope bounds and the domain of validity of the sector conditions $\mathcal{X}_0$, compute the gains K_x and K_ϕ in order to find a bound on the maximum symmetrical allowable jitter, denoted by σ (*i.e.*, $\mathcal{T}_1 = \mathcal{T}_{nom} - \sigma$, $\mathcal{T}_2 = \mathcal{T}_{nom} + \sigma$) and obtain an estimate of the region of attraction for which the stability of the closed-loop system (50) is ensured.

P13. Given $\mathcal{T}_1$, $\mathcal{T}_2$ and the domain of validity of the sector conditions $\mathcal{X}_0$, compute the gains K_x and K_ϕ in order to maximize the sector and slope upper bounds given by the diagonal matrix Ω, and obtain an estimate of the region of attraction for which the stability of the closed-loop system (50) is ensured.

P14. Given $\mathcal{T}_1$, $\mathcal{T}_2$, the sector and slope bounds and the domain of validity of the sector conditions $\mathcal{X}_0$, compute the gains K_x and K_ϕ in order to improve the temporal response by maximizing μ, and obtain an estimate of the region of attraction for which the stability of the closed-loop system (50) is ensured and the decay rate at the sampling instants is maximized.

Observe that the conditions in *Theorem 9* are quasi-LMIs, since there exists involved nonlinearities which comes from the product of ε, β and $\overline{\Lambda}$ with the decision variables. To handle this issue, we will use the PSO algorithm described by *Algorithm 1*. As in the previous section, we must assign to each optimization problem a fitness function $f(\cdot)$ in order to identify the combination of the optimization parameters that leads to the best solution. The fitness function tests the feasibility of the LMIs (127)-(129) for the input particle, where each element of the particle corresponds to an optimization parameter. Two possible outcomes are assigned to the fitness function for the problems P11-P14, as detailed in Table 21.

Table 21: Regional Synthesis - Outputs of the fitness function for each optim. problem.

Problem	Fitness Function	Feasible	Infeasible
P11	$f_5([\varepsilon,\beta,\overline{\Lambda},\mathcal{T}_2])$	$f_5 = \mathcal{T}_2$	$f_5 = -1$
P12	$f_6([\varepsilon,\beta,\overline{\Lambda},\sigma])$	$f_6 = \sigma$	$f_6 = -1$
P13	$f_7([\varepsilon,\beta,\overline{\Lambda},\Omega])$	$f_7 = \Omega$	$f_7 = -1$
P14	$f_8([\varepsilon,\beta,\overline{\Lambda},\mu])$	$f_8 = \mu$	$f_8 = -1$

From Table 21, we have that if the LMIs are feasible for a given particle, f_5, f_6, f_7 and f_8 will return, respectively, $\mathcal{T}_2$, σ, Ω and μ. Otherwise, the respective functions will return -1. Following the same reasoning as in the previous section, a procedure to solve problems P11-P14 is given by the following steps:

Step 1/3 - Solve the corresponding optimization problem:

$$\begin{cases} \max\ \mathcal{T}_2\ (\text{or } \sigma,\ \text{or } \Omega,\ \text{or } \mu) \\ \text{subject to } (127), (128), (129). \end{cases} \tag{133}$$

Step 2/3 - From the matrices obtained in Step 1, recover P and Λ and then determine the maximum level set of the Lyapunov function such that $\mathcal{L}(V_R, \rho) \subset \mathcal{X}_0$. This can

be accomplished through the following optimization problem:

$$\begin{cases} \max \rho \\ \text{subject to (131). (Asymmetric case)} \\ \qquad\qquad (132). \text{ (Symmetric case)} \end{cases} \tag{134}$$

Step 3/3 - If the obtained level set does not touch at least one of the boundaries of the validity region $\mathcal{X}_0$, then increase ρ until this condition is satisfied. Therefore, this new level set defines an estimate of the region of attraction.

In the first step, we solve the quasi-LMIs as in the global synthesis case with the help of the PSO algorithm. Then, we recover the matrices P and Λ from the matrices obtained by the synthesis according to the relations detailed in the proof of *Theorem 8* to search a posteriori for the maximum level set that is included in $\mathcal{X}_0$. Since the conditions that guarantee this inclusion are based on an outer approximation of $\mathcal{L}(V_R, \rho)$, in the last step we increase ρ until the level set touches the boundaries of the validity region, thus giving a better estimate of the region of attraction.

5.3.2 Numerical Examples

Example: Consider system (18) given by the following matrices:

$$A = \begin{bmatrix} -2 & 1 \\ 1 & 1 \end{bmatrix}, B_u = \begin{bmatrix} 1 & 0 \\ 0 & 1 \end{bmatrix}, B_\phi = \begin{bmatrix} 1 & 0 \\ 0 & 2 \end{bmatrix} C = \begin{bmatrix} 0 & 1 \\ 1 & 0 \end{bmatrix}, D_\phi = \begin{bmatrix} 0 & 0 \\ 0 & 0 \end{bmatrix}.$$

Suppose that this system is fed back by nonlinearities $\phi_1(y_1) = \text{sgn}(y_1)y_1^2$ and $\phi_2(y_2) = \text{sgn}(y_2)y_2^2$ and that we are interested to stabilize it in the interval y_1, $y_2 \in [-1, 1]$. The sector and slope bounds are given by $\underline{\delta}_1 = \underline{\delta}_2 = 0$, $\overline{\delta}_1 = \overline{\delta}_2 = \Omega$, $\underline{\gamma}_1 = \underline{\gamma}_2 = 0$ and $\overline{\gamma}_1 = \overline{\gamma}_2 = 2\Omega$. The parameters chosen for the PSO algorithm were $\omega = 0.7298$ and $c_1 = c_2 = 1.4962$. Also, we defined $n_p = 100$, $n_{sw} = 75$ and the search space over $\varepsilon \in [0.01, 2]$, $\beta \in [0.01, 50000]$ and over the diagonal elements of $\overline{\Lambda}$ in $[0, 10]$. To reduce the number of optimization variables, we assume in this case equal values for the diagonal elements of $\overline{\Lambda}$, that is, $\overline{\Lambda} = \begin{bmatrix} \overline{\lambda} & 0 \\ 0 & \overline{\lambda} \end{bmatrix}$, as discussed in *Remark 12*. Initial velocities $\underline{s}_d$, $\overline{s}_d$ were set until 5% of the maximal value of the interval for each optimization variable.

The results for P11 are detailed in Table 22, by considering $\mathfrak{T}_1 = 0.1$ ms and $\Omega = 1$. The maximum intersampling time that we guarantee stability was $\mathfrak{T}_2 = 0.4758$ s. Moreover, the functions V_R and V_{QG} leads to the same results for the optimization problems with $\mu = 0$, $\mu = 0.5$ and $\mu = 1.0$, which are greater about 6.8%, 8.6% and 8.6% than those obtained with V_Q and V_L, respectively.

Table 22: Regional synthesis, Ex. 1 - Maximum $\mathfrak{T}_2$ for different μ and function V.

	Parameter	V_Q	V_{QG}	V_L	V_R
$\mu = 0$	β	49895.44	42185.35	31910.32	38624.45
	ε	0.1650	0.1409	0.1658	0.1408
	$\overline{\lambda}$	-	-	0.0000	0.0000
	$\boldsymbol{\mathfrak{T}_2}$	**0.4455**	**0.4758**	**0.4455**	**0.4758**
$\mu = 0.5$	β	50000.00	26549.95	38794.50	6800.99
	ε	0.5517	0.3886	0.5513	0.3884
	$\overline{\lambda}$	-	-	0.0000	0.0000
	$\boldsymbol{\mathfrak{T}_2}$	**0.3897**	**0.4236**	**0.3897**	**0.4236**
$\mu = 1.0$	β	3769.74	50000.00	8678.69	26415.92
	ε	1.0094	0.7325	1.0086	0.7330
	$\overline{\lambda}$	-	-	0.0000	0.0000
	$\boldsymbol{\mathfrak{T}_2}$	**0.3476**	**0.3776**	**0.3476**	**0.3776**

The results for P12 are detailed in Table 23, by considering $\mathfrak{T}_{nom} = 0.3$ s and $\Omega = 1$. Note that for $\mu = 0$ we could guarantee stability for $\mathfrak{T}_1 = 0.1240$ s and $\mathfrak{T}_2 = 0.4760$ s. For $\mu = 0.05$, the results of σ with the functions V_R and V_{QG} were 22.4% greater than the ones obtained with V_L and V_Q. For $\mu = 0.15$, this percentage increases to 25.7%.

Table 23: Regional synthesis, Ex. 1 - Maximum σ for different μ and function V.

	Parameter	V_Q	V_{QG}	V_L	V_R
$\mu = 0$	β	35488.32	45778.99	49600.35	26123.27
	ε	0.1652	0.1397	0.1655	0.1400
	$\overline{\lambda}$	-	-	0.0000	0.0000
	$\boldsymbol{\sigma}$	**0.1456**	**0.1760**	**0.1456**	**0.1760**
$\mu = 0.05$	β	50000.00	11238.27	50000.00	49710.49
	ε	0.1991	0.1628	0.1987	0.1627
	$\overline{\lambda}$	-	-	0.0000	0.0000
	$\boldsymbol{\sigma}$	**0.1393**	**0.1706**	**0.1393**	**0.1706**
$\mu = 0.15$	β	32211.20	45781.19	48093.45	40380.92
	ε	0.2711	0.2087	0.2717	0.2094
	$\overline{\lambda}$	-	-	0.0000	0.0000
	$\boldsymbol{\sigma}$	**0.1272**	**0.1599**	**0.1272**	**0.1599**

For P13, considering $\mathfrak{T}_1 = 0.1$ ms and $\mathfrak{T}_2 = 0.5$ s, results are depicted in Table 24. In this case, for $\mu = 0$, $\mu = 0.05$ and $\mu = 0.15$, the results of Ω with the functions V_R and V_{QG} were 10.2%, 10.8% and 12.1% greater than the ones obtained with V_L and V_Q, respectively.

Table 24: Regional synthesis, Ex. 1 - Maximum Ω for different μ and function V.

	Parameter	V_Q	V_{QG}	V_L	V_R
$\mu = 0$	β	23407.53	23241.00	32518.99	46866.68
	ε	0.1598	0.1387	0.1596	0.1389
	$\overline{\lambda}$	-	-	0.0000	0.0000
	Ω	**0.8467**	**0.9331**	**0.8467**	**0.9331**
$\mu = 0.05$	β	39589.07	34242.51	48809.92	32656.42
	ε	0.1919	0.1610	0.1914	0.1612
	$\overline{\lambda}$	-	-	0.0000	0.0000
	Ω	**0.8272**	**0.9170**	**0.8272**	**0.9170**
$\mu = 0.15$	β	10357.67	19423.37	50000.00	41529.69
	ε	0.2615	0.2074	0.2612	0.2073
	$\overline{\lambda}$	-	-	0.0000	0.0000
	Ω	**0.7877**	**0.8836**	**0.7877**	**0.8836**

Finally, for P14, the results are presented in Table 25, with $\mathcal{T}_1 = 0.1$ ms, $\mathcal{T}_2 = 0.3$ s and $\Omega = 1$. Again, the results with the function V_{QG} and V_R were less conservative than the ones with V_Q and V_L. Note that the variable $\overline{\Lambda}$ does not help to improve the solutions.

Table 25: Regional synthesis, Ex. 1 - Maximum μ for different function V.

Parameter	V_Q	V_{QG}	V_L	V_R
β	26722.32	33441.68	26938.03	25328.33
ε	1.8318	1.9988	1.8311	1.9994
$\overline{\lambda}$	-	-	0.0000	0.0000
μ	**1.7548**	**2.0897**	**1.7548**	**2.0897**

Let us consider the results from P11 (Table 22, $\mu = 0$). The estimate of the region of attraction corresponding to the solutions of P11 for different functions V is presented in Fig. 27, along with the boundaries of the region of validity. The obtained level set for the function V_R was $\rho = 3.1390 \cdot 10^4$, with the matrices

$$P = 10^5 \cdot \begin{bmatrix} 2.1687 & -0.9072 & -0.0257 & 0.2695 \\ -0.9072 & 0.6934 & 0.0730 & -0.0122 \\ -0.0257 & 0.0730 & -0.0074 & -0.1157 \\ 0.2695 & -0.0122 & -0.1157 & -0.0721 \end{bmatrix}, \quad \Lambda = \begin{bmatrix} 0 & 0 \\ 0 & 0 \end{bmatrix}.$$

In this case, the validity region in $\mathbb{R}^n$ can be described as $\mathcal{X}_0 = \{x \in \mathbb{R}^n | -1 \leq x_i \leq 1, i = 1, 2\}$, as shown in Fig. 27. Observe that with the functions V_{QG} and V_R the estimates cover a smaller region in comparison to the estimates with V_Q and V_L, but we emphasize that this area ensures stability for a larger $\mathcal{T}_2$. Furthermore, the estimates of the region of attraction with the functions V_{QG} and V_R do not touches the validity region. It was observed that occurs an atypical, unexpected behavior when we increase ρ in relation to the previous computed. This is illustrated in Fig. 28, through the level sets of V_R.

Figure 27 – Regional synthesis, Ex. 1 - Estimate of the region of attraction for P11 with different V.

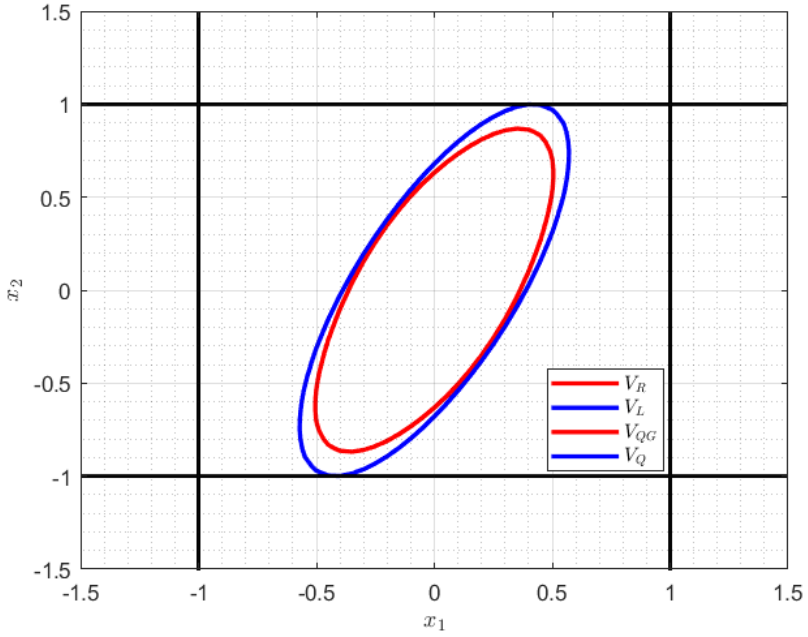

Font: Author.

Figure 28: Regional synthesis, Ex. 1 - Level sets of V_R.

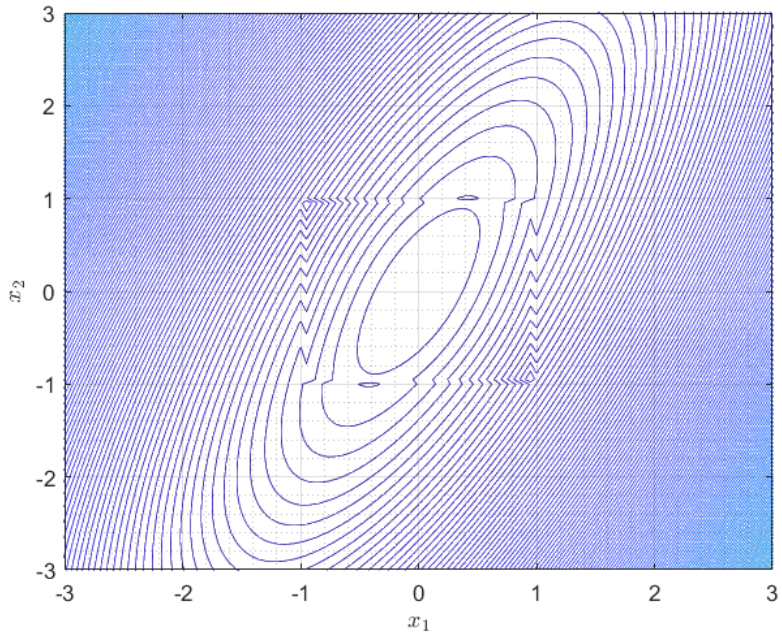

Font: Author.

Figure 28 depicts the level sets of V_R. Note that for a value of ρ slightly greater than the one obtained from problem (134), the level set is no longer compact and does not belong to the domain $\mathcal{X}_0$. So the computed ρ is actually the maximal one. Moreover, some "sawtooth" behavior can be observed at the level sets which crosses the validity region.

To show that stability is guaranteed for the obtained region, we simulate the closed-loop system (50), as presented in Fig. 29, by considering the solution of P11 with V_R and $T_k \in [0.0001, 0.4758]$. As observed in Fig. 29, the continuous-time trajectories starting at $\partial\mathcal{L}(V_R, \rho)$ with $\rho = 3.1390 \cdot 10^4$ converge to the origin. Finally, we aim to show the effectiveness of the synthesis method which allows to improve the time-response of the closed-loop system in terms of decay rate through the parameter μ. In this case, the gains obtained with performance constraint $\mu = 0$, $\mu = 0.5$ and $\mu = 1.0$ are given in Table 26.

Figure 29: Regional synthesis, Ex. 1 - Trajectories of the closed-loop system for P11.

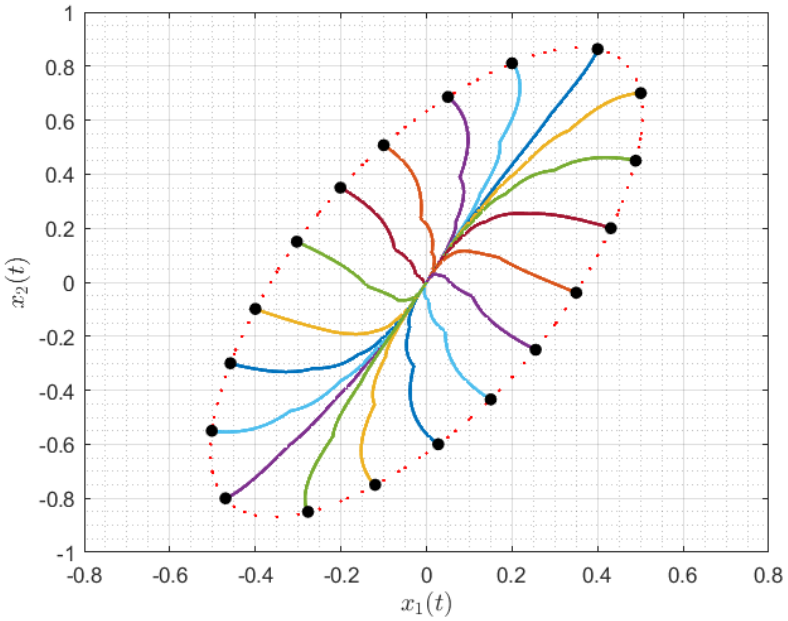

Font: Author.

Table 26: Regional synthesis, Ex.1 - Gains obtained from P11 with the function V_R.

	K_x	K_ϕ
$\mu = 0$	$\begin{bmatrix} -0.0805 & -0.4091 \\ 0.1567 & -1.9873 \end{bmatrix}$	$\begin{bmatrix} -0.6923 & -0.0356 \\ -0.1205 & -1.6127 \end{bmatrix}$
$\mu = 0.5$	$\begin{bmatrix} -0.0317 & -0.4139 \\ 0.1147 & -2.2404 \end{bmatrix}$	$\begin{bmatrix} -0.7461 & -0.1133 \\ -0.1318 & -1.7026 \end{bmatrix}$
$\mu = 1.0$	$\begin{bmatrix} -0.4846 & -0.2309 \\ 0.3811 & -2.6941 \end{bmatrix}$	$\begin{bmatrix} -0.7896 & -0.1875 \\ -0.1293 & -1.7253 \end{bmatrix}$

To show that asymptotic stability holds for these cases, we choose the intersampling interval in the range $T_k \in [0.0001, 0.3776]$, which is the result for $\mu = 1$. The control action and the states for different values of μ are presented in Figs. 30 and 31, by considering $x(0) = [0.4\ 0.8]^T$.

Figure 30: Regional synthesis, Ex. 1 - Control action of the closed-loop system.

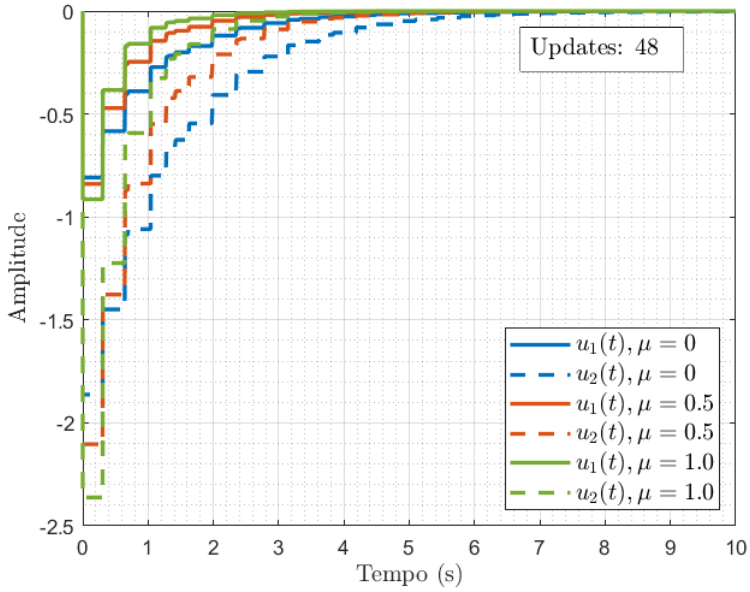

Font: Author.

Figure 31: Regional synthesis, Ex. 1 - States of the closed-loop system.

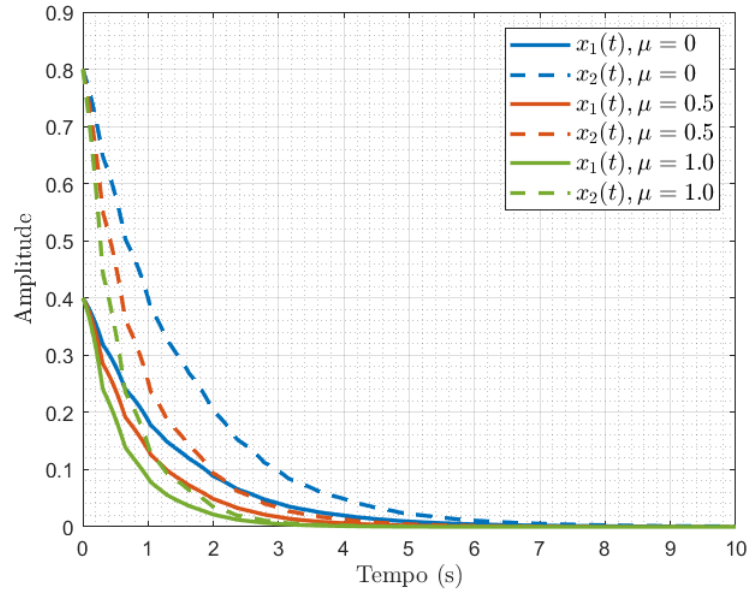

Font: Author.

Note that with $\mu = 1$ the states x_1 and x_2 converge faster to the origin, as expected, at the cost of higher control action.

5.4 Final Comments

This chapter presented the latest contributions of this dissertation, which provides new conditions for the synthesis of stabilizing controllers in the form of quasi-LMIs for both global and regional contexts, based on the results of the previous chapter.

Optimization problems are stated aiming to compute the gains K_x and K_ϕ in a way to maximize the intersampling intervals, the sector bounds or to improve the time-response of the closed-loop system. An estimate of the region of attraction is also provided for the regional case. Since there exists involved nonlinearities between the product of β, ε and $\overline{\Lambda}$ with the decision variables in the presented conditions, we propose a heuristic-based algorithm called Particle Swarm Optimization to search for the best combination of these ones while testing the feasibility of the LMI constraints.

The results from the numerical examples shows that the function V_R reduce the conservatism in comparison to the other functions in some cases. However, we should point out that the requirement on the positivity of the Lure coefficients and on the nonlinearities to be monotonically increasing are limiting factors to obtain less restrictive results.

6 CONCLUSIONS

This dissertation presented a new method for stability analysis and synthesis of sampled-data control for Lure systems subject to aperiodic sampling and nonlinearities that are sector and slope restricted. The method is based on a looped-functional approach that relates the discrete and continuous-time behavior of the SDC, combined with a generalized Lure function. The motivation for this study is given by the lack of results concerning stability and stabilization of sampled-data control Lure systems and due to the fact that many physical systems can be represented in this form. In the sequence, we summarize the main conclusions from each chapter of this dissertation and, afterwards, some future perspectives are discussed.

In Chapter 3, a representation of the sampled-data Lure system was given in the looped-functional framework. As preliminary results, we stated two main theorems that provides asymptotic stability conditions for the trajectories of the continuous-time closed-loop system under a generic sampled-data control law, respectively, in global and local contexts. From these theorems, we started addressing the choice of the functional candidate, which has terms that depend both on the states, nonlinearities and its derivatives. A main feature of this approach is that we do not need to impose the positivity of the functional in the global case, differently from LKF-based approaches. Next, we presented the generalized Lure function, which structure contains a quadratic term on the states and on the nonlinearities and has a Lure-Postnikov integral term, allowing the relaxation on the positivity of the Lure-Postnikov coefficients as well of the quadratic terms. From these results and from the classical sector conditions, we obtained the necessary ingredients to proceed to the analysis and synthesis problems.

In Chapter 4, preliminary results given by *Theorem 4* were initially used to derive conditions in the form of linear matrix inequalities to ensure the global asymptotic stability of the origin of the sampled-data Lure system. Optimization problems regarding the maximization of the admissible intersampling intervals or the maximal sector bounds were formulated, which could be solved through LMI feasibility tests and bisection algorithms. Numerical examples were provided. Also, the method was compared to the one of (SEIFULLAEV; FRADKOV, 2015), yielding in greater results on the upper intersam-

pling bound. Afterwards, we treated about the stability in a regional context, based on the results of *Theorem 5*. In this case the sector and slope bounds hold only in a domain of validity, and the main interest is to obtain an estimate of the region of attraction for which stability is ensured. On this basis, we provided sufficient conditions to guarantee the inclusion of the level sets of a function V into symmetric or asymmetric validity regions and then we formulated different optimization problems. Numerical examples illustrated the efficiency of the results.

Finally, in Chapter 5, the conditions obtained in the analysis problems are modified in an appropriate way to derive synthesis conditions in both global and regional contexts, *i.e.*, to compute feedback gains such that the stabilization of the closed-loop system is guaranteed. The resulting inequalities are quasi-LMIs, that is, are LMIs by fixing some variables, which implies that nonlinearities arises from the product between some decision variables. To tackle this problem, we proposed a Particle Swarm Optimization algorithm, which searches for the best combination of the optimization variables while supporting feasibility of LMIs. Optimization problems analogous to analysis ones were provided, highlighting the potentialities of the method. An additional condition to improve the time response of the closed-loop system in terms of decay rate at the sampling instants was also presented. It should be highlighted that, after the synthesis procedures, the analysis methods which are based on less conservative assumptions, can be used to still improve the bounds on $\mathcal{T}_2$, σ or Ω obtained.

Finally, we conclude that this work provides an evolution of the theory for stability assessment and stabilization of sampled-data control Lure systems. In addition, it attempts to fill a gap in the literature, since to date synthesis results considering SDC have been lacking in both global and local cases.

6.1 Perspectives and Future Work

The results presented in the previous chapters point to some perspectives and themes that can be explored in the continuation of this work, as described below:

- *The use of new looped-functionals*. If the functional satisfies the conditions stated in *Theorem 4* and *Theorem 5*, then it can be directly incorporated into the LMIs. Moreover, the development of less restrictive functionals is still an open field of research;

- *Analysis and synthesis for a given region of stability*. In this case, the choice of the optimization criteria is essential so that the estimates of the region of attraction are not conservative;

- *Systems with uncertain parameters*. This can be incorporated to the LMI conditions by considering polytopic or norm bounded uncertainties. From a practical

viewpoint, the resulting conditions will be more restrictive and the difficulty to find feasible solutions is increased;

- *Analysis and synthesis of dynamic output feedback controllers*. This extension could be explored by considering a more realistic hypothesis that the controller is a function of a generic output $z(t_k)$. Thus, the available information for sampling is reduced to what is in the output of the plant, and static or dynamic output feedback control laws should be investigated (GOMES DA SILVA JR *et al.*, 2016).

- *A sampled-data control system with delayed inputs*. In this case, $u(t) = K_x x(t_k - \tau(t)) + K_\phi \phi(t_k - \tau(t))$ for the states and nonlinearities feedback or $u(t) = Kz(t_k - \tau(t))$ for the dynamic output feedback. This extension would represent more accurately the delays coming from the NCS, since the delay induced by the communication protocols and data acquisition, along with the uncertain sampling intervals already considered, is a major aspect of this topology;

- *Multi-rate sampled-data under aperiodic sampling*. Inspired in (PARK; PARK, 2020), in some cases the measurements from the sensors are acquired with different sampling rates, due to different sensing methods or due to calculus of data coming from different sensors. In addition, the data of the sensors are transferred aperiodically in the networks even under uniformly sampling, since network delays and packet losses may occur;

- *Sampling as a control parameter*. As discussed in (HETEL *et al.*, 2017), this concerns the case when the sampling interval t_k, or equivalently the sequence of sampling $\{t_k\}_{k\in\mathbb{N}}$, is considered to be a control parameter that can be modified in order to ensure desired properties in terms of stability and resource/network utilization. This formulation corresponds to design a scheduling mechanism in real time control that triggers the sampler.

6.2 Publications

This work allowed the following article to be prepared, describing the preliminary results obtained:

- TITTON, M. G.; GOMES DA SILVA JR., J. M.; VALMORBIDA, G. Stability of sampled-data control for Lurie systems with slope-restricted nonlinearities. In: CONGRESSO BRASILEIRO DE AUTOMÁTICA XXIII, 23., 2020. **Anais [...]** SBA, 2020. v2. n.1.

REFERENCES

ANTSAKLIS, P.; BAILLIEUL, J. Special issue on technology of networked control systems. **Proceedings of the IEEE**, New York, v. 95, n. 1, p. 5–8, 2007.

ARCAK, M.; LARSEN, M.; KOKOTOVIĆ, P. Circle and Popov criteria as tools for nonlinear feedback design. **Automatica**, Amsterdam, v. 39, n. 4, p. 643–650, 2003.

ÅSTRÖM, K. J.; WITTENMARK, B. **Computer-controlled systems**: theory and design. New York: Dover Publications, Inc., 2013.

BANSAL, J. C. *et al.* Inertia weight strategies in particle swarm optimization. *In*: THIRD WORLD CONGRESS ON NATURE AND BIOLOGICALLY INSPIRED COMPUTING, 3., 2011, Salamanca. **Proceedings [...]** New York: IEEE, 2011. p. 633–640.

BOYD, S. P. *et al.* **Linear matrix inequalities in system and control theory**. Philadelphia: SIAM, 1994. v. 15.

BRIAT, C. Convex conditions for robust stability analysis and stabilization of linear aperiodic impulsive and sampled-data systems under dwell-time constraints. **Automatica**, Amsterdam, v. 49, n. 11, p. 3449–3457, 2013.

BRIAT, C. Theoretical and numerical comparisons of looped functionals and clock-dependent Lyapunov functions - The case of periodic and pseudo-periodic systems with impulses. **International Journal of Robust and Nonlinear Control**, Chichester, v. 26, n. 10, p. 2232–2255, 2016.

BRIAT, C.; SEURET, A. A looped-functional approach for robust stability analysis of linear impulsive systems. **Systems & Control Letters**, Amsterdam, v. 61, n. 10, p. 980–988, 2012.

BRIAT, C.; SEURET, A. Convex dwell-time characterizations for uncertain linear impulsive systems. **IEEE Transactions on Automatic Control**, New York, v. 57, n. 12, p. 3241–3246, 2012.

CAO, Y.-Y.; SUN, Y.-X.; CHENG, C. Delay-dependent robust stabilization of uncertain systems with multiple state delays. **IEEE Transactions on Automatic Control**, New York, v. 43, n. 11, p. 1608–1612, 1998.

CASTELAN, E. B.; TARBOURIECH, S.; QUEINNEC, I. Control design for a class of nonlinear continuous-time systems. **Automatica**, Amsterdam, v. 44, n. 8, p. 2034–2039, 2008.

CHEN, T.; FRANCIS, B. A. **Optimal sampled-data control systems**. London: Springer Science & Business Media, 2012.

CHIU, W.-Y. Method of reduction of variables for bilinear matrix inequality problems in system and control designs. **IEEE Transactions on Systems, Man, and Cybernetics: Systems**, New York, v. 47, n. 7, p. 1241–1256, 2016.

CLERC, M.; KENNEDY, J. The particle swarm - explosion, stability, and convergence in a multidimensional complex space. **IEEE Transactions on Evolutionary Computation**, New York, v. 6, n. 1, p. 58–73, Feb 2002.

DULLERUD, G. E.; LALL, S. Asynchronous hybrid systems with jumps - analysis and synthesis methods. **Systems & Control Letters**, Amsterdam, v. 37, n. 2, p. 61–69, 1999.

FAGUNDES, A. S.; GOMES DA SILVA JR., J. M.; JUNGERS, M. Stability of control systems under aperiodic sampling and input saturation with clock-dependent Lyapunov functions. *In:* SIMPÓSIO BRASILEIRO de AUTOMAÇÃO INTELIGENTE, 14., 2019, Ouro Preto. **Anais [...]**. Campinas: Galoá, 2019. Available in: https://proceedings.science/sbai-2019/papers/stability-of-control-systems-under-aperiodic-sampling-and-input-saturation-with-clock-dependent-lyapunov-functions. Access in: 19 feb. 2021.

FIACCHINI, M.; GOMES DA SILVA JR., J. M. Stability of sampled-data control systems under aperiodic sampling and input saturation. *In*: IEEE CONFERENCE ON DECISION AND CONTROL (CDC), 57, 2018, Miami. **Proceedings [...]** New York: IEEE, 2018. p. 6644–6649.

FRIDMAN, E. Use of models with aftereffect in the problem of the design of optimal digital-control systems. **Automation and remote control**, New York, v. 53, n. 10, p. 1523–1528, 1992.

FRIDMAN, E. A refined input delay approach to sampled-data control. **Automatica**, Amsterdam, v. 46, n. 2, p. 421–427, 2010.

FRIDMAN, E. **Introduction to time-delay systems**: analysis and control. New York: Springer, 2014.

FRIDMAN, E.; SEURET, A.; RICHARD, J.-P. Robust sampled-data stabilization of linear systems: an input delay approach. **Automatica**, Amsterdam, v. 40, n. 8, p. 1441–1446, 2004.

FUJIOKA, H. Stability analysis of systems with aperiodic sample-and-hold devices. **Automatica**, Amsterdam, v. 45, n. 3, p. 771–775, 2009.

GAO, H.; CHEN, T. Network-Based $\mathcal{H}_\infty$ Output Tracking Control. **IEEE Transactions on Automatic control**, New York, v. 53, n. 3, p. 655–667, 2008.

GOEBEL, R.; SANFELICE, R. G.; TEEL, A. R. Hybrid dynamical systems. **IEEE control systems magazine**, New York, v. 29, n. 2, p. 28–93, 2009.

GOEBEL, R.; SANFELICE, R.; TEEL, A. **Hybrid Dynamical Systems**: modeling, stability, and robustness. New Jersey: Princeton University Press, Princeton (NJ), 2012.

GOMES DA SILVA JR, J. M. *et al.* Regional stability analysis of discrete-time dynamic output feedback under aperiodic sampling and input saturation. **IEEE Transactions on Automatic Control**, New York, v. 61, n. 12, p. 4176–4182, 2016.

GOMES DA SILVA JR, J. M. *et al.* Dynamic output feedback stabilization for systems with sector-bounded nonlinearities and saturating actuators. **Journal of the Franklin Institute**, Philadelphia, v. 350, n. 3, p. 464–484, 2013.

GONZAGA, C. A.; JUNGERS, M.; DAAFOUZ, J. Stability analysis of discrete-time Lur'e systems. **Automatica**, Amsterdam, v. 48, n. 9, p. 2277–2283, 2012.

HADDAD, W. M.; KAPILA, V. Absolute stability criteria for multiple slope-restricted monotonic nonlinearities. **IEEE Transactions on Automatic Control**, New York, v. 40, n. 2, p. 361–365, 1995.

HALE, J. K.; LUNEL, S. M. V. **Introduction to functional differential equations**. New York: Springer Science & Business Media, 2013. v. 99.

HAO, F.; ZHAO, X. Absolute stability of Lurie networked control systems. **International Journal of Robust and Nonlinear Control**, Chichester, v. 20, n. 12, p. 1326–1337, 2010.

HESPANHA, J. P.; LIBERZON, D.; TEEL, A. R. Lyapunov conditions for input-to-state stability of impulsive systems. **Automatica**, Amsterdam, v. 44, n. 11, p. 2735–2744, 2008.

HESPANHA, J. P.; NAGHSHTABRIZI, P.; XU, Y. A Survey of recent results in networked control systems. **Proceedings of the IEEE**, New York, v. 95, n. 1, p. 138–162, 2007.

HETEL, L. *et al.* Recent developments on the stability of systems with aperiodic sampling: an overview. **Automatica**, Amsterdam, v. 76, p. 309–335, 2017.

HOU, L.; MICHEL, A. N.; YE, H. Some qualitative properties of sampled-data control systems. **IEEE Transactions on Automatic Control**, New York, v. 42, n. 12, p. 1721–1725, 1997.

HU, L.-S. *et al.* A linear matrix inequality (LMI) approach to robust $\mathcal{H}_2$ sampled-data control for linear uncertain systems. **IEEE Transactions on Systems, Man, and Cybernetics, Part B (Cybernetics)**, New York, v. 33, n. 1, p. 149–155, 2003.

HU, T.; HUANG, B.; LIN, Z. Absolute stability with a generalized sector condition. **IEEE Transactions on Automatic Control**, New York, v. 49, n. 4, p. 535–548, 2004.

JIANG, X. *et al.* A New $\mathcal{H}_\infty$ Stabilization criterion for networked control systems. **IEEE Transactions on Automatic control**, New York, v. 53, n. 4, p. 1025–1032, 2008.

KABAMBA, P. T.; HARA, S. Worst-case analysis and design of sampled-data control systems. **IEEE Transactions on Automatic Control**, New York, v. 38, n. 9, p. 1337–1358, 1993.

KENNEDY, J. The particle swarm: social adaptation of knowledge. *In*: IEEE INTERNATIONAL CONFERENCE ON EVOLUTIONARY COMPUTATION (ICEC'97), 1., 1997, New York. **Proceedings [...]** New York: IEEE, 1997. p. 303–308.

KENNEDY, J.; EBERHART, R. Particle swarm optimization. *In*: ICNN'95 - INTERNATIONAL CONFERENCE ON NEURAL NETWORKS, 4., 1995. **Proceedings [...]** New York: IEEE, 1995. p. 1942–1948.

KHALIL, H. K. **Nonlinear systems**. 3rd. ed. Upper Saddle River: Prentice-Hall, 2002.

KOLMANOVSKII, V.; MYSHKIS, A. **Applied theory of functional differential equations**. Dordrecht: Springer Science & Business Media, 2012. v. 85.

LIU, K.; SUPLIN, V.; FRIDMAN, E. Stability of linear systems with general sawtooth delay. **IMA Journal of Mathematical Control and Information**, New York, v. 27, n. 4, p. 419–436, 2010.

LOUIS, J.; JUNGERS, M.; DAAFOUZ, J. Sufficient LMI stability conditions for Lur'e type systems governed by a control law designed on their Euler approximate model. **International Journal of Control**, London, v. 88, n. 9, p. 1841–1850, 2015.

MICHEL, A. N.; HU, B. Towards a stability theory of general hybrid dynamical systems. **Automatica**, Amsterdam, v. 35, n. 3, p. 371–384, 1999.

MIHEEV, Y. V.; SOBOLEV, V. A.; FRIDMAN, È. M. Asymptotic analysis of digital control systems. **Avtomatika I Telemekhanika**, New York, n. 9, p. 83–88, 1988.

MIRKIN, L. Some remarks on the use of time-varying delay to model sample-and-hold circuits. **IEEE Transactions on Automatic Control**, New York, v. 52, n. 6, p. 1109–1112, 2007.

MOREIRA, L. *et al.* Stability analysis of rational nonlinear sampled-data control systems: a looped-functional approach. *In*: AMERICAN CONTROL CONFERENCE (ACC), 37, 2019, Philadelphia. **Proceedings [...]** New York: IEEE, 2019. p. 2414–2419.

MOUSA, M.; MILLER, R.; MICHEL, A. Stability analysis of hybrid composite dynamical systems: descriptions involving operators and difference equations. **IEEE Transactions on Automatic Control**, New York, v. 31, n. 7, p. 603–615, 1986.

NAGHSHTABRIZI, P.; HESPANHA, J. P.; TEEL, A. R. Exponential stability of impulsive systems with application to uncertain sampled-data systems. **Systems & Control Letters**, Amsterdam, v. 57, n. 5, p. 378–385, 2008.

OLIVEIRA, M. C.; SKELTON, R. E. Stability tests for constrained linear systems. *In*: MOHEIMANI, S. O. R. (Ed.). **Perspectives in robust control**. London: Springer, 2001. p. 241–257.

PALMEIRA, A. H. K.; GOMES DA SILVA JR, J. M.; FLORES, J. V. Regional stabilization of nonlinear sampled-data control systems: A quasi-LPV approach. **European Journal of Control**, In Press, 2020.

PALMEIRA, A. H. K. *et al.* Sampled-data control under magnitude and rate saturating actuators. **International Journal of Robust and Nonlinear Control**, Chichester, v. 26, n. 15, p. 3232–3252, 2016.

PARK, J.; PARK, P. An improved stability criterion for linear systems with multi-rate sampled data. **Nonlinear Analysis: Hybrid Systems**, Amsterdam, v. 38, p. 100947, 2020.

PARK, P. Stability criteria of sector-and slope-restricted Lur'e systems. **IEEE Transactions on Automatic Control**, New York, v. 47, n. 2, p. 308–313, 2002.

PARK, P.; BANJERDPONGCHAI, D.; KAILATH, T. The asymptotic stability of nonlinear (Lur'e) systems with multiple slope restrictions. **IEEE Transactions on Automatic Control**, New York, v. 43, n. 7, p. 979–982, 1998.

SEIFULLAEV, R. E.; FRADKOV, A. L. Sampled-data control of nonlinear oscillations based on LMIs and Fridman's method. **IFAC Proceedings Volumes**, Caen, v. 46, n. 12, p. 95–100, 2013.

SEIFULLAEV, R. E.; FRADKOV, A. L. Sampled-data control of nonlinear systems based on Fridman's analysis and passification design. **IFAC-PapersOnLine**, Saint-Petersburg, v. 48, n. 11, p. 685–690, 2015.

SEIFULLAEV, R. E.; FRADKOV, A. L. Robust nonlinear sampled-data system analysis based on Fridman's method and S-procedure. **International Journal of Robust and Nonlinear Control**, Chichester, v. 26, n. 2, p. 201–217, 2016.

SEURET, A. Stability analysis for sampled-data systems with a time-varying period. *In*: IEEE CONFERENCE ON DECISION AND CONTROL (CDC) HELD JOINTLY WITH 2009 28TH CHINESE CONTROL CONFERENCE, 48., 2009, New York. **Proceedings [...]** New York: IEEE, 2009. p. 8130–8135.

SEURET, A. A novel stability analysis of linear systems under asynchronous samplings. **Automatica**, Amsterdam, v. 48, n. 1, p. 177–182, 2012.

SEURET, A.; GOMES DA SILVA JR., J. M. Taking into account period variations and actuator saturation in sampled-data systems. **Systems & Control Letters**, Amsterdam, v. 61, n. 12, p. 1286–1293, 2012.

SHI, Y.; EBERHART, R. A modified particle swarm optimizer. *In*: IEEE INTERNATIONAL CONFERENCE ON EVOLUTIONARY COMPUTATION PROCEEDINGS. IEEE WORLD CONGRESS ON COMPUTATIONAL INTELLIGENCE (CAT. NO. 98TH8360), 5., 1998, Anchorage. **Proceedings [...]** New York: IEEE, 1998. p. 69–73.

SIVASHANKAR, N.; KHARGONEKAR, P. P. Characterization of the $\mathcal{L}_2$-induced norm for linear systems with jumps with applications to sampled-data systems. **SIAM Journal on Control and Optimization**, Philadelphia, v. 32, n. 4, p. 1128–1150, 1994.

SUN, W.; NAGPAL, K. M.; KHARGONEKAR, P. P. $\mathcal{H}_\infty$ control and filtering for sampled-data systems. **IEEE Transactions on Automatic Control**, New York, v. 38, n. 8, p. 1162–1175, 1993.

SUYKENS, J.; VANDEWALLE, J.; DE MOOR, B. An absolute stability criterion for the Lur'e problem with sector and slope restricted nonlinearities. **IEEE Transactions on Circuits and Systems I: Fundamental Theory and Applications**, New York, v. 45, n. 9, p. 1007–1009, 1998.

TOIVONEN, H. T. Sampled-data $\mathcal{H}_\infty$ optimal control of time-varying systems. **Automatica**, Amsterdam, v. 28, n. 4, p. 823–826, 1992.

TURNER, M. C.; KERR, M. Lyapunov functions and $\mathcal{L}_2$ gain bounds for systems with slope restricted nonlinearities. **Systems & Control Letters**, Amsterdam, v. 69, p. 1–6, 2014.

VALMORBIDA, G.; DRUMMOND, R.; DUNCAN, S. R. Positivity conditions of Lyapunov functions for systems with slope restricted nonlinearities. *In*: AMERICAN CONTROL CONFERENCE (ACC), 34., 2016, New York. **Proceedings [...]** New York: IEEE, 2016. p. 258–263.

VALMORBIDA, G.; DRUMMOND, R.; DUNCAN, S. R. Regional analysis of slope-restricted Lurie systems. **IEEE Transactions on Automatic Control**, New York, v. 64, n. 3, p. 1201–1208, 2018.

VIDYASAGAR, M. **Nonlinear systems analysis**. Philadelphia: SIAM, 2002.

YE, H.; MICHEL, A. N.; HOU, L. Stability theory for hybrid dynamical systems. **IEEE Transactions on Automatic Control**, New York, v. 43, n. 4, p. 461–474, 1998.

YU, M. *et al.* Stabilization of networked control systems with data packet dropout and transmission delays: continuous-time case. **European Journal of Control**, London, v. 11, n. 1, p. 40–49, 2005.

ZAMPIERI, S. Trends in networked control systems. **IFAC Proceedings Volumes**, Seoul, v. 41, n. 2, p. 2886–2894, 2008.

ZANI, A.; FLORES, J. V.; GOMES DA SILVA JR., J. M. Synchronization Analysis of Piecewise-Linear Lur'e Systems under Sampled-Data Control. **IFAC-PapersOnLine**, Florianópolis, v. 51, n. 25, p. 234–239, 2018.

ZENG, H.-B.; TEO, K. L.; HE, Y. A new looped-functional for stability analysis of sampled-data systems. **Automatica**, Amsterdam, v. 82, p. 328–331, 2017.

ZENG, H.-B. *et al.* Absolute stability and stabilization for Lurie networked control systems. **International Journal of Robust and Nonlinear Control**, Chichester, v. 21, n. 14, p. 1667–1676, 2011.

ZENG, H.-B. *et al.* New insights on stability of sampled-data systems with time-delay. **Applied Mathematics and Computation**, Philadelphia, v. 374, p. 125041, 2020.

ZHANG, X.-M. *et al.* Networked control systems: a survey of trends and techniques. **IEEE/CAA Journal of Automatica Sinica**, New York, v. 7, n. 1, p. 1–17, 2019.

APPENDIX A BASIC CONCEPTS

In this section, it will be presented some concepts related to the stability of nonlinear systems, considering Lyapunov's theory.

A.1 Stability in the sense of Lyapunov

Characterization of the stability of nonlinear systems is a fundamental problem in control theory. For the case where systems does not have disturbances or exogenous signals, the main focus is in ensuring the stability of the equilibrium point. The following statements makes precise the notion of stability in the sense of Lyapunov to conceptualize internal stability for the nonlinear, continuous-time system:

$$\dot{x}(t) = f(x(t)), \quad x(t_0) = x(0), \tag{135}$$

where $x \in \mathbb{R}^n$, $t \geq 0$.

Definition 3 (Equilibrium Point)**.** *A point $x = x_e$ in the state space is defined as a equilibrium point if whenever the state of the system start x_e, it will remain at x_e for all future time, or equivalently, $f(x_e) = 0, \forall t \geq 0$.*

In general, it is supposed that the equilibrium point of the system is the origin. However, if it is not, the equilibrium point x_e can be translated to the origin, making 0 the equilibrium point of the translated system (KHALIL, 2002).

Definition 4 (Stability)**.** *The equilibrium point $x_e = 0$ is a stable equilibrium point if $\forall t_0 \geq 0$ and $\varepsilon > 0$, there exists $\delta(t_0, \varepsilon)$ such that*

$$\|x(0)\| < \delta(t_0, \varepsilon) \Rightarrow \|x(t)\| < \varepsilon, \ \forall t \geq t_0, \tag{136}$$

where $x(t)$ is the solution of the system starting in $x(0)$, on time $t = t_0$.

If an equilibrium point is not stable, then it is unstable.

Definition 5 (Asymptotic stability)**.** *The equilibrium point $x_e = 0$ is an asymptotically stable equilibrium point if*

i) $x_e = 0$ *is a stable equilibrium point;*

ii) $x_e = 0$ *is attractive , i.e., there exists a* $\delta(t_0)$ *such that*

$$\|x(0)\| < \delta(t_0) \Rightarrow \lim_{t\to\infty} \|x(t)\| = 0. \tag{137}$$

Define now

$$\mathcal{B}(r) = \{x \in \mathbb{R}^n | \ \|x - x_e\| \leq r, r > 0\}. \tag{138}$$

Consider regions $\mathcal{B}(\delta)$ and $\mathcal{B}(\varepsilon)$ similarly to that presented in (138). According to Definition 4, for an equilibrium point to be stable, the trajectories starting inside from the region represented by $\mathcal{B}(\delta)$ with radius δ must not leave the region $\mathcal{B}(\varepsilon)$ with radius ε, which is centred on the equilibrium point x_e. Thus, it can be said that the system has a stable equilibrium point. Moreover, if the trajectories converge to the equilibrium point x_e and stays there for all t, then the equilibrium point is asymptotically stable. This definition of stability is illustrated in Figure 32.

Figure 32: Stability in the sense of Lyapunov.

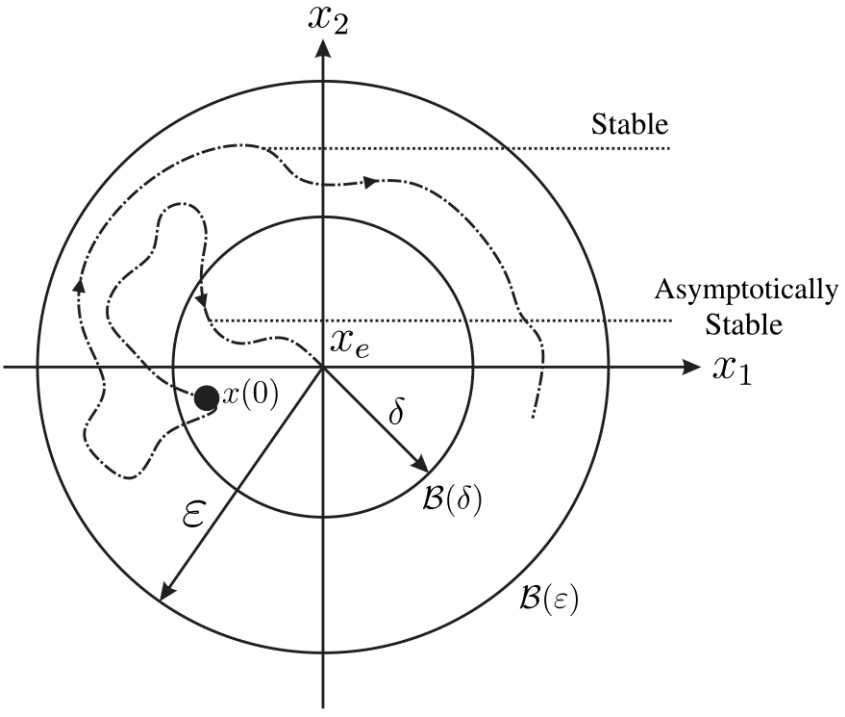

Font: Author.

Definition 6 (Global asymptotic stability)**.** *The equilibrium point* $x_e = 0$ *is a globally asymptotically stable equilibrium point if it is stable and*

$$\lim_{t\to\infty} x(t) = 0, \ \forall x(0) \in \mathbb{R}^n. \tag{139}$$

A.2 Linear Matrix Inequality

This section will present the theory related to linear matrix inequalities (LMIs), which are used to solve a wide variety of problems arising in system and control theory. The main feature of this approach is that many of control problems which does not have an analytic solution can be solved numerically through LMI restrictions in a reliable way (BOYD *et al.*, 1994).

Definition 7 (Linear Matrix Inequality)**.** *A linear matrix inequality has the following structure:*

$$F(x) = F_0 + \sum_{i=1}^{m} x_i F_i \succ 0, \tag{140}$$

where $x \in \mathbb{R}^n$ is a vector of decision variables and the symmetric matrices $F_i \in \mathbb{S}^n$, $i = 0, \ldots, m$ are given. The inequality symbol in (140) means that $F(x)$ is positive definite, i.e., $u^T F(x) u > 0$ for all nonzero $u \in \mathbb{R}^n$, which is equivallent to a set of n polynomial inequalities in x, or in other words, the leading principal minors of $F(x)$ must be positive. Inequality (140) can be also strictly negative, i.e., $F(x) \prec 0$ or nonstrict, in the form $F(x) \succeq 0$ or $F(x) \preceq 0$.

The main interest of developing problems in an LMI form is that (140) is a convex constraint on x, i.e., the set $\{x | F(x) \succ 0\}$ is convex. This property is fundamental to treat constraints and optimization problems that arises in control theory as SDP problems, i.e., convex optimization problems that minimizes a linear objective function of a decision variable vector $x \in \mathbb{R}^n$, as for example

$$\begin{cases} \min\limits_{x} \ c^T x \\ \text{subject to } F(x) \succ 0, \end{cases} \tag{141}$$

with F an affine function of x, or evaluate the feasibility of LMI restrictions.

A.3 Finsler's Lemma

Finsler's Lemma allows to obtain equivalent conditions in LMI forms by adding or eliminating some variables. This lemma is stated as follows.

Lemma 11 (Finsler's Lemma (OLIVEIRA; SKELTON, 2001))**.** *Let $\xi \in \mathbb{R}^n$, $\mathcal{L} \in \mathbb{S}^n$, $\mathcal{B} \in \mathbb{R}^{q \times n}$, with rank$(\mathcal{B}) < n$ and $\mathcal{B}\mathcal{B}_\perp = 0$. Then the following statements are equivalent:*

$$i) \quad \xi^T \mathcal{L} \xi < 0, \ \forall \xi \in \mathbb{R}^n, \ \xi \neq 0, \mathcal{B}\xi = 0; \tag{142}$$

$$ii) \quad \mathcal{B}_\perp^T \mathcal{L} \mathcal{B}_\perp < 0; \tag{143}$$

$$iii) \quad \exists \mu \in \mathbb{R} : \mathcal{L} - \mu \mathcal{B}^T \mathcal{B} \prec 0; \tag{144}$$

$$iv) \quad \exists \mathcal{X} \in \mathbb{R}^{n \times q} : \mathcal{L} + \mathcal{X}\mathcal{B} + \mathcal{B}^T \mathcal{X}^T \prec 0. \tag{145}$$

A.4 Schur's Complement

The Schur Complement (BOYD *et al.*, 1994) is used to convert non-linear convex inequalities into a LMI form and vice-versa. This artifice is formally presented below.

Lemma 12 (Schur's Complement (BOYD *et al.*, 1994))**.** *Let $Q(x) = Q(x)^T$, $R(x) = R(x)^T$ and $S(x)$ real matrices of appropriate dimensions. Then:*

$$i) \quad Q(x) - S(x)R(x)^{-1}S(x)^T \succ 0, \quad R(x) \succ 0, \tag{146}$$

$$ii) \quad \begin{bmatrix} Q(x) & S(x) \\ S(x)^T & R(x) \end{bmatrix} \succ 0, \tag{147}$$

are equivalent.

Thus, the set of non-linear inequalities (146) can be represented by the LMI (147), which allows the treatment through computational methods.

A.5 S-Procedure

The S-Procedure is used to obtain an LMI formulation that guarantees that a function will be defined in signal whenever another function is defined in signal (BOYD *et al.*, 1994). The case for strict inequalities and quadratic forms, i.e., quadratic functions without constant or linear terms, will be presented below.

Lemma 13 (S-Procedure (BOYD *et al.*, 1994))**.** *Let $T_0, \ldots, T_p \in \mathbb{S}^n$. If there exists scalars $\tau_1 \geq 0, \ldots, \tau_p \geq 0$, such that*

$$T_0 - \sum_{i=1}^{p} \tau_i T_i \succ 0, \tag{148}$$

then

$$\zeta^T T_0 \zeta \succ 0 \ \text{ for all } \ \zeta \neq 0 \ \text{ such that } \ \zeta^T T_i \zeta \succeq 0, \ \ i = 1, \ldots, p \tag{149}$$

holds.

Note that (148) is an LMI in the variables T_0 and $\tau_1 \ldots, \tau_p$.

A.6 Other concepts

Lemma 14 (Strictly Positive Real Transfer Function (KHALIL, 2002))**.** *Let $G(s)$ be a $m \times m$ proper rational transfer function matrix, and suppose det$[G(s) + G^T(-s)]$ is not identically zero. Then, $G(s)$ is strictly positive real if and only if*

- *$G(s)$ is Hurwitz, that is, poles of all elements of $G(s)$ have negative real parts;*

- $G(j\omega) + G^T(-j\omega)$ *is positive definite for all* $\omega \in \mathbb{R}$*, and*
- *either* $G(\infty) + G^T(\infty)$ *is positive definite or it is positive semidefinite and* $\lim_{\omega\to\infty} \omega^2 M^T[G(j\omega) + G^T(-j\omega)]M$ *is positive definite for any* $m \times (m-q)$ *full-rank matrix* M *such that* $M^T[G(\infty) + G^T(\infty)]M = 0$*, where* $q =$ *rank*$[G(\infty) + G^T(\infty)]$.